GP-RSS

International Joint Graduate Program in Resilience and Safety Studies

The 7th International Symposium on Water Environment Systems

---with Perspective of Global Safety

(November 14th – 16th, 2019)

Department of Civil and Environmental Engineering
Graduate School of Engineering
Tohoku University

TOHOKU
UNIVERSITY

Sponsors

International Joint Graduate Program in Resilience and Safety Studies of Tohoku University

http://gp-rss.tohoku.ac.jp/

Department of Civil and Environmental Engineering, Graduate School of Engineering, Tohoku University

http://www.eng.tohoku.ac.jp/

ORGANIZERS

Dr. So KAZAMA	(Professor, Tohoku University)
Dr. Yu-You LI	(Professor, Tohoku University)
Dr. Daisuke KOMORI	(Associate Professor, Tohoku University)
Dr. Daisuke SANO	(Associate Professor, Tohoku University)

SECRETARIES

Assistant Professor, Yoshiya TOUGE
yoshiya.touge.a6@tohoku.ac.jp

Assistant Professor, Yu QIN
yu.qin.e8@tohoku.ac.jp

DC Student, Yemei LI
li.yemei.s5@dc.tohoku.ac.jp

DC Student, Ying SONG
song.ying.q2@dc.tohoku.ac.jp

DC Student, Yuanyuan REN
ren.yuan.yuan.t7@dc.tohoku.ac.jp

Schedule

Nov. 14th, 2019

15:00~17:30 | Registration

Venue

Graduate School of Engineering, Aobayama campus, Tohoku University

Lectures and oral presentations

Room 110, Engineering Laboratory Complex building (総合研究棟) (C10)

Posters exhibition

Room 201, Engineering Laboratory Complex building (総合研究棟) (C10)

Net-work party

Center hall Aoba restaurant (工学部中央棟)

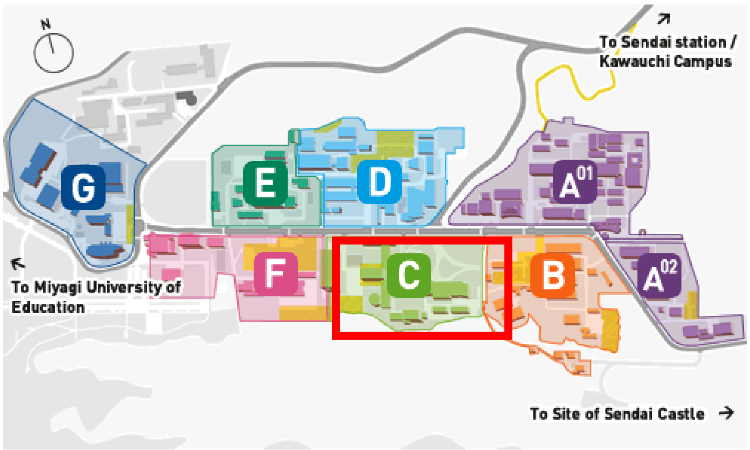

- A01 Mechanical and Aerospace Engineering
- A02 Quantum Science and Energy Engineering
- B Materials Science and Engineering
- C Center Square
- D Electrical Engineering and Applied Physics
- E Applied Chemistry, Chemical Engineering and Biomolecular Engineering
- F Civil Engineering and Architecture
- G Various Area

Engineering Laboratory Complex building(総合研究棟)

Access to Aobayama Campus (Subway)

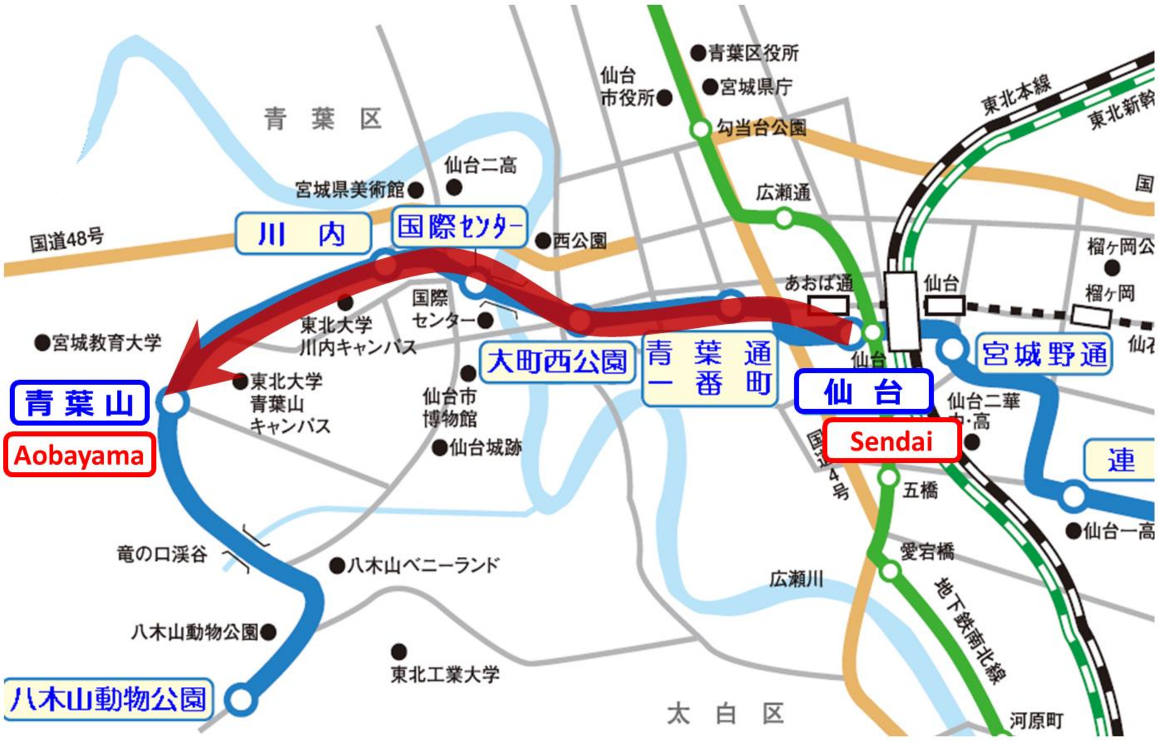

Map of **East-west line subway(地下鉄 東西線)** in Sendai

Please take this subway line and get off on the stop **Aobayama（青葉山）**.

Tips

If you start from Sendai Station, please make sure you are entering **East-west line subway（地下鉄 東西線）** rather than South-north line subway（**地下鉄 南北線**） nor JR station.

Nov. 15th, 2019

The 7th International Symposium on Water Environment Systems

Place: Room 101, Engineering Laboratory Complex building, Tohoku University

8:55 ~ 9:00	**Opening address**	
Section I	**Invited Keynote Speech**	
9:00 ~ 9:30	Anaerobic treatment of a low pH high strength dissolved organic wastewater in a membrane bioreactor George A. EKAMA *University of Cape Town*	1
9:30 ~ 10:00	Moving inventions to innovations in wastewater and sludge treatment Guang-Hao CHEN *The Hong Kong University of Science and Technology*	2
10:00 ~ 10:05	**Coffee break**	
Section II	**Water, Wastewater and Waste Management**	
10:05 ~ 10:20	Source water odor in one reservoir in hot and humid areas of southern China: diagnosis and possible mitigation measures Chao RONG, Jianwei YU, Xiaobo Han, Jinsong ZHANG *Harbin Institute of Technology Shenzhen Graduate School & Shenzhen Water Affairs (Group) Co.*	3
10:20 ~ 10:35	Human health risk of Legionella pneumophila infection caused by the groundwater usage in a decentralized drinking water system Arief Nurul UMAM, Mohan AMARASIRI, Daisuke SANO *Tohoku University*	5
10:35 ~ 10:50	Applicability of anaerobic dynamic membrane bioreactor (AnDMBR) for domestic wastewater treatment at short HRTs Yisong HU, Yuan YANG, Xiaochang C. WANG & Yu-You LI *Xi'an University of Architecture and Technology & Tohoku University*	7
10:50 ~ 10:55	**Coffee break**	
10:55 ~ 11:10	Startup and performance of a novel one-stage partial nitritation-anammox system for reject water treatment Yunzhi QIAN, Huaji MA, Yongzhi CHI, Hongying YUAN, Yanmei DING *Tohoku University*	9
11:10 ~ 11:25	Effects of phosphate and Ca/P ratio on the Anammox-hydroxyapatite (HAP) crystallization process Lan LIN, Yanlong ZHANG, Tong OUYANG, Yu-You LI *Tohoku University & Xiamen University*	11

11:25 ~ 11:40	Sulfate in anaerobic co-digester accelerates methane production from food waste and waste activated sludge Feixiang Zan, Tianwei Hao *The Hong Kong University of Science and Technology*	13
11:40 ~ 11:45	**Coffee break**	
11:45 ~ 12:00	Trace metal element supplementation impact in methane fermentation of fish processing wastewater Eli Hendrik SANJAYA, Yu-You LI *Tohoku University & State University of Malang (Universitas Negeri Malang)*	15
12:00 ~ 12:15	Experimental study on filtrate of thermal hydrolysis of sludge as an additional carbon source for denitrification Lu HAN, Yun HAN, Yuan GAO *Xi' an University of Architecture and Technology &Tohoku University*	17
12:15 ~ 12:30	Co-digestion of cow and sheep manure: Performance evaluation and relative microbial activity Yu Li, Jing Zhao, Gert-Jan Euverink *University of Groningen*	19
12:30 ~ 12:45	Anaerobic co-digestion of paper waste and sewage sludge: The effects of paper waste ratio Aijun ZHU, Yu Qin, Jing WU, Yu-You LI *Tohoku University*	21
12:45 ~ 12:55	**Group photo**	
13:00 ~ 15:00	**Poster Exhibition**	

Place: Room 201, Engineering Laboratory Complex building, Tohoku University

・	Estimation of vulnerable spots for overtopping by using 3-D point cloud data generated by UAV-SfM approach Masakazu Hashimoto, Shosuke Sato, Ken Ichikawa, Susumu Naradate, Kaori Amaya, Keiji Sato, Arata Nasuno *Tohoku University*	
・	Understanding flood hazard and crop yield loss relationship using hydrodynamic and remote sensing model Vempi Satriya, Daisuke Komori *Tohoku University*	34
・	Assessing the impact of human-induced land-use change on natural water cycle at watershed scale based on land surface model Linghao Meng, Daisuke Komori *Tohoku University*	36
・	Estimation of the flood damage caused by Climate change and effect of the adaptation Tao Yamamoto, So Kazama, Yoshiya Touge, Tsuyoshi Tada, Takeshi Yamashita *Tohoku University*	38

Section III Global Climate Assessment

15:00 ~ 15:30	Manifold Analysis of Pacific Islands Climate Data Ming-Che HU, Yi-Hsuan Shih, Tai-Yi Liu *National Taiwan University*	23
15:30 ~ 16:00	A preliminary study on development flood early warning system in Southeast Sulawesi Province Nurul Fajar Januriyadi *Universitas Pertamina*	25
16:00 ~ 16:25	Application of a large ensemble climate simulation for flood risk assessment Satoshi Watanabe *University of Tokyo*	
16:25 ~ 16:50	Data Assimilation Research for Global Weather Prediction: Past Achievements and Future Perspectives Shunji Kotsuki *Chiba University*	
16:50 ~ 17:05	**Coffee break**	
17:05 ~ 17:30	Spatial Representativity of AMeDAS Gauge Rainfall over Radar/Raingauge-Analysed Precipitation Masafumi Yamada *Kyoto University*	28
17:30 ~ 17:50	Estimating Irrigated Area through a Combined Use of MODIS and Land Surface Model in the Amu Darya Delta Jacqueline Muthoni Mbugua, Yoshiya Touge, So Kazama *Tohoku University*	30
17:50 ~ 18:10	Estimating fire severity map based on representative plots in Kamaishi 2017 forest fire Grace Puyang Emang, Yoshiya Touge, So Kazama *Tohoku University*	32
18:10 ~ 18:20	**Closing speech**	
18:30 ~ 20:00	**Dinner party**	

Nov. 16th, 2019

Technical Tour: Energy recovery & New technology

Place: Sendai Senen Sewage Treatment Plant

Biogas typically refers to a gas produced by the anaerobic digestion of organic matter including manure, sewage sludge, municipal solid waste and other biodegradable waste. The biogas for electricity system of Senen sewage treatment plant was implemented in 2018 with 7 electric generator installed. The total electric generation and yearly generation is 350 kW and 1,880,000 kWh respectively, which could supply electricity consumption of 407 generations (4618 kWh/Year/household). The emission of CO_2 can be reduced by 1040t-CO_2/year.

・The biogas for electricity system in Senen sewage treatment plant

AnMBR and One-stage Anammox is a new technology to develop an energy-positive innovative sewage treatment system integrating an anaerobic membrane bioreactor (AnMBR) and anaerobic ammonium oxidation (Anammox) process. The pilot plant in Senen sewage treatment plant has a working volumes of 20 L for the AnMBR and 7 L for One-stage Anammox reactor and completed with a capacity of 20 m^3/d after a 140-day operation.

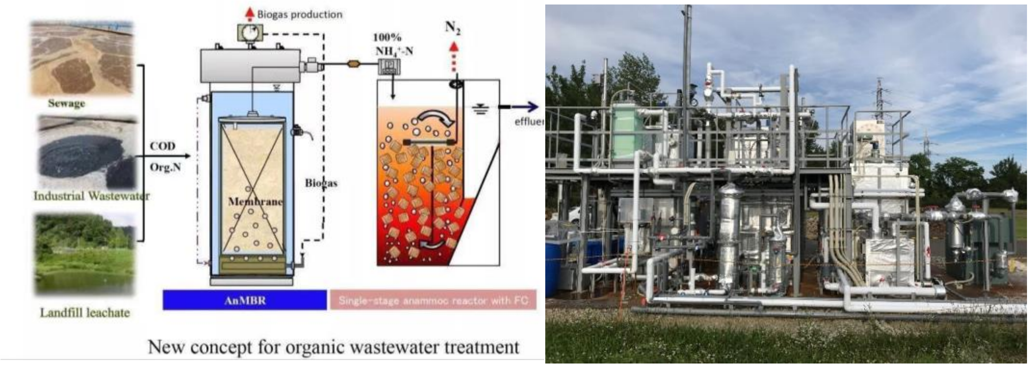

New concept for organic wastewater treatment

・Pilot plant of AnMBR and One-stage Anammox in Senen sewage treatment plant

Anaerobic treatment of a low pH high strength dissolved organic wastewater in a membrane bioreactor

○ Ekama GA[1]
[1]University of Cape Town, South Africa.

Abstract

An Anaerobic Membrane Bio-Reactor (AnMBR) was developed for the treatment of Fischer-Tropsch reaction water (FTRW) originating in Sasol's coal to fuel synthesis process. The laboratory-scale AnMBR used A4-size submerged flat panel ultra filtration membranes for 100% solids-liquid-separation. Membrane scour to reduce fouling was provided by biogas recirculation. The FTRW has a high strength (18000 mgCOD/L) and comprises mostly C_2 to C_6 short chain fatty acids (SCFA). Although the pH of the FTRW is low (3.8), only a low alkalinity (NaOH) dose is required to neutralize the low residual (effluent) VFA to maintain a reactor pH of 7.1.

The AnMBR was operated at a steady state organic loading rate (OLR) = 15 kgCOD/m^3/d for a period of 800 days and yielded a total effluent COD of only 35 mgCOD/L. The alkalinity requirement was only 0.067 kgNaOH/kgCOD removed and the MLSS concentration could be increased up to 30gTSS/L resulting in an organic loading rate (OLR) of 30 kgCOD/m^3 reactor/d. The sludge production of the AnMBR was 0.021 kgTSS/kgCOD removed.

Compared with aerobic treatment of FTRW, the advantages of anaerobic treatment are not only very low sludge production and energy consumption and high quality water recovery, but also, more importantly, the CH_4 produced can be added to the producer gas fed to synthesis process, which significantly reduces the carbon footprint of the coal to fuel synthesis process.

Biography

Professor George Ekama, who has been at the University of Cape Town (UCT) for 40 years, is well known for his work on activated sludge such as biological nutrient removal, secondary settling tank performance, filamentous bulking and kinetic modelling, some of which was adopted into the IWA activated sludge models (ASM1&2). He has published over 150 journal papers, 10 books and 25 PhD and 40 MSc students qualified under his supervision. His current research interests are (1) developing integrated chemical, physical and biological processes complete CHONPS element mass balanced three phase (aqueous-gas-solid) steady state and dynamic kinetic simulation models for plant wide municipal and industrial aerobic and anaerobic wastewater treatment modelling, (2) impact of source separation of urine, enhanced primary separation and discharge of food waste to sewer on biological wastewater treatment, nutrient removal, anaerobic digestion and energy recovery. Although retired since 2018, he continues to be active at UCT, Hong Kong University of Science and Technology (HKUST) and the UNESCO-IHE in the Netherlands teaching post-graduate courses and supervising PhD and MSc students.

Moving inventions to innovations in wastewater and sludge treatment

○ Guang-Hao CHEN[1]
[1]The Hong Kong University of Science and Technology, Hong Kong, China.

Abstract

This talk shares our experiences in development of a couple of key novel technologies (Sulfate reduction Autotrophic denitrification Nitrification Integrated (SANI) process and Sulfated Polysaccharides (SP) production from sludge) in sewage treatment from ideas, concept-proofs, and scale-up trials into potential applications. Challenges, approaches, funding and collaboration opportunities, project risk control and market exploration are also discussed.

Biography

GH Chen obtained his PhD in Environmental Engineering from Kyoto University in 1990 and has joined the Hong Kong University of Science and Technology (HKUST) since 1995. Currently he is a chair professor of Civil and Environmental Engineering at HKUST, Director of Water Technology Center of HKUST, Head of the CNERC for control and treatment of heavy metal pollution (Hong Kong Branch), and an Associated Director of the Institute for the Environment of HKUST. GH was selected Distinguished Fellow of the International Water Association (IWA) (DFIWA) in 2015, received four international awards including the Global Honor Award of IWA Project Innovation Awards (PIA) in 2012, a winner of the first Chinese National Innovation Pioneer Awards in 2018; a bronze winner of IWA PIA of Breakthroughs in Research Development in 2018, and 2018 Gold Prize of Hong Kong Green Innovation Awards. He has published nearly 200 journal papers, including 74 papers published in Water Research.

Source water odor in one reservoir in hot and humid areas of southern China: diagnosis and possible mitigation measures

○ Chao RONG[1,3*], Jianwei YU [2], Xiaobo Han[3], Jinsong ZHANG[3]
[1]Harbin Institute of Technology Shenzhen Graduate School, Shenzhen 518055, China.
[2]Key Laboratory of Drinking Water Science and Technology, Research Center for Eco-Environmental Sciences, Chinese Academy of Sciences, Beijing 100085, China.
[3]Shenzhen Water Affairs (Group) Co., Ltd., Shenzhen 518048, China.
*E-mail: rong.chao.p7@dc.tohoku.ac.jp.

Abstract

Taste and odor (T&O) are an important esthetic index to indicate the quality of drinking water and it is a direct hint for users to judge the drinking water whether is safe. In this study, aiming at a major water source reservoir in hot and humid areas in southern China, which encountered seasonable odor problems caused by 2-MIB in recent years, an integrated approach including GC/MS, algal enumeration and quantitative real-time polymerase chain reaction (qPCR) was adopted to investigate the odor problem. The results indicated that *Pseudanabaena* sp. is the main 2-MIB producer in the reservoir, which was confirmed as a benthic filamentous algae. The release of 2-MIB from the *Pseudanabaena* sp. cells is affected by temperature and light. The risk of sudden increase of 2-MIB will be reduced by raising the depth of water in the reservoir. COD_{Mn} and DOC also have great influence on *Pseudanabaena* sp. growth, further measures to reduce the COD_{Mn} and DOC input should be performed.

Keywords: Drinking water; Earthy-musty odor; *Pseudanabaena* sp.; 2-MIB; qPCR.

1 Introduction

T&O problem occurrence in drinking water was widely reported worldwide. Although no researches have shown that the presence of some odorants in the drinking water will cause harm to human health, the unpleasant smell of drinking water will undoubtedly affect the quality of consumers' life and the impression of water supply enterprise.

Due to the low odor threshold concentration (OTC) of the odorants, for instance, 2-MIB (2-methylisoborneol) and geosmin were reported as 10 ng/L and 8 ng/L, respectively, and the limited removal efficiency with conventional water treatment process, it is difficult for water treatment plant to adopt applicable control measures once encountering T&O episodes in drinking water. Previous research has proved that most T&O occurrence in reservoir or lake source water is linked to some cyanobacterial metabolites, such as 2-MIB and geosmin. As a result, identifying the odorant-producer and take effective measures in the water resource is considered the key point to reduce the T&O problem in drinking water. However, it should be noted that this process is difficult since there are many algal species in the reservoir, and not all phytoplankton produce these compounds, such as 2-MIB and geosmin, < 50 of the more than 2000 species classified to date have been directly confirmed as producers. In addition, the mechanism of algae growth, synthesis and release of odorants in algae cells are complex, as it affected by many environmental factors such as water temperature, precipitation, light, and nutrients.

Fortunately, in recent years, the genes involved in the synthesis of odorants have studied a lot, and detection of odorants producing algae with qPCR method has been widely used. Wang et al. have revealed genes involved in cyanobacteria and first studied the correlation between the gene (*mic*) and 2-MIB concentration (10-60 fg 2-MIB per *mic* copy). This provides a new way to identify the odorants-produced algae and must be more accurate than previous method.

Shiyan reservoir (SY) is a representative water resource in hot and humid regions of China and encountered seasonable T&O problems, especially in April to July which is one typical high temperature and rainy season. Our previous research has confirmed that 2-MIB is the major odorant and blamed to the T&O problem. In this study, the further research has conducted to the occurrence procedure and cause. By comparing to one nearby reservoir with no odor occurrence, the odor-producing algae, key environmental affecting factors and possible control measures for reducing odor occurrence risk in SY reservoir were systematically investigated. The results of this study will be helpful for further improvement of the drinking water quality and water management suffering from odor problems.

2 Materials and methods

2.1 Field sites and sampling

Samples were taken from the intake (0.5m below the surface) of two reservoirs from October 2016 to May 2018, and total of 66 samples were collected. Samples were collected weekly in the spring and summer (April to September), and approximately monthly at other times of the period. The samples from October 28, 2016, May 8, 2017 (odor event) and September 26, 2017 were used for odorant-producer identification analysis. During the April to July, 2018, additional sampling sites (1–6#) were added in SY. Sample sites 1–2# were close to the water inlet of the reservoir and the water depth is only about 3 meters. For other sample sites, the water depth is > 10 m.

2.2 Analysis Methods

2.2.1 Algal enumeration

The water sample was added 5% Lugol' s iodine and static settlement by 48 h, then pre-concentrated 100×and kept in dark until cell counting. The algal cell density was determined by the Uterml technique using a Sedgewick-Rafter counting chamber under a microscope (Nikon Eclipse 50i) with phase contrast and bright field illumination. A magnification of 160 × was used to enumerate the cells. Triplicates of 1 mL concentrate samples were collected separately and counted.

2.2.2 Real-time PCR

The genomic DNA was extracted from *Pseudanabaena* sp. (FACHB1277) which is 2-MIB producer. Field samples were filtered through 0.22 μm polycarbonate filter (GTTP type, Millipore, USA) before genomic DNA extraction. The Fast DNA®SPIN KIT for Soil (MP Biomedicals, USA) kit was used and operated according to the manufacturer's instructions. The primer pair MIB-R(f/r)(MIB-Rf 5′ -CGA CAGCTTCTACAYCYCCATGAC-3′ , MIB-Rr 5′ -CGC CGCAATCTGTAGCACCAT-3′) was used to amplify the *mic* fragments. The PCR instrument used was C1000™ Thermal Cycler (Bio-Rad, USA). PCR amplification was carried out in 1 × DynaZyme II buffer (Thermo Scientific, USA) with 0.2 mM of each primer, 200 mM of dNTPs, 0.4 U of DynaZyme II, and 20–50 ng of genomic DNA as template. The PCR protocol was 94 °C for 3 min, 35 cycles of 94 °C for 30 s, 59 °C for 30 s, 72 °C for 60 s, and 72 °C for 5 min. Then, the amplification product is subjected to a purification operation with SanPrep KIT (Sangon Biotech, China) and performed according to the manufacturer's instructions.

3 Results and discussion

During the odor event, the total amount of algae in SY was as high as 100 million, which was significantly higher than the other two times. The relative abundance of some cyanobacteria species, especially *Pseudanabaena sp.*, increased significantly. In previous studies, *Pseudanabaena* sp. has been identified as one of the 2-MIB producers in the aquatic ecosystem.

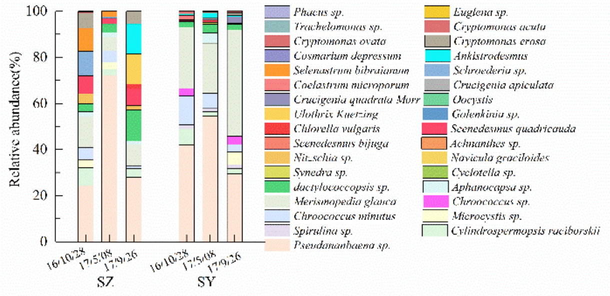

Fig. 1. The variation of phytoplankton in SZ and SY before, after, and during the odor event by genus

The relationship between algae biovolume represented by chlorophyll-a and 2-MIB indicates was 0.766 (P < 0.01), when the *Pseudanabaena* sp. is the dominant species.

Table 1 correlation analysis of chlorophyll-a and 2-MIB of SY after data selected

		Chl.a	2-MIB
Chl.a	Pearson Correlation	1	0.766**
	Sig.(2-tailed)		0.000
	N	19	19
2-MIB	Pearson Correlation	0.766**	1
	Sig.(2-tailed)	0.000	
	N	19	19

**correlation is significant at the 0.01 level (2-tailed).

The relationship between the number of *mic* and 2-MIB concentration in the filed simples is shown in Fig. 2(a. The results indicated that the number of *mic* genes was closely correlated with 2-MIB concentration by linear regression (R^2 = 0.746, P < 0.001), and show that one *mic* represent about 10 fg 2-MIB.

Principal compound analysis (PCA) was used to analyze the difference of physio-chemical variables in SZ and SY, and the result proved that COD_{Mn} and DOC are the key factors cause of the difference in phytoplankton.

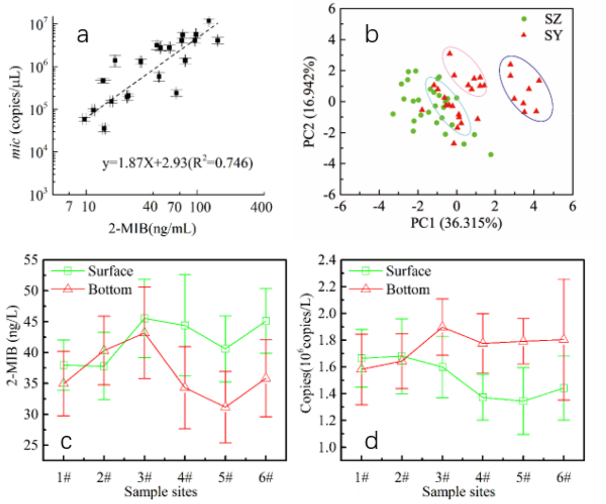

Fig. 2. Comprehensive analysis result of *mic*, environmental factors and 2-MIB concentration: (a. Relationship between 2-MIB concentration and *mic*. (b. PCA plot based on the physio-chemical variables in SZ and SY. (c. 2-MIB distribution in surface and bottom of different sites in SY. (d. *mic* distribution in surface and bottom of different sites in SY

The concentration of 2-MIB at 4–6# in the surface layer is much higher than 1–3# close to the inlet, while the 2-MIB in the bottom layer presents the opposite phenomenon. The distribution of *mic* genes is significantly different from 2-MIB, showing the opposite situation in 3–6# (Fig. 2(d). This may be attributed to the fact that the *Pseudanabaena* sp. is one typical benthic alga, which prefers to grow near the sediment to obtain enough nutrients. increase of water level may also cause nutrient dilution and decrease of water temperature, which is not only inhibit the growth of algae, but also detrimental to the production and release of 2-MIB in the cell.

Conclusions

Pseudanabaena sp. is the main 2-MIB producer in Shiyan reservoir. COD_{Mn} and DOC had higher effects on *Pseudanabaena* sp. growth, reduce the COD_{Mn} and DOC input which might be a useful measure for controlling the growth of *Pseudanabaena* sp. *Pseudanabaena* sp. is a benthic filamentous algae, and the risk of sudden increase of 2-MIB will be reduced by raising the depth of water to reduce the temperature and light in the reservoir.

Reference

[1] RONG C. et al, Source water odor in one reservoir in hot and humid areas of southern China: occurrence, diagnosis and possible mitigation measures, Environ Sci Eur, 30:45 (2018) doi: 10.1186/s12302-018-0175-8.

Human health risk of *Legionella pneumophila* infection caused by the groundwater usage in a decentralized drinking water system

○ Arief Nurul UMAM[1], Mohan AMARASIRI[3], Daisuke SANO[1,2,3]
[1]Department of Environmental Studies, Tohoku University, Sendai 980-8579, Japan.
[2] Department of Frontier Science for Advanced Environment, Tohoku University, Sendai 980-8579, Japan.
[3]Department of Civil and Environmental Engineering, Graduate School of Engineering, Tohoku University, Sendai 980-8579, Japan
*E-mail: arief.nurul.umam.s3@dc.tohoku.ac.jp

Abstract

Daily usage of poorly-treated water poses human health risks owing to the presence of harmful microorganisms. This study evaluated the health risks caused by *Legionella pneumophila* in untreated groundwater used as source of a decentralized drinking water system. Quantitative Microbial Risk Assessment (QMRA) was performed for two exposure scenarios; toilet flushing, and showering. The result indicated that showering scenario had a higher health risk with the median loss of disability-adjusted life years per person per year (DALYpppy loss) with 1.19 x 10^{-5}, compared to toilet flushing scenario with 1.30 x 10^{-8} DALYpppy loss. This estimated disease burden was mitigated by the introduction of ultrafiltration membrane to the system, and the DALYpppy loss were decreased significantly below 10^{-6}, which is recommended by WHO as a tolerable disease burden.

Keywords: QMRA; *Legionella pneumophila*; groundwater usage; DALY

1 Introduction

United Nation’s Sustainable Development Goals (SDGs) target number 6.1, that explicitly calls for full coverage of safely managed drinking water for all, still has a tough challenge, especially in rural areas. Up until 2017, it was only approximately 53 % of the total population in rural areas across the world were covered with safely managed drinking water systems[1]. The reason for this low coverage percentage is the cost of a reliable centralized water supply system is often too high for the population to afford. People live in a rural or remote area usually rely on decentralized water supply (DWS), which refers to small scale purification and distribution systems of water in a single household or a small community, and uses locally available water sources such as groundwater, river water, spring water, etc.

DWS still has challenges in providing water that free of physical, chemical, and microbiological contaminants since environmental waters, such as groundwater and river water, are prone to many natural and anthropogenic harmful contaminants. *Legionella pneumophila*, a rod-shaped gram-negative bacterium, is one that threatens to the usage of DWS. This bacterium infects lung tissues and causes a severe pneumonia-like disease called Legionnaires. It can be found in diverse environments and naturally occur in freshwater. Unlike traditional fecal-oral route pathogens, *L. pneumophila* can disperse into aerosolized waterdrops, and be inhaled by the victim[2]. *L. pneumophila* then enter and multiply in the alveolar macrophages that may cause the destruction of the pulmonary tissues.

In this research, the risk of infection of *L. pneumophila* from the direct usage of groundwater/river water is evaluated in two scenarios, showering and toilet flushing. Quantitative Microbial Risk Assessment (QMRA) model was built and applied for showering and toilet flushing’s exposure routes. The usage of membrane filtration as a countermeasure that can potentially reduce the concentration of the *L. pneumophila* was also incorporated into the study.

2 Materials and methods

QMRA for *L. pneumophila* exposure resulting from river water usage was performed in the four steps described below :

Hazard identification

Data sets of *L. pneumophila* in the rural ground water was taken from Stojek & Dutkiewicz (2006)[3] that characterize *L. pneumophila* concentration in 107 potable water samples collected from Lublin region, Poland. Among these samples, 32 samples were taken from wells situated in rural areas. These 32 *L. pneumophila* concentration data sets were then fitted into log normal distribution using fitdistrplus package in R, representing *L. pneumophila* probability distribution in the groundwater from rural area.

Exposure assessment

Two exposure scenarios were evaluated for aerosol contaminated with *L. pneumophila* inhalation during showering and toilet flushing modelled by equation 1[4]. Each scenario was modelled based on the inhalation of aerosols of various diameters that are large enough to hold *L. pneumophila* bacteria but small enough to deposit at the alveoli. The effect of ultrafiltration membrane log removal value (LRV) also studied on each exposure routes.

$$dose = C_{leg} 10^{-k} Bt \sum_{i=1}^{n} C_{aer,i} V_{aer,i} \sum_{i=1}^{n} F_i D_i \qquad (1),$$

where C_{leg} = the concentration of *L. pneumophila* in water, $C_{aer,\ j}$= the concentration of aerosols of diameter i, where i=1:10 µm, $V_{aer,\ i}$ is the volume of aerosol for size i, k=LRV, B = breathing rate (m^3 / min), t = exposure duration (min), F_i = the fraction of *L. pneumophila* that partitions to the applicable size diameter aerosols, and D_i = alveolar deposition efficiency of size i diameter aerosols.

Dose response

Dose response analysis was performed using exponential dose-response equation [2]:

$$P_{inf,daily} = 1 - e^{-rd} \qquad (2),$$

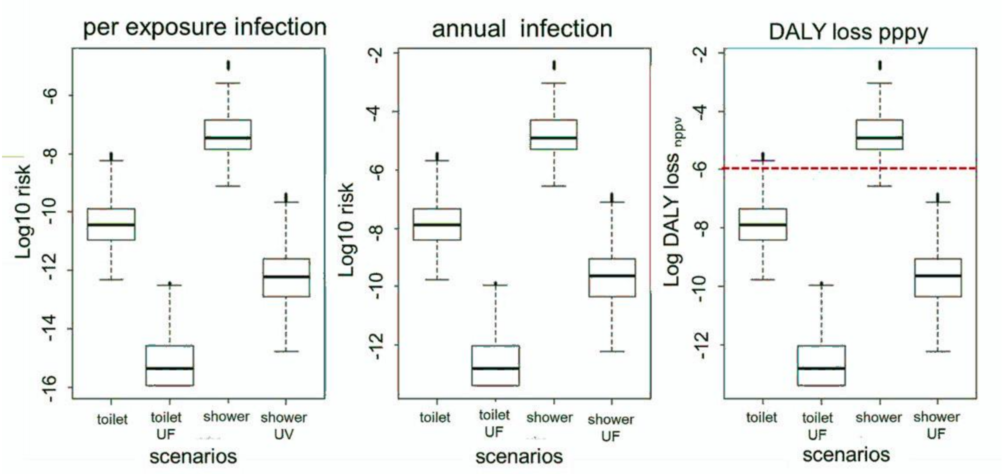

Figure 1 Monte carlo simulation result: per exposure risks , annual risks, and DALY loss per person per year

where $P_{inf,\ daily}$ = daily probability of infection, d= dose, and r is a parameter of the exponential dose response model. Monte carlo simulation with 10,000 iteration, was performed for each calculation.

Risk Characterization

Annual risk was calculated as equation [3]:

$$P_{inf,ann} = 1 - \prod_{2}^{nfj}\left(1 - P_{inf,daily}\right) \qquad (3),$$

where $P_{inf,\ ann}$= annual risk of infection, n = the yearly frequency, and f = the daily frequency of the activity j. Additionally, the annual risks were converted to the disability adjusted life years (DALY) metric using the following equation[4]:

$$DALY = \frac{DALY}{infection} P_{inf,ann} \qquad (4).$$

All risk computations were performed in R using mc2d package and 100,000 monte carlo iterations.

3 Results and discussion

Figure 1 shows the per exposure risk, annual risk, and the loss of DALY per person per year (DALYpppy) from *L. pneumophila* infection for the initial concentration calculated from Stojek & Dutkiewicz (2006), in which the rural groundwater concentration of *L. pneumophila* data were indicated. The showering scenario showed higher risk than toilet flushing scenario both in per exposure and annual risk of infection. The median of per exposure and annual risk for showering scenario were 3.37 x 10^{-8} and 1.23 x 10^{-5}, respectively. While the median per exposure and annual risk for toilet flushing scenario were 3.66 x 10^{-11} and 1.34 x 10^{-8}. The much higher risk from showering is possible because during the showering event, the aerosols concentration is higher than during the toilet flushing.

This high risk of *L. pneumophila* infection in showerin scenario, bring consequences to its DALYpppy loss. The data showed that the median of showering scenario's DALYpppy loss has exceeded 10^{-6}, which is recommend by WHO as a tolerable disease burden. The median of DALY for showering scenario was $10^{-4.92}$ DALYpppy.

The application of membrane ultrafiltration led to the decreasing of *L. pneumophila* risk of infection. Both scenarios showed that the DALYpppy loss reduced to under the 10^{-6} with the application of membrane ultrafiltration, by filtering out the *L. pneumophila* concentration in the source water.

4 Conclusions

In this study, *L. pneumophila* risk from the usage of groundwater in showering and toilet flushing scenarios at a decentralized drinking water system was modeled using QMRA approach. The results indicated that showering gave a significant disease burden (higher than 10^{-6} DALYpppy loss). The introduction of ultrafiltration membrane into the system mitigated the disease burden, indicating that the additional membrane filtration led to promising result for reducing *L. pneumophila* concentration in the source water, thus significantly decrease the risk of infection.

Reference

[1] "The WHO/UNICEF JMP global database includes estimates of progress in household drinking water, sanitation, and Hygiene since 2000." [Online]. Available: https://washdata.org/data. [Accessed: 30-Aug-2019].

[2] T. W. Armstrong and C. N. Haas, "Quantitative microbial risk assessment model for Legionnaires' disease: Assessment of human exposures for selected spa outbreaks," *J. Occup. Environ. Hyg.*, vol. 4, no. 9, pp. 634–646, 2007.

[3] N. M. Stojek and J. Dutkiewicz, "Legionella and other Gram-negative bacteria in potable water from various rural and urban sources," *Ann Agric Env. Med*, vol. 13, p. :323-335, 2006.

[4] K. A. Hamilton *et al.*, "Risk-Based Critical Concentrations of Legionella pneumophila for Indoor Residential Water Uses," *Environ. Sci. Technol.*, vol. 53, no. 8, pp. 4528–4541, 2019.

Applicability of anaerobic dynamic membrane bioreactor (AnDMBR) for domestic wastewater treatment at short HRTs

○ Yisong HU[1,2*], Yuan YANG[1], Xiaochang C. WANG[1] & Yu-You LI[2]
[1]School of Environmental and Municipal Engineering, Xi'an University of Architecture and Technology, Xi'an 710055, P.R. China
[2]Department of Civil and Environmental Engineering, Tohoku University, Miyagi 980-8579, Japan
[*]E-mail: yshu86@163.com.

Abstract

An upflow anaerobic dynamic membrane bioreactor (AnDMBR) was applied for real domestic wastewater treatment at room temperature and short hydraulic retention time (HRT = 8 h, 4 h, 2 h, and 1 h). Following continuous operation for 93 days with stepwise decreased HRT, stable average chemical oxygen demand (COD) removal was achieved (between 77.3% and 70.6%) when HRT was reduced from 8 h to 4 h, then 2 h with flux varying from 22.5 to 90 L/m^{2}h. At these three HRTs, the rate of increase in trans-membrane pressure (TMP) was 0.4, 0.38, and 0.57 kPa/d, and average CH_4 production was 0.12, 0.10, and 0.08 L/g $COD_{removed}$, respectively. Further decreasing the HRT to 1 h resulted in less COD being removed (60.4%) and lower CH_4 production (0.05 L/g $COD_{removed}$) as well as a faster rate of TMP increase (2.11 kPa/d). Various analytical methods were applied to characterize the morphology and composition of the dynamic membrane (DM) layers. With reduced HRT, increased accumulation of organic substances was noted in the DM layer, especially when the HRT was shortened to 1 h. AnDMBR was applicable to wastewater treatment at room temperature with short HRTs, 2 h could be the HRT limit to maintain stable operation.

Keywords: AnDMBR; wastewater treatment; methane production; hydraulic retention time

1 Introduction

In the AnMBRs, the continuous attachment of foulants on the UF/MF membrane surface is a common phenomenon resulting in cake layer fouling. This problem accounts for over 80% of the total filtration resistance. Meanwhile, the cake layer could function as a "secondary membrane" or filter to enhance pollutant removal, possibly due to the physical rejection and biodegradation effects of active biomass. Thus, researchers have attempted to strengthen cake layer formation on coarse pore materials (such as non-woven cloths and meshes) to replace conventional UF/MF membrane during wastewater or waste solids treatment. The successful formation of a heterogeneous cake layer, which is commonly termed "dynamic membrane" (DM) has a robust structure and stable filterability and is observed both in anaerobic dynamic membrane bioreactors (AnDMBRs) and aerobic dynamic membrane bioreactors (AeDMBRs). Both systems possess several unique advantages such as high membrane flux, low membrane cost, and easy membrane cleaning [1]. Here, the DM can transform one of the most critical disadvantages of membrane fouling, into a competitive advantage.

It is known that real municipal wastewater is generally in the complex wastewater category due to its large amount of particulate substances and moderate biodegradability. Thus, challenges encountered for anaerobic municipal wastewater treatment at temperate area. For real municipal wastewater treatment in low-temperature areas, utilizing the AnDMBR at room temperature could be an appropriate alternative. However, studies on the application of the emerging AnDMBR process in real municipal wastewater treatment are lacking, and its potential has not been fully understood until recently. According to one review regarding the application of AnDMBR, when treating municipal wastewater, the shortest HRT reported was 2.6 h, with other studies reporting HRTs of 8 h or longer.

Thus, the main objective of this work is to investigate the application of an upflow AnDMBR for real domestic wastewater treatment at short HRTs (decreasing from 8 h to 1 h) at room temperature (20-25 °C), with a focus on treatment performance and DM filterability during a long-term operation period (93 d) [2]. Moreover, the characteristics of the DM layer, including the morphology, component substances, and retention function, were discussed. No such investigation has yet assessed the impacts of extreme conditions (relatively short HRT, low temperature, and high particulate content wastewater) on AnDMBR performance

2 Materials and methods

2.1 Experimental setup and operation

The AnDMBR set-up was made of plexiglass with a total working volume of 3.6 L and comprised an upflow bioreactor and a submerged DM module located at the top of the bioreactor. The nylon mesh (75 μm pore size) served as the supporting material for DM formation with a total filtration area of 0.02 m^2. Real domestic wastewater was fed into the bioreactor using a peristaltic, which was connected to a water level sensor to maintain a constant water level in the bioreactor. Permeate was collected using a second peristaltic pump. To achieve the target HRTs, the membrane flux was changed by regulating the flow rate of the effluent pump. An on-line pressure sensor located on the permeate line recorded the trans-membrane pressure (TMP). The volume of the produced biogas was measured by a wet-type gas flowmeter.

The AnDMBR was inoculated with sludge from a local full-scale anaerobic digester The feed wastewater was collected from a local WWTP in Xi'an, China. The

AnDMBR was operated at 20-25 °C covering four phases. At the first phase, the HRT was 8 h, then it was shortened to 4 h, 2 h, and 1 h at the subsequent phases, with fluxes of 22.5, 45, 90 and 180 L/m^{2}h, respectively. During the four stages, the OLR was 0.82, 1.63, 3.01, and 6.8 kg COD/m^3·d.

2.2 Analytical methods

Various analytical methods are adopted and listed below: particle size distribution (PSD) analysis, scanning electron microscopy (SEM) - energy diffusive X-ray (EDX) analysis, fluorescent excitation–emission matrix (EEM) analysis, Fourier transform infrared (FTIR) analysis, specific methanogenic activity (SMA) analysis as well as others, such as VFAs, EPS, COD/SCOD, MLSS/MLVSS and SO_4^{2-}, and biogas composition.

3 Results and discussion

Fig. 1(a) shows that increasing filtration flux from 22.5 to 180 L/m^{2}h is adopted to achieve stepwise decrease of HRT from 8 h to 1 h. The time course of TMP is shown in Fig. 1(b) at different HRTs. TMP increased steadily when HRTs were 8 h, 4 h and 2 h, with increasing rate of 0.4, 0.38 and 0.57 kPa/d, respectively. TMP increasing rate was much higher during HRT of 1 h (2.11 kPa/d). Apparently, HRTs at the 2-8 h TMP increasing rates were acceptable and not affected by the high filtration flux (22.5-90 L/m^{2}h). However, at extremely short HRT (1 h) and high flux (180 L/m^{2}h) with a quick TMP increase coupled with an even unsustainable flux appeared.

As shown in Fig. 1(c), at HRTs of 8 h, 4 h and 2 h, the effluent turbidity maintained within a relatively stable range with the average values as 21.4, 19.2 and 24.4 NTU, respectively, this was when influent turbidity was 139.4 NTU on average. However, at HRT of 1 h, the effluent turbidity increased to 37.9 NTU on average, indicating a reduction of filtration performance. The DM layers at the end of operation at HRT of 2 h and 1 h were chosen to investigate the effects of short HRTs on the DM layer.

The potential reasons were presented as follows. It is worth noting that at HRT of 1 h the high flux (180 L/m^{2}h) was seldom reported to date in the AnDMBRs and also in the AnMBRs. Increased upflow velocity (1.7 m/h) at HRT of 1 h resulted in turbulence of the sludge blanket, more small flocs, colloids and biopolymers were presented in the supernatant, which can be verified by supernatant turbidity (67 and 102 NTU at HRT of 2 h and 1 h on average) and supernatant COD concentrations. On the other hand, the drag force was much higher to maintain high flux, which may accelerate the deposition of flocs, colloids and biopolymers on support material. This process induced the formation of a thicker and denser cake layer,

As shown in Fig. 2, the black gray cake layers were both formed on the support material at two HRTs. In addition, SEM images were taken to determine the morphology of the DM layer. It can be seen that the virgin nylon mesh was smooth and the pores were clear. At HRT of 2 h and 1 h, the DM layers were covered by microbial flocs or biopolymers, and seemed to be dense, rough and uneven. Meanwhile, the SEM images revealed showed that the DM layer at HRT of 1 h appears to be denser, and more compact when compared with that at HRT of 2 h.

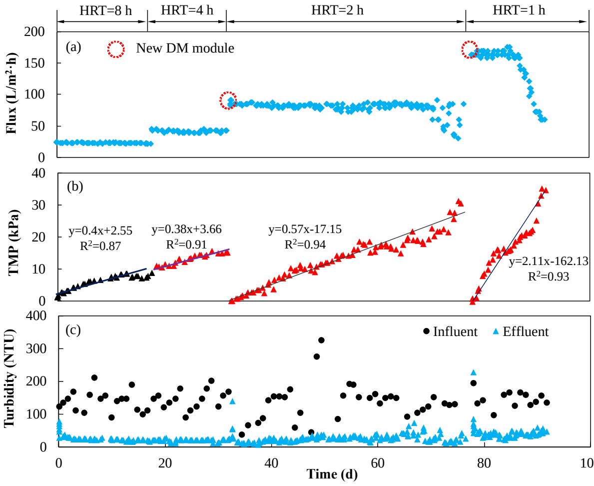

Fig. 1. Profiles of (a) flux, (b) TMP and (c) effluent turbidity in the AnDMBR at different HRTs.

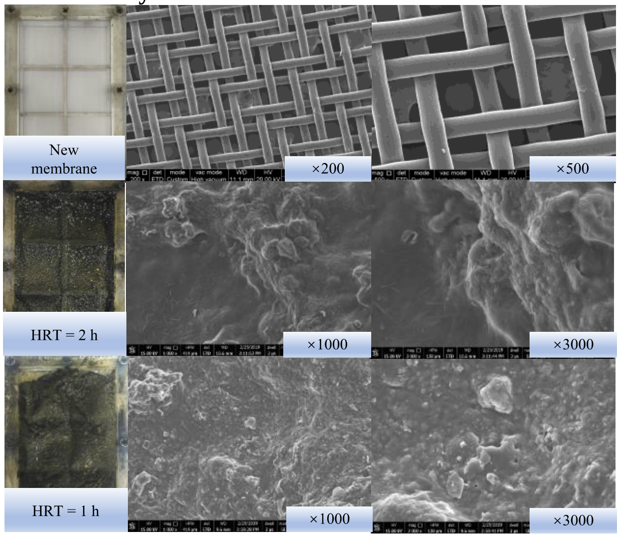

Fig. 2. Photos and SEM images of virgin mesh and DM layers at HRTs of 2 h and 1 h.

4 Conclusions

(1) When HRT no less than 2 h satisfactory COD removal and appreciable CH_4 production could be guaranteed.

(2) Further shortening HRT to 1h affected the process performance as COD removal rate dropping to 60%, methane production decreasing to 0.05 L CH_4/g COD and TMP increasing rapidly (2.11 kPa/d). Enhanced accumulation of foulants in the DM layer resulted in severer membrane fouling issue.

(3) AnDMBR can be a promising alternative for wastewater treatment under extremely environment and operation conditions.

Reference

[1] Y.S. Hu, X.C. Wang, H.H. Ngo, Q.Y. Sun, Y. Yang, Anaerobic dynamic membrane bioreactor (AnDMBR) for wastewater treatment: A review, Bioresour. Technol., 247 (2018) 1107-1118.

[2] Y. Yang, Y. Zang, Y.S. Hu, X.C. Wang, H.H. Ngo, Upflow anaerobic dynamic membrane bioreactor (AnDMBR) for wastewater treatment at room temperature and short HRTs: Process characteristics and practical applicability, Chem. Eng. J., (2019) 123186.

Startup and performance of a novel one-stage partial nitritation-anammox system for reject water treatment

○ Yunzhi QIAN[1*], Huaji MA[2], Yongzhi CHI[2] , Hongying YUAN[2] & Yanmei DING[2]
[1]Graduate School of Environmental Studies, Tohoku University, Miyagi 980-8579, Japan.
[2]School of Environmental and Municipal Engineering, Tianjin Chengjian University, Tianjin 300384, China.
[*]E-mail: qian.yunzhi.q8@dc.tohoku.ac.jp

Abstract

A novel internal circulation contact oxidation membrane bioreactor (ICCOMBR) was constructed to investigate the nitrogen removal of reject water. The nitrosation process, partial nitrosation process and one-stage partial nitrosation-anammox (PN/A) process were established gradually. The stable nitrite accumulation rate (NAR) of 87.5% was achieved with nitrogen loading rate (NLR) increased from 0.1 to 0.64gN/(L·d). The transition from nitrosation process to partial nitrosation process could be achieved by reducing the aeration rate (AR) from 1.65L/min to 0.8L/min, and the ratio of NO_2^-/NH_4^+ in the effluent was 1.15±0.04. With the dissolve oxygen (DO) concentration of 0.50mg/L and the NLR of 0.4gN/(L·d), the one-stage PN/A process was built in 27 days after inoculated anammox granular sludge. The one-stage PN/A process was successfully operated under 0.4-0.6gN/(L·d), 0.50-0.55mgDO/L, and 82% nitrogen removal effectively.

Keywords: One-stage partial nitrosation-anammox; Reject water; Partial nitrosation; Biofilm carriers.

1 Introduction

The wastewater produced by sludge anaerobic digestion is called reject water. The flow rate of reject water is about 2% of WWTP influent and the nitrogen load accounts for about 15 to 40% of the WWTP. Besides, the characteristics of high-strength ammonia concentration (500-2000mg/L) and low C/N (≤1) lead to difficulties in treating reject water with nitrification-denitrification process.

For the low operating cost and no requirement of external carbon sources, partial nitrosation/anammox (PN/A) has been the emerging environment-friendly and energy-saving process for biological nitrogen removal, especially for high-strength ammonia wastewater such as reject water. The one-stage PN/A system is more potential for application due to space saving. However, only the ammonia-oxidizing bacteria (AOB) of partial nitrosation process and the anammox bacteria of anammox process are coexist efficiently in one reactor can the one-stage PN/A system could achieve the stable nitrogen removal performance. Besides, the nitrite oxidizing bacteria (NOB) usually coexist in the microbial community and compete nitrite with anammox bacteria.

To solve the above challenges, dissolved oxygen (DO) concentration control is used in one-stage PN/A system. DO concentration below 1.0mg/L is widely used in the startup and stable operational of one-stage PN/A system to restrain ammonia over oxidation and avoid inhibition of anammox activity at higher DO level. Additionally, contact oxidation reactor was wildly used to startup and operate the one-stage PN/A system[1]. In these reactors, the microorganisms rely on the biofilm carriers to form a two-layer biofilm. Among them, the anammox bacteria live in an anaerobic environment and the AOB lives in an aerobic environment. However, there are problems that the microorganisms could lost with effluent before successful forming biofilm or the inadequate biomass of anammox bacteria in inoculation sludge, resulting in prolonged start-up time of one-stage PN/A system. Membrane bioreactor (MBR) is suitable for slow-growth-rate microorganisms such as anammox bacteria and AOB due to the complete biomass retention. Therefore, by coupling suitable bio-fillers and membrane separation technology, this could more potential to achieve the fast start-up and stable operation of one-stage PN/A system.

In this study, a novel internal circulation contact oxidation membrane bioreactor (ICCOMBR) was setup to evaluate the start-up characteristics and nitrogen removal performance of one-stage PN/A system. The stable operation of nitrosation process and the mechanism of transformation from nitrosation process to partial nitrification process were studied.

2 Materials and Methods

2.1 Biofilm carriers

The biofilm carriers used in this study was made of high-density polyethylene (HDPE) modified material, which has an H×D=10mm×7mm, the specific surface area of 1000m^2/m^3, and the specific gravity is 0.96~0.98.

2.2 Reactor setup and operation

The ICCOMBR system was equipped with an 8.5L ICCOMBR reactor, a substrate tank and a pretreatment tank. The ICCOMBR reactor has an H/D of 12:1. Operation temperature was kept at 35℃ with a water bath heater. Influent was pumped by a peristaltic pump. Effluent recirculation was pumped by a peristaltic pump to dilute the substrate concentration in the reactor. The U-type microfiltration membrane module was made of polyvinylidene fluoride (PVDF) with a membrane pore size of 0.22μm and a membrane effective surface area of 0.1 m^2 .The bio-filler with a packing ratio of 84.5% was fixed with nylon thread.

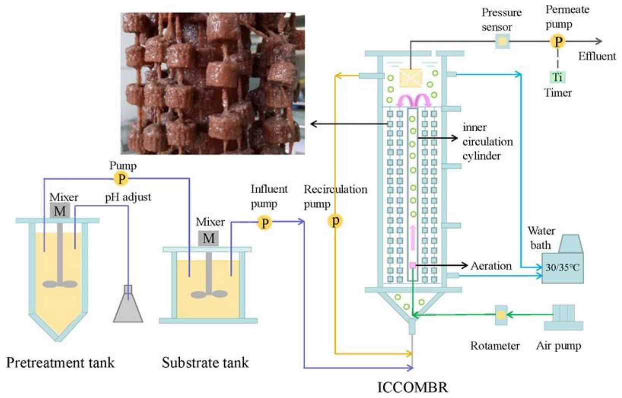

Fig. 1. Schematic diagram of the ICCOMBR reactor

2.3 Influent and seed sludge

Reject water was generated from digestive sludge dewatering treatment, which was treated with struvite precipitation for phosphorus recovery and pretreated by poly aluminium chloride (PAC) coagulationand sedimentation. The molar ratio of HCO_3^-/NH_4^+ in reject water was 2:1 by adding $NaHCO_3$. The main compositions of reject water were NH_4^+-N 584±140mg/L, TP 0.56 ±0.16mg/L, COD 232±47mg/L and SS 47±8mg/L, respectively.

Activated sludge was inoculated to start the nitrosation process, with SS was 3.3g/L and VSS/SS was 0.46. The anammox granular sludge was taken from an UASB reactor treat high strength ammonia synthetic wastewater, with the SS was 56 g/L and VSS/SS was 0.44.

2.4 Analysis Methods

Influent and effluent samples were measured daily and processed immediately for analysis. The samples were filtered through 0.45μm filter prior to measurements. Ammonia, nitrite and nitrate were analyzed according to standard methods[2] .

Nitrite accumulation rate (NAR), ammonia removal efficiency (ARE), volume nitrosation rate (v_1) and volume nitrification rate (v_2) were calculated as Eq. (1)-(4).

$$\text{NAR}=\frac{NO_2^-\text{-}N_{eff}}{NO_2^-\text{-}N_{eff}+NO_3^-\text{-}N_{eff}}\times100\% \qquad (1)$$

$$\text{ARE}=\frac{NH_4^+\text{-}N_{inf}-NH_4^+\text{-}N_{eff}}{NH_4^+\text{-}N_{inf}}\times100\% \qquad (2)$$

$$v_1=\frac{NO_2^-\text{-}N_{eff}\times Q-NO_2^-\text{-}N_{inf}\times Q}{V\times1000} \qquad (3)$$

$$v_2=\frac{NO_3^-\text{-}N_{eff}\times Q-NO_3^-\text{-}N_{inf}\times Q}{V\times1000} \qquad (4)$$

Where Q and V are inflow rate and reactor volume, respectively.

3 Results and Discussion

Fig. 2 showed the startup and operation performance of the ICCOMBR reactor. Fig.2 (a) - (c) showed the startup and operation of nitrosation process. After influent NH_4^+-N concentration higher than 250mg/L, the nitrosation process could achieve the stable operation with NAR of 87.6±3.5% while NOB was successfully inhibited in a low level of 0.05±0.02gNO_3^--N/L/d. Fig.2 (d) - (f) showed the startup and operation of partial nitrosation process. After the AR was adjusted from 1.65L/min to 0.8L/min, the partial nitrosation process was startup in 5 days and the effluent ratio of NO_2^--N/NH_4^+-N was kept in a stable level of 1.15 ±0.04. It suggested that the partial nitrosation process can be fast started by reducing the AR to about 50% of the nitrosation process. AR was the key control parameter for the transition from nitrosation process to partial nitrosation process. Fig.3 (g) - (i) showed the startup and operation of one-stage PN/A process. The one-stage PN/A process was built in 27 days after inoculated anammox granular sludge and was successfully operated under nitrogen loading rate of 0.4-0.6gN/(L·d), DO of 0.50-0.55mg/L, and with a nitrogen removal effectively of 82%.

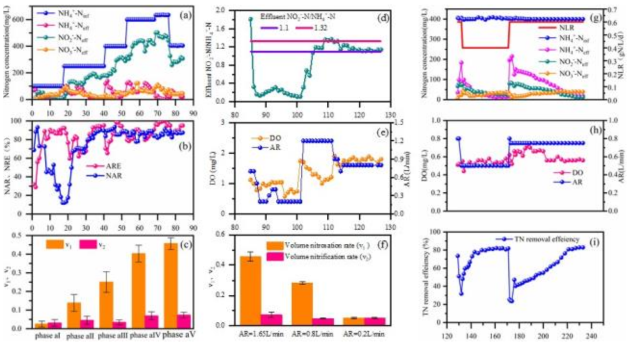

Fig. 2. The startup and operation performance of the ICCOMBR reactor. ((a)the nitrogen concentrations, (b)NAR and ARE, and (c) v_1 and v_2 of nitrosation process; (d)effluent substrate ratio, (e)DO and AR, and (f) v_1 and v_2 of partial nitrosation process; (g) the nitrogen concentrations and NLR, (h)DO and AR, and (i)TN removal effeiency of one-stage PN/A process.

4 Conclusions

(1) The nitrosation process could achieve fast startup and stable operation while NOB was successfully inhibited when influent NH_4^+-N concentration was higher than 250mg/L.

(2) The partial nitrosation process can be fast started by reducing the AR to about 50% of the nitrosation process.

(3) The one-stage PN/A process could successfully operated under NLR of 0.4-0.6gN/(L·d) and nitrogen removal effectively of 82%.

Reference

[1] Liu, Y., Niu, Q.G., Wang, S.P., Ji, J.Y., Zhang, Y., Yang, M., Hojo, T., Li, Y.Y. 2017. Upgrading of the symbiosis of Nitrosomanas and anammox bacteria in a novel single-stage partial nitritation-anammox system: Nitrogen removal potential and Microbial characterization. Bioresource Technology, 244, 463-472

[2] APHA. 2005. Standard Methods for the Examination of Water and Wastewater. American Water Works Association and Water Environment Federation, Washington, DC,USA.

Effects of phosphate and Ca/P ratio on the Anammox-hydroxyapatite (HAP) crystallization process

○ Lan LIN[1,2,*], Yanlong ZHANG[2], Tong OUYANG[2] & Yu-You LI[3]
[1]Department of Civil and Environmental Engineering, Tohoku University, Miyagi 980-8579, Japan.
[2]College of the Environment & Ecology, Xiamen University, Xiang'an District, Xiamen, Fujian 361102, China.
[3]Department of Frontier Science for Advanced Environment, Tohoku University, Miyagi 980-8579, Japan.
[*]E-mail: lnkhl06@163.com.

Abstract

Based on the requirements for advanced treatment and resource recovery of nitrogen and phosphorus pollutants in wastewater, the coupled anammox and hydroxyapatite (HAP) crystallization process was studied with an aim of achieving high efficiency and low energy consumption during simultaneous nitrogen and phosphorus removal. In this study, the effects of phosphate and calcium-phosphorus (Ca/P) ratio on the coupled anammox-HAP system were investigated through batch tests. The inhibition effects of phosphate and free HAP were analyzed by the modified 2-P logistic model to obtain the threshold concentrations of inhibitors. And a reference formula of calcium dosage was obtained to provide theoretical basis for practical engineering application of this system.

Keywords: Anammox; hydroxyapatite crystallization; phosphate; Ca/P ratio; calcium dosage.

1 Introduction

Excess nitrogen and phosphorus have been released into waterbodies due to excessive use of fertilizer in agriculture. And the worldwide phosphorus reserves have been sharply reduced, and apparently a global shortage situation will be unavoidable in the near future. Therefore, recycling and reusing released phosphorus resources is a possible solution for eutrophication.

The anammox process was discovered to be an advanced and promising technology for nitrogen removal, which can greatly cut down the energy consumption and sludge production in contrast to the traditional biological process. However, phosphorus cannot be removed from wastewater by a single anammox process. The traditional phosphorus removal process mainly uses the bioenrichment and chemical precipitation methods, while the former has low removal efficiency and the latter is not suitable for treatment of wastewater with a low phosphorus concentration and also costly.

The anammox biological process was coupled with hydroxyapatite (HAP) crystallization and combined into an anammox-HAP crystallization process in this study. The HAP was produced through the effects of both biologically induced mineralization and biologically controlled mineralization via anammox. The produced HAP was combined with the anammox microorganism and finally acted as a carrier of the anammox biofilm. Since HAP has the advantages of excellent bio-compatibility and high crystallinity, this structure can enhance the mechanical stability and sedimentation performance of sludge granules and improve the ability of sludge to withstand compression. In addition, it offers a way to recover phosphorus from wastewater in the form of HAP, which is also an essential product in industry.

Based on this, it is of significance to investigate the effects of phosphate and calcium-phosphorus (Ca/P) ratio on the coupled anammox-HAP system. Since higher phosphate concentrations can inhibit anammox activity and the Ca/P ratio is an important factor in the HAP crystallization process. Furthermore, the phosphorus concentration varies in a range in practical water treatment, thus the optimal amount of calcium added also differs.

In this study, an anammox attached film expanded bed (AAFEB) reactor was used to start up the anammox-HAP crystallization process. Through batch tests, the effects of phosphate concentration and Ca/P ratio on the specific anammox activity (SAA) and phosphorus removal performance were investigated. And the data were fitted by models to analyze and discuss the results.

2 Materials and methods

2.1 Batch Tests

The effects of phosphate and Ca/P ratio were investigated through the determination of the SAA and phosphorus removal efficiency. The phosphorus removal efficiency was obtained by analyzing filtered samples using ammonium molybdate spectrophotometry method.

The steps of the SAA test were as follows. The tests were conducted in serum flasks with a working volume of 150 mL and incubated in a thermostatic shaker (110 rpm) at 35 °C. The substrate was basically consistent with the influent of AAFEB reactor system, which had total nitrogen content of 200 mg N/L, a NO_2^--N to NH_4^+-N ratio of 1.32:1 and an initial pH value of 7.8. The substrate was also sparged with nitrogen gas to obtain anoxic conditions. Sludge granules were taken from the middle of AAFEB reactor and washed with nutrient solution to remove substrate residue. By recording the amount of gas produced, a curve of gas production over time was obtained. The modified Gompertz equation model (Eq. (1)) was used to fit the data:

$$P = P_0 \times \exp\{-\exp[R_{\max} \cdot \mathrm{e} \cdot (\lambda\text{-}t)/P_0 + 1]\} \qquad (1)$$

where P is the cumulative nitrogen production (mL), P_0 is the theoretical maximum nitrogen gas production (mL), R_{max} is the maximum nitrogen production rate, e is a constant (= 2.718281828), t is the reaction time, and λ is the lag phase time (h). The P_0, R_{max} and λ parameters are obtained by fitting, and the SAA is calculated using these fitted parameters.

2.2 Model Description

The modified 2-P logistic model is used to fit the inhibitory effect, and the threshold concentrations of inhibitor are defined as the IC_{10} (at which the inhibition rate is 10%), IC_{50} and IC_{90}. The modified 2-P logistic model can be expressed as:

$$I = 100 - \frac{100}{1+(X/X_0)^P} \tag{2}$$

where I is the inhibition ratio (%), X is the inhibitor concentration, X_0 is the half maximal inhibitory concentration (IC_{50}), and P is a constant.

The Monod equation model is a kinetic model used to describe the relationship between the cell growth rate and substrate concentration. It was used in this study to fit the effect of Ca/P ratio on the phosphorus removal rate. The Monod equation used in the batch test can be expressed as:

$$P = P_m \cdot r/(k_r + r) \tag{3}$$

where P is the phosphorus removal efficiency (%), P_m is the maximum phosphorus removal efficiency (%), r is the Ca/P ratio, and k_r is half of the Ca/P ratio corresponding to the P_m.

3 Results and discussion

3.1 Effects of Phosphate Concentration

Fig. 1(a)-1(b) shows the SAA variation with the phosphate concentration and the inhibition curve fitted by the modified 2-P logistic model. The SAA value decreased to 0.0676 ±0.0046 when the phosphate concentration reached 600 mg/L and further decreased to 0.0069±0.0042 when the phosphate concentration was 1500 mg/L. Higher phosphate concentrations inhibited anammox activity and the the IC_{10}, IC_{50} and IC_{90} of phosphate for the system were 375, 651, and 1221 mg P/L, respectively.

3.2 Inhibition Due to Free HAP

In this study, a phosphorus concentration of 600 mg/L, which is similar to the IC_{50} of phosphate inhibition (651 mg/L), and a Ca/P ratio range of 0~1.0 were selected to investigate the effect of the calcium dosage. The SAA results (Fig. 1(c)) show that when the Ca/P was higher than 0.1, an increase in the Ca dosage deteriorated rather than alleviated the inhibition induced by high phosphate.

In addition, the phosphorus concentrations after reaction at Ca/P ratios of 0.5, 0.7, and 1.0 (295.14, 236.20 and 164.16 mg/L, respectively) were lower than the IC_{10} (375 mg/L). Therefore, under these Ca/P ratios, the inhibitory effect of high phosphate was considered to be eliminated. Meanwhile, many white crystals formed in the serum flasks, and more white crystals formed under higher Ca/P ratios. XRD characterization revealed that the white crystals were HAP. Therefore, the reaction system may be inhibited by these generated free HAP crystals. The inhibition curve of free HAP was obtained by the modified 2-P logistic model (Fig. 1(d)) and the IC_{10}, IC_{50} and IC_{90} values of free HAP were 6.34, 8.74, and 12.05 g/L, respectively.

3.3 Reference Formula of Calcium Dosage

Different initial phosphorus concentrations (5.7, 11.4, 40, and 600 mg/L) were used to investigate the effect of different Ca/P ratios on phosphorus removal (Fig. 1(e)). With the increase in Ca/P ratios at the low phosphorus concentrations, the rate of increase of phosphorus removal was slow. When the concentration increased, the Ca/P ratio had a more significant effect on phosphorus removal, and the phosphorus removal rate tended to be constant in the end. In addition, the initial phosphorus concentration had a great influence on its removal rate. For a specified Ca/P ratio, a higher phosphorus concentration would give rise to higher phosphorus removal efficiency.

The Monod equation model was used to fit the data points in Fig. 1(e), and the P_m was substituted into the equation to obtain the corresponding optimal Ca/P ratio (calcium dosage). A quadratic equation of the calcium dosage versus the phosphorus concentration was then obtained by nonpolynomial fitting (Fig. 1(f)). Thus, the reference formula of calcium dosage was:

$$D_{Ca} = 1.79E\text{-}05\ C_P^2 + 0.00163\ C_P + 0.312 \tag{4}$$

where D_{Ca} is the calcium dosage (g/L), and C_P is the phosphorus concentration (mg/L) in the wastewater.

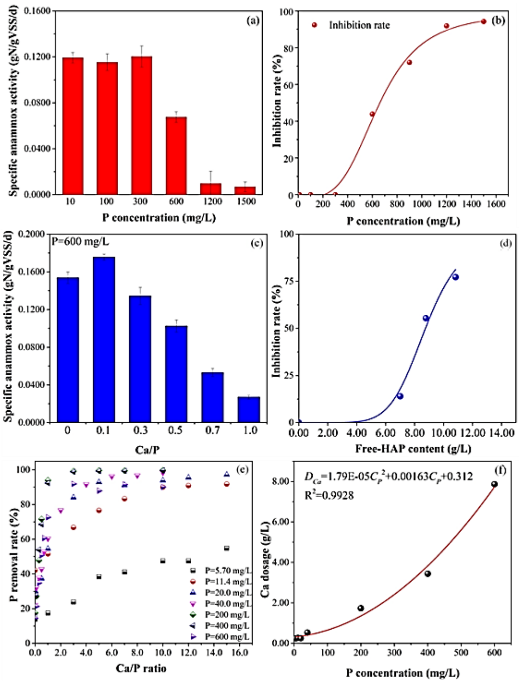

Fig. 1. SAA for different phosphate concentrations (a) and different Ca/P ratios (c), inhibition rate fitting curve of phosphate (b) and free HAP (d); phosphorus removal results for different initial concentrations (e) and calcium dosage curve (f).

4 Conclusions

(1) Higher phosphate concentration had an adverse effect on the coupled anammox-HAP system and higher Ca/P ratio could inhibit this system through the formation of free HAP.

(2) The inhibition thresholds of phosphate and free HAP on the coupled system and a reference formula of the calcium dosage were obtained.

Reference

[1] Zhang, Y.L. et al, Long-term operation performance and variation of substrate tolerance ability in an anammox attached film expanded bed (AAFEB) reactor, Bioresour. Technol., 211 (2016a) 31-40.

Sulfate in anaerobic co-digester accelerates methane production from food waste and waste activated sludge

○ Feixiang Zan[1], Tianwei Hao[2]*

[1] Department of Civil and Environmental Engineering, The Hong Kong University of Science and Technology, Clear Water Bay, Hong Kong, China

[2] Department of Civil and Environmental Engineering, Faculty of Science and Technology, University of Macau, Macau, China

*E-mail: thao@connect.ust.hk.

Abstract

The presence of sulfate in food waste (FW) and waste activated sludge (WAS) threatens the anaerobic co-digestion for methane production. In this study, methane production from the anaerobic co-digestion of FW and WAS at sulfate concentrations from 50 to 400 mg S/L was not affected, but instead deteriorated at 200–300 mg S/L. However, a model-based kinetic analysis reveals that sulfate can significantly promote the conversion of rapidly biodegradable substrates. From a point of thermodynamic view, the presence of sulfate can stimulate sulfate reducing bacteria acting as acetogens to convert propionate to acetate, providing an alternative metabolic pathway for methanogenesis. In the anaerobic co-digestion, regulation of sulfate at a proper concentration can be a potential strategy to improve the efficiency of methane production. However, more research is needed to optimize the sulfate concentration and substrate types in the anaerobic co-digester.

Keywords: Sulfate; Anaerobic co-digestion; Food waste; Waste activated sludge.

1 Introduction

Anaerobic digestion (AD) is a versatile biotechnology capable of stabilizing organic waste while simultaneously recovering energy in the form of methane. A high organic substrate such as FW can be effectively converted into bioenergy through the AD process for energy recovery and solids reduction. However, the mono-digestion of FW can be inhibited by the improper ratio of carbon-to-nitrogen (C/N) and the imbalanced nutrients. To overcome the disadvantages of mono-digestion, the co-digestion of FW and waste activated sludge (WAS) is done in view of optimizing the C/N ratio and improving the nutrients balance. However, the sulfur content in FW, from 0.2% to 0.6% of the dry matter, is usually overlooked in the anaerobic co-digestion. Besides, sewage sulfate concentrations of 20 to 300 mg S/L can inevitably end up in the anaerobic digesters through the seawater intrusion, application of sulfate-containing flocculants and/or discharge of sulfate-laden industrial wastewater. Sulfate reducing bacteria (SRB) thrive in the presence of sulfate and impact negatively on methane production. SRB compete with methanogens or fermentative bacteria for carbon sources and electrons, while the produced sulfide by SRB can inhibit both methanogens and fermentative bacteria. Other than the competition, an active syntrophic relationship between methanogens and SRB have been extensively identified. In this study, it was hypothesized that the sulfate concentration could be the key driver for diverse SRB-related anaerobic metabolisms in the anaerobic co-digestion of FW and WAS; sulfate could potentially determine the functional role of SRB in AD.

Hence, the main objective of this study is to investigate the role of sulfate at a proper concentration in the anaerobic co-digestion of FW and WAS. Biochemical methane potential (BMP) tests were conducted to evaluate the methane production from the co-digestion of FW and WAS at different sulfate concentrations. A model-based kinetic analysis was used to evaluate the hydrolysis rates and methane production potential of the substrates at various co-digesters sulfate concentrations.

2 Materials and methods

The WAS was collected from a secondary sedimentation tank in a local saline wastewater treatment plant (WWTP) in Shatin of Hong Kong with an average solids retention time of about 15 days. The total solids (TS), volatile solids (TS) and pH were 15.85 ± 0.14 g/L, 9.60 ± 0.07 g/L and 6.53 ± 0.02, respectively. Inoculum for BMP tests were obtained from a mesophilic anaerobic digester (AD) at the same WWTP with 30.15 ± 0.27 g TS/L, 16.20 ± 0.20 g VS/L and pH of 6.60 ± 0.02. The FW was prepared according to previous study[1]. The FW slurry was characterized with 30.83 ± 0.32 g TS/L, 30.50 ± 0.49 g VS/L and pH of 6.04 ± 0.02. To assess the impacts of different sulfate concentrations on the co-digestion of FW and WAS, BMP tests were conducted with an Automatic Methane Potential Test unit (AMPTS II, Bioprocess Control, Sweden) with a reactor volume of 500 mL. All tests were carried out in duplicate and last for 30 days.

To investigate the impacts of sulfate on the reaction rates and biodegradability in the anaerobic co-digestion of FW and WAS, two kinetic models were applied to fit the cumulative methane production data from the BMP tests. First, one substrate-based first-order kinetic model Eq. (1) was used[2], and the model parameters were calculated by minimizing the least square difference between the observed and predicted values.

$$B(t)=B_u\cdot(1-\exp(-k_{hyd}\cdot t)) \qquad (1)$$

Where, B(t) represents the cumulative methane production (L CH_4/kg VSadded); B_u is the ultimate biochemical methane potential (L CH_4/kg VS_{added}); k_{hyd} is the hydrolysis rate (1/d); and t is the length of the test duration (d).

3 Results and discussion

Methane production from the co-digestion of FW and WAS at different sulfate concentrations are shown in Fig. 1. The presence of sulfate at 200 and 300 mg S/L in the reactors resulted in a considerable drop in methane production. The nonlinear inhibition of sulfate or sulfide was observed and the underlying reason why methane production deteriorated at sulfate concentrations of 200–300 mg S/L or remained unaffected at 400 mg S/L is unclear at this stage. Sulfide production by sulfate reduction during the tests was monitored. The presence of sulfide can inhibit different microorganisms. This can be attributed to the diffusion of sulfide into the cell membrane and deactivation of native protein in the form of hydrogen sulfide. Moreover, there is a potential competition for electron donor between SRB and MA in the system, which can divert the electron flow from methane production to sulfate reduction. More research must be conducted to verify this observation. Although the addition of sulfate of 50 to 400 mg S/L did not improve the total methane production, over 80% of the maximum accumulated methane production was achieved within the first ten days by adding sulfate concentrations of 50 to 400 mg S/L, suggesting that the rate of methane production can be increased by the presence of sulfate. Sulfate at a proper concentration can be beneficial for methane production given that it accelerates the substrate degradation through the mediation of SRB serving as acetogens.

The simulated methane production curves using one-substrate model are illustrated in Fig. 2, which show agreement with the experimental results of methane production (R2>0.98 in all studied cases). The highest estimated values of B_u were obtained without sulfate addition (i.e. sulfate is 0 mg S/L) in the co-digestion of FW and WAS. There were slight decreases in B_u at the sulfate concentrations of 50, 100 and 400 mg S/L, whereas significant decreases were obtained at the sulfate concentrations of 200 and 300 mg S/L. Also, it is clear that the estimated values of k_{hyd} were significantly improved by 70% up to 144% at sulfate concentrations greater than 50 mg S/L. The hydrolysis rates of substrates increased with the presence of sulfate at different concentrations as shown by the one-substrate kinetic model. From a point of thermodynamic view, the presence of sulfate can stimulate sulfate reducing bacteria acting as acetogens to convert propionate to acetate, which provides an alternative metabolic pathway for methanogenesis.

In the presence of sulfate, propionate is first converted to acetate by a group of SRB. The produced acetate can be either directly used for acetotrophic methanogens or indirectly converted to hydrogen and CO_2 for hydrogenotrophic methanogens. Further research into microbial communities is deemed necessary to confirm the key functional microorganisms in the degradation pathways with the addition of sulfate. The proper addition of sulfate in the anaerobic co-digestion of FW and WAS can improve the hydrolysis rates of rapidly biodegradable substrates and accelerate the methane production. The kinetic analysis reveals the substantial increases in k_{hyd} with sulfate at different concentrations through the one-substrate model. The regulation of sulfate concentration in the anaerobic digester can be a potential strategy to optimize methane production with the assistance of SRB. However, identifying the substrate types and effective sulfate concentration control strategy are necessary to sustain the optimum productivity of the anaerobic digester.

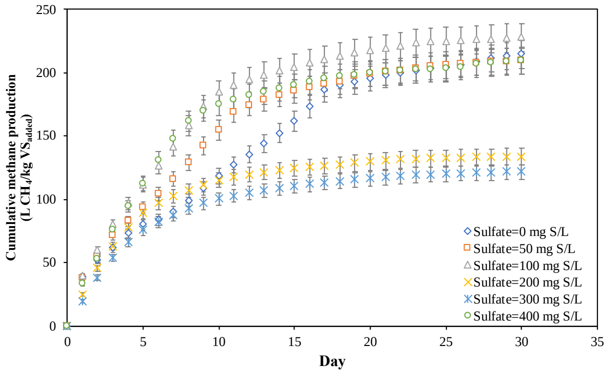

Fig. 1. Cumulative methane production from the co-digestion of FW and WAS with different sulfate concentrations (0, 50, 100, 200, 300, and 400 mg S/L).

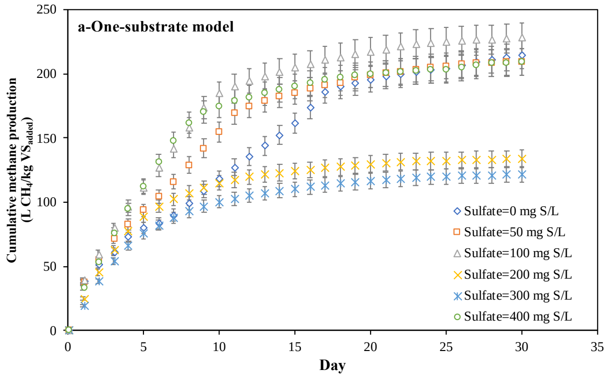

Fig. 2. Observed and predicted methane production (from FW and WAS co-digestion) in the BMP tests (the symbols represent the experimental measurements and the lines represent the model fits) using one-substrate model.

4 Conclusions

This study demonstrated that the presence of sulfate can accelerate the methane production by improving the hydrolysis rate, at sulfate concentrations of 50 to 400 mg S/L. The kinetic analysis reveals that sulfate at proper concentrations can increase the hydrolysis rates.

Reference

[1] Zan, F., Dai, J., Hong, Y., Wong, M., Jiang, F., Chen, G., 2018. The characteristics of household food waste in Hong Kong and their implications for sewage quality and energy recovery. Waste Manag. 74, 63–73.

[2] Rao, M.S., Singh, S.P., Singh, A. K., Sodha, M.S., 2000. Bioenergy conversion studies of the organic fraction of MSW: assessment of ultimate bioenergy production potential of municipal garbage. Appl. Energy 66, 75–87.

Trace metal element supplementation impact in methane fermentation of fish processing wastewater

○ Eli Hendrik SANJAYA[1,2*] and Yu-You LI[1]

[1] Department of Civil and Environmental Engineering, Tohoku University, 6-6-06 Aoba, Aramaki, Aoba-ku, Sendai, Miyagi, 980-8579, Japan.

[2] Department of Chemistry, State University of Malang (Universitas Negeri Malang), Jl. Semarang No. 5, Malang, East Java, 65145, Indonesia.

*E-mail: eli.hendrik.fmipa@um.ac.id

Abstract

Trace metal elements are an important and essential element needed for enzyme complex synthesize and also as growing factor. Fe, Ni, Co, Zn and Mo/W were reported as essential elements needed to form enzyme/cofactor in acetogenesis and methagonesis process. It is linear with the fact that in methabolic pathways, methanogenesis is one of the most enzymatic pathways with the metal-rich content. However, their optimum concentration in the anaerobic digestion system will be different for every reactor and substrate. The effect of trace metal elements in Fish processing wastewater (FPW) fermentation was studied in both batch experiment and self-agitated anaerobic baffled reactor (SA-ABR). Based on the four batch experiments, the three best performance of sole element addition were resulted from Ca^{2+}, Co^{2+}, and Fe^{2+} elements. On the other hand, the three best metal combinations were $Ca^{2+}+Mg^{2+}+Fe^{2+}+Co^{2+}+Ni^{2+}$, $Fe^{2+}+Ni^{2+}+Co^{2+}$, and $Ca^{2+}+Mg^{2+}$. Supplementing 15 mg/L Ca^{2+} on the SA-ABR could increase the performance significantly at OLR 3.115 gCOD/L/d. COD, protein, carbohydrates removal and gas production were growing up. Moreover, the VFA concentration was dropped from 4901.74 to 765.63 mg/L at OLR 3.115. The performance was quite stable at OLR 4.750 gCOD/L/d.

Keywords: trace element; methane fermentation; fish processing wastewater (FPW).

1 Introduction

As one method in organic waste treatment, produce energy, and offset the global warming all at once, anaerobic digestion has been used in most advanced countries and followed by developing countries [1]. Various reactors such as up-flow anaerobic sludge blanket reactor (UASB), completely stirred tank reactor (CSTR), anaerobic baffled reactor (ABR), membrane (MBR), etc. have been developed to treat solid and liquid biomass. Moreover, many researchers also innovated those reactors in order to improve the performance especially for highly methane production and organic removal efficiency. For instance, it was self-agitated anaerobic baffled reactor (SA-ABR) developed by Kobayashi and Li (2011).

The development and innovation of anaerobic digestion is so fast, however, it does not mean without any troubles and obstacles. Stability of reactor performance, removal efficiency, inhibition, and lack of several nutrients or elements are the most problem in the anaerobic digestion [3]–[5].

Many studies resulted that anaerobic process were not only requiring main macronutrients such as carbon (C), nitrogen (N), sulphur (S) and phosphorus (P), but also trace metal elements at relatively lower concentration [6]

Trace metals are an important and essential element needed for enzyme complex synthesize and also as the growing factor. Iron (Fe), nickel (Ni), cobalt (Co), zink (Zn) and molybdenum (Mo)/ wolfram (W) were reported as essential elements needed to form enzyme or cofactor in acetogenesis and methagonesis process [6].

On the other hand, related to the trace metal problem in anaerobic digestion, less trace elements in the reactor is one problem that sometimes cannot be avoided. Commonly this comes from the substrate characteristic itself or caused by the substrate pretreatment such as dilution. This research studied several trace metals supplementing impact to the methane fermentation of FPW in both batch and lab scale of SA-ABR experiments.

2 Materials and methods

Batch experiment did by using vial bottle 120mL with the working volume 80mL, sludge 2g VSS, fish wastewater as substrate was 8 mL at first and second round and 16 mL at third and fourth round. It was operated at temperature 35±1°C. Supplementing was various for sole and combination of metal ions. SA-ABR was operated started from OLR 3.115 gCOD/L/day. Sludge was taken from SA-ABR which was operated for methane fermentation of FPW during 460 days operation.

3 Results and discussion

Batch experiment result at the 1st round show that as initial the gas production in all vials were still very low (below 25mL accumulated in 9 days). The addition of Ca^{2+}, Mg^{2+}, $Ca^{2+}+Mg^{2+}$, Mn, and Fe has positive effect for anaerobic digestion of FPW with the strength of effect in order from high to low is Ca^{2+} to Fe^{2+}. At the 2nd round, the metals which resulted positive effect were little bit changed. These were Fe^{2+}, Co^{2+}, $Ca^{2+}+Mg^{2+}+Fe^{2+}+Co^{2+}+Ni^{2+}$, and Ca^{2+} with Fe^{2+} were the best one. At the 3rd and 4th round, the amount of substrate was multiplied into two times. The results at the 3rd round show that the combination of $Ca^{2+}+Mg^{2+}+Fe^{2+}+Co^{2+}+Ni^{2+}$ defeated Ca^{2+}, $Ca^{2+}+Mg^{2+}$, Co^{2+}, $Fe^{2+}+Co^{2+}+Ni^{2+}$, and Fe^{2+}. At the last round, the result was not so much different with the 3rd round result, with the order of strength in positive effect were Ca^{2+}+Mg^{2+}+Fe^{2+}+Co^{2+}+Ni^{2+}, Fe^{2+}+Co^{2+}+Ni^{2+}, Co^{2+}, Ca^{2+}, Ca^{2+}+Mg^{2+}, and Fe^{2+}.

Based on the all batch experiment, the three best performance of sole element addition were resulted from Ca, Co, and Fe elements. On the other hand, the three best metal combinations were Ca^{2+}+Mg^{2+}+Fe^{2+}+Co^{2+}+Ni^{2+}, Fe^{2+}+Co^{2+}+Ni^{2+}, and Ca^{2+}+Mg^{2+}.

Batch experiment result show that trace metal ion supplementation was not only resulting positive effect but also negative effect. Addition of Ca^{2+}, Co^{2+}, Fe^{2+}, and Mg^{2+} gave the positive effect. Surprisingly result was the the supplementing Ca^{2+} had an immediately impact, it could be seen that addition Ca^{2+} could improve the gas production and became the best at the 1st round defeated Fe^{2+} and Co^{2+}. On the other hand, addition Co^{2+} and Fe needed more time to get the best impact to escalate the gas production. Co^{2+} and Fe^{2+} could beat Ca^{2+} at the 2nd round. It also proved when the amount of substrate was multiplied into two times higher than at the 1st and 2nd round. At the 3rd round, Ca^{2+} came back defeated Co^{2+} and Fe^{2+}, but Co^{2+} addition could be higher than Fe^{2+} addition. On the other hand, at the 4th round, the effect of addition Fe was still below Ca^{2+} addition. It might be caused by the concentration of Fe^{2+} in the vial bottle was below the optimum condition.

The metal ion addition of sole Ni^{2+}, Zn^{2+} and Mn^{2+} did not have significant effect to the fermentation performance. Their gas productions were almost the same with the blank. However, supplementing Mo^{6+} could inhibit the anaerobic digestion. It can be seen in Fig.1, the gas production in the vial which was added Mo^{6+} was very low, even far below the blank. It was suggested that on the vial added Mo^{6+} had high ammonia concentration which could be inhibiting the anaerobic digestion process since the chemical in stock solution was $(NH4)_6Mo_7O_{24}\cdot 4H_2O$ which is in the water solution it can release NH_4^+.

Based on the batch experiment result, the semi continues SA-ABR was operated started from OLR 3.115 gCOD/L/d without supplementing any elements. On the day 63, both reactor and substrate were added 15 mg/L of Ca^{2+}. The performance was significantly increased. It can be seen in Table 1, COD, protein, carbohydrates removal and gas production were growing up. Moreover, the VFA concentration was dropped from 4901.74 to 765.63 mg/L. This performance was stable even at the higher OLR (4.750 gCOD/L/d).

Table 1. SA-ABR Performance in FPW treatment

OLR gCOD/L/d	3.115		4.75
Added Ca^{2+}	before	after	After
COD (%)	66.21	87.46	89.98
Protein (%)	55.22	79.44	85.80
Carbohydrate (%)	50.28	76.83	78.75
Gas Production (L/d)	11.01	14.57	21.4
Methane Composition (%)	76.32	74.32	74.17
TAN (mg/L)	5334.64	5334.64	5172.81
VFA (mg/L)	4901.74	765.63	527.95
pH	7.88	7.96	7.99
Alkalinity (mg/L)	12066.67	11077.78	10128.57

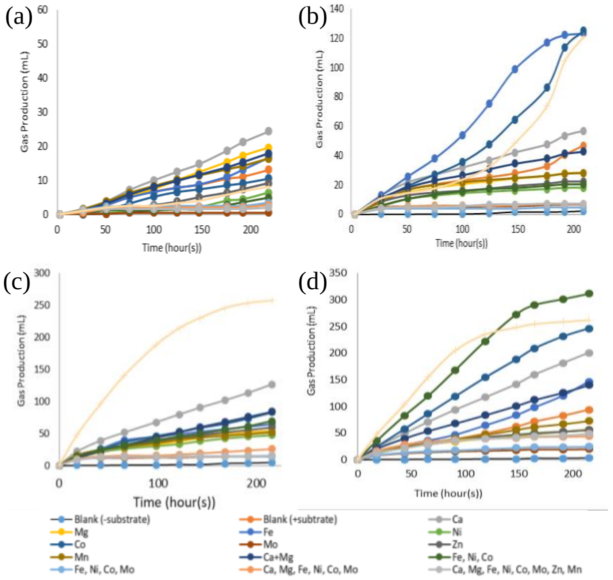

Fig. 1. Accumulation of Gas Production During 9 days Batch Experiment. (a) first round, (b) second round, (c) third round, and (d) fourth round.

4 Conclusions

Batch experiment resulted the three best performances of sole element addition were resulted from Ca^{2+}, Co^{2+}, and Fe^{2+} elements. On the other hand, the three best metal combinations were Ca^{2+}+Mg^{2+}+Fe^{2+}+Co^{2+}+Ni^{2+}, Fe^{2+}+Co^{2+}+Ni^{2+}, and Ca^{2+}+Mg^{2+}. Supplementing 15 mg/L Ca^{2+} on the SA-ABR could increase the performance significantly at OLR 3.115 gCOD/L/d. COD, protein, carbohydrates removal and gas production were growing up. Moreover, the VFA concentration was dropped from 4901.74 to 765.63 mg/L at OLR 3.115. The performance was quite stable at OLR 4.750 gCOD/L/d.

Reference

[1] H. Qiang, D.-L. Lang, and Y.-Y. Li, “High-solid mesophilic methane fermentation of food waste with an emphasis on Iron, Cobalt, and Nickel requirements,” *Bioresour. Technol.*, vol. 103, no. 1, pp. 21–27, Jan. 2012.

[2] T. Kobayashi and Y.-Y. Li, “Performance and characterization of a newly developed self-agitated anaerobic reactor with biological desulfurization,” *Bioresour. Technol.*, vol. 102, no. 10, pp. 5580–5588, May 2011.

[3] Y. Chen, J. J. Cheng, and K. S. Creamer, “Inhibition of anaerobic digestion process: A review,” *Bioresour. Technol.*, vol. 99, no. 10, pp. 4044–4064, Jul. 2008.

[4] F. G. Fermoso *et al.*, “Fate of Trace Metals in Anaerobic Digestion,” *Adv. Biochem. Eng. Biotechnol.*, vol. 151, pp. 171–195, 2015.

[5] M. Ye *et al.*, “Improving the stability and efficiency of anaerobic digestion of food waste using additives: A critical review,” *J. Clean. Prod.*, vol. 192, pp. 316–326, Aug. 2018.

[6] Y. Y. Choong, I. Norli, A. Z. Abdullah, and M. F. Yhaya, “Impacts of trace element supplementation on the performance of anaerobic digestion process: A critical review,” *Bioresour. Technol.*, vol. 209, pp. 369–379, Jun. 2016.

Experimental study on filtrate of thermal hydrolysis of sludge as an additional carbon source for denitrification

○Lu HAN[1,3], Yun HAN[1,2*] &Yuan GAO[1]
[1]School of Municipal and Environmental Engineering, Xi' an University of Architecture and Technology, Xi' an 710055, China.
[2]Key Laboratory of Northwest Water Resources, Environment and Ecology, Ministry of Education, Xi' an 710055,China.
[3]Department of Civil and Environment, Tohoku University, Miyagi 980-8579, Japan
*E-mail: hanyun@xauat. edu. cn.

Abstract

This study presents a strategy to improve the removal efficiency of nitrogen and phosphorus from municipal sewage by feeding sequencing batch reactor(SBR) with the filtrate of thermal hydrolysis of sludge(FTHS) as carbon sources. High solid sludge (solid content 10%) was subjected to thermal hydrolysis pretreatment at different temperatures (140°C, 170°C, 200°C, 230°C, 260°C) for 30 min. Through the analysis of the FTHS, the optimal temperature was determined to be 170°C. The biodegradability of the FTHS was also analyzed. The FTHS as an additional carbon source added to the low C/N ratio sewage. The chemical oxygen demand(COD), ammonia nitrogen(NH_4^+-N), phosphate of the low C/N ratio influent was 300 mg/L, 80 mg/L and 5 mg/L, respectively. In addition, the microbial communities in the activated sludge of the treatment system with carbon source was analyzed. This paper provides an effective way to solve the problem of insufficient organic carbon source in biological nitrogen and phosphorus removal of low C/N wastewater.

Keywords: Thermal hydrolysis of sludge; Filtrate; Additional carbon source; Low C/N ratio; SBR

1 Introduction

It is well known that exceeded discharge of nutrients(N and P) to nature water bodies usually causes eutrophication. At present, most wastewater treatment plants(WWTPs) use the biological method to remove the nitrogen and phosphorus. However, due to the shortage of carbon source in urban sewage, nitrogen and phosphorus in the effluent can not reach the preset standard simultaneously. WWTPs usually increase the influent dissolved chemical oxygen demand (SCOD) concentration by adding carbon source such as sodium acetate or methanol. This operation will result in a significant increase in the operating costs of the WWTPs.

After thermal hydrolysis, a large amount of insoluble organics in the high solid sludge was converted into soluble organics and transferred to the hydrolyzate. After the hydrolyzate was dehydrated, the filtrate contains a large amount of organics. At present, thermal hydrolyzate(TH) mainly focuses on dehydration and anaerobic digestion, and there are few studies on the recycling of carbon, nitrogen and phosphorus. If the FTHS is applied as a carbon source supplement for biological denitrification, the problem of insufficient carbon source can be solved. Moreover, the recycling of resources in the TH can be realized. This study provides a new idea for the efficient treatment of sludge and solves the problem of treatment and outlet of FTHS.

In this study, the SBR system was used to simulate anoxic/oxic(A/O) process. The influent of A/O process was low C/N ratio urban sewage. The feasibility of the FTHS as an additional carbon source and its difference with sodium acetate were analyzed.

2 Materials and methods

2.1 Test devices and operation mode

The thermal hydrolysis test device is an autoclave (KCF-5, Beijing Century Senlang). The effective volume is 5L. The working temperature is<350℃. The working pressure is <10MPa. During the test, 1.2L of sludge was added to the reactor and thermally hydrolyzed at the set temperature for 30 min. The hydrolyzate was stored in a refrigerator at 4°C for analysis. The effective volume of the SBR is 5.2L. The oxic stage used an air pump to charge the reactor with air. The anoxic stage is stirred by an agitator(JHS-1/60). The SBR were operated under same conditions with four cycles per day. Each cycle of the SBRs consisted of 5min of influent, 160min of anoxic, 160min of oxic, 30min of settling, 5min of effluent.

2.2 Sludge and sewage source

The thermal hydrolysis sludge was collected from a WWTP located in Xi`an, China. The WWTP used the A^2O process.The main physicochemical characteristics of the test sludge are as follows: pH of 7.01, total chemical oxygen demand(TCOD) of 96.3g/L, suspended chemical oxygen demand(SCOD) of 1.65g/L, suspended solids(SS) of 99.98 g/L, volatile suspended solids(VSS) of 67.99g/L.

The inoculated sludge of the SBR reactor was also collected from the WWTP. The physicochemical characteristics of the inoculated sludge are as follows: pH of 7.01, SS of 6.33 g/L, VSS of 3.81g/L.

The influent of the second stage SBR reactor was a dilution of the FTHS. The dilution factor is 100 times. The main physicochemical characteristics of the influent are as follows: pH of 7.00, COD of 508.71mg/L, biochemical oxygen demand (BOD_5) of 114.35mg/L, total nitrogen(TN) of 36.10mg/L, NH_4^+ -N of 13.41mg/L, total phosphorus(TP) of 7.55mg/L, phosphate of 7.33mg/L.

The influent of the third stage SBR reactor was low C/N ratio of municipal sewage. The COD, NH_4^+-N, phosphate was 300mg/L, 80mg/L and 5 mg/L, respectively.

2.3 Thermal hydrolysis pretreatment

The sludge were thermally hydrolyzed at temperatures of 140, 170, 200, 230, 260℃. The obtained TH was collected to measure total protein, total carbohydrate, TCOD, TN,and TP. And a certain amount of TH was centrifuged. The obtained solution was measure dissolved protein, dissolved carbohydrate, SCOD, dissolved TN, and dissolved TP in the filtrate.

2.4 Biodegradability of the FTHS

The SBR was employed in the current study. The influent of the SBR is the dilution of the FTHS.

2.5 Analysis methods

pH was measured by a pH meter(PHS-3C). DO was measured by a portable dissolved oxygen analyzer. COD, BOD_5, TN, NH_4^+-N, TP, Phosphate, protein and carbohydrate were measured by the standard methods.

3 Results and discussion

3.1Determination of optimal thermal hydrolysis temperature of high solid sludge

Table.1 showed the sludge characteristics before and after thermal hydrolysis pretreatment.

Table.1.Sludge characteristics before and after thermal hydrolysis pretreatment

Detection Indexes		Unit	Pretreatment sludge characteristics	Sludge characteristics after pretreatment at different temperatures				
				140℃	170℃	200℃	230℃	260℃
pH			7.01	5.91	5.53	5.44	6.58	6.69
COD	T	g/L	93.39	92.84	89.06	89.79	83.08	84.78
	S	g/L	1.65	35.73	40.71	40.37	40.08	38.31
BOD_5		g/L	0.03	11.16	12.33	11.43	11.56	10.74
TN	T	g/L	6.52	6.76	6.59	6.75	6.17	6.40
	S	g/L	0.17	3.78	3.56	3.98	4.22	4.70
NH_4^+-N		g/L	0.01	0.61	0.99	0.77	0.76	2.12
TP	T	g/L	2.49	2.40	2.37	2.35	2.29	2.41
	S	g/L	0.15	0.78	0.82	0.79	0.67	0.53
Protein	T	g/L	46.30	42.25	42.03	33.16	32.15	28.05
	S	g/L	0.14	18.80	20.56	11.68	16.87	14.93
Carbohy drate	T	g/L	15.49	15.43	14.73	10.81	6.06	6.59
	S	g/L	0.93	11.74	9.10	1.92	0.79	0.65
SS		g/L	99.97	62.43	55.77	53.36	52.48	50.78
VSS		g/L	67.99	37.39	40.20	28.55	26.23	22.25

Compared with the untreated sludge, the SCOD, BOD_5, TN, etc. in the FTHS were greatly increased. The thermal hydrolysis pretreatment made the organics enter the liquid phase from the solid phase. Then increasing the SCOD concentration of the FTHS. The SCOD in the FTHS reached a maximum at 170℃(40.71 ± 0.11 g/L). In addition, compared with other temperatures, the TN in the FTHS at 170℃ is the least (3.56 g/L). Therefore, the FTHS at 170℃ can ensure that the amount of TN introduced is reduced while introducing the carbon source.

3.2 Biodegradability test of the FTHS

Fig.1 shows the influent and effluent water quality of the SBR and removal rate of the pollutants. The average pH of the SBR influent is about 7.0, and the effluent pH is 7.14. The effluent concentration of COD is about 136.32 mg/L, and the average removal rate is 73.3%. The effluent concentration of NH_4^+-N is about 3.1 mg/L, and the average removal rate is 77.12%. The effluent concentration of TN is about 13.58 mg/L, and the removal efficiency is about 63.0%. The effluent concentration of TP is about 3.56 mg/L, and the removal efficiency is about 54.3%. The average effluent concentration of phosphate is 3.06 mg/L, and the removal efficiency is about 59.1%. It can be seen that the removal rate of organics and phosphorus by the anoxic/oxic process is very low. According to Huang Qingtao et al.(2017), the removal efficiency of COD, NH_4^+-N and phosphate was 90%, 91% and 82%, respectively by the anaerobic/oxic/anoxic(A/O/A) process. Therefore, in order to improve the removal efficiency of nitrogen and phosphorus, the next stage will use A/O/A process.

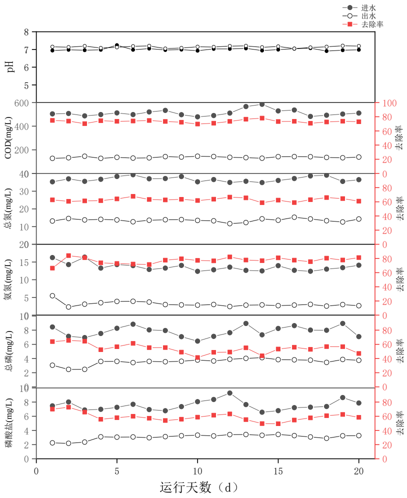

Fig.1.Influent and effluent water quality of the SBR and removal rate of pollutants

4 Conclusions

(1)The optimal temperature for the thermal hydrolysis of the sludge was determined to be 170℃.

(2)The removal rate of organics and phosphorus in the influent water is very low by the A/O process.

(3)In order to improve the removal efficiency of nitrogen and phosphorus, the next test will use the A/O/A process.

Reference

[1] HUANG, Q, T. et al, Influences of extra carbon sources on the removal of nitrogen and phosphate by AOA -SBR process, Industrial Water Treatment, 37(2017)26-29.

Co-digestion of cow and sheep manure: Performance evaluation and relative microbial activity

○ Yu Li[1*], Jing Zhao[1] & Gert-Jan Euverink[1]

Faculty of Science and Engineering, University of Groningen, Nijenborgh 4, 9747 AG Groningen, The Netherlands

*E-mail:yu.li@rug.nl

Abstract

This study investigated the feasibility of anaerobic co-digestion of cow manure (CM) with sheep manure (SM) at varying volatile solid (VS) ratios under mesophilic condition (37˚C) in batch system. Synergistic effects of co-digesting CM and SM were obtained in the batch experiment, with the most effective degradation of cellulose (56%) and hemicellulose (55%), and thus, the highest cumulative methane yield (210 mL/gVSadded) when CM and SM were mixed at a ratio of 1:3. Microbial analysis indicated that cellulase activities were observed in SM instead of CM. Enzymes involved in methane metabolism excreted by *Candidatus Cloacimonas* and *Methanocelleus* were found more variable in high SM addition (≥50%) compared with CM alone. Prolonged positive influence of SM on anaerobic digestion (AD) of CM in continuous experiment was observed as well. Results implied that compared with mono-digestion of CM, co-digestion of CM and SM contributed to the biodegradation of lignocellulosic compounds in CM and thus favoured the growth of *Candidatus Cloacimonas* and *Methanocelleus* to boost the methane yield.

Keywords: Anaerobic co-digestion; cow manure; sheep manure; microbial community.

1 Introduction

Intensive livestock farming has been increasingly developed over the last decades to satisfy our overwhelming demand of meat and dairy products. Despite the benefits these farms bring to human beings, these farms inevitably contribute to a considerable amount of manure waste annually. Anaerobic digestion (AD) is regarded as a cost-effective method for manure disposal because through this process, simultaneous waste treatment and production of biogas can be achieved.

Cow manure (CM) is served as the substrate in AD worldwide due to its high availability, which is similar in the Netherlands. However, the use of CM in AD generally leads to low production of biogas, probably due to a high percentage of lignocellulosic materials (cellulose, hemicellulose and lignin). One of the energy-consuming approaches to improve the degradation of lignocellulosic materials including management of the biogas process to ensure growth of microorganisms with efficient degradation capabilities. Hence, effort can be done by co-digesting CM with another substrate which either contains low lignocellulosic compounds or contains active fibre-degrading microbes.

Compared with CM, sheep manure (SM) is rarely mentioned as a substrate in AD. However, based on FAO’s data, SM can no longer be overlooked since its high amount. (1.3 billion tons annual). Unlike CM, SM is generally believed to contain lower lignocellulosic compounds. Another intriguing point for SM is that it may contain active microbes which could boost the hydrolysis step in AD. These merits of SM hint it could be a good idea to mix CM and SM in AD.

This study investigated the performance of co-digesting cow and sheep manures at the mesophilic condition. Both batch and continuous digestion were comprehensively evaluated. Microbial community diversity and community as well as key functional enzymes were determined to elucidate the mechanisms of biogas production during manure co-digestion.

2 Materials and methods

2.1 Subtrate and Inoculum

The CM and SM were taken from a farm. The inoculum was taken from the anaerobic digester in a wastewater treatment plant (WWTP). Before use, the inoculum was acclimated in an incubator at 37 ˚C for 10 days.

2.2 Reactor set-up and operation

The batch AD of CM and SM was carried out at five CM/SM ratios based on volatile solid (VS): 1:0, 0:1, 1:1, 3:1, 1:3. The experiments were performed in 500 mL glass bottles capped with butyl rubber stoppers with a working volume of 400 mL. For each treatment, an initial substrate concentration of 25 gVS/L was used. The substrate to inocula ratio (ISR) was set 0.5. After adding the proper amounts of substrate and inoculum, each bottle was filled with distilled water to achieve the working volume. The bottles were then flushed with pure nitrogen gas for 5 min to ensure anaerobic conditions. Finally the bottles were placed in a shaking incubator (140 rpm) at 37±1˚C.

A single stage laboratory-scale continuously stirred tank reactor (CSTR) with a working volume 2.4 L was established in this study. The experiment lasted 200 days. The reactor was fed once a day by a peristaltic pump. Hydrolytic retention time (HRT) was set 25 days based on batch experiment, and organic loading rate (OLR) was 0.5 g VS $L^{-1}d^{-1}$ from day 0 to day 50 and then adjusted to 1g VS $L^{-1}d^{-1}$ afterwards. The temperature was maintained at 37˚C±1˚C by a water bath. The speed of stirring was constantly set at 120rpm. The reactor was initiated with 2.4L same seed sludge coming from WWTP as used in batch experiment, followed by feeding once per day with CM alone or CM and SM.

2.3 Analytical methods

Biogas volume in batch test was recorded by displacing 75% saturated solution of sodium chloride, which was acidified to pH 2.0. Wet meter was used for continuous experiment.Biogas composition was analyzed by gas chromatography (C2V-200 Micro GC Thermal Scientific). The TS VS were measured based on National Renewable Energy Laboratory (NREL). For lignocellulosic compounds measurement, CM and SM were pre-treated according to the method in NREL. Extractive-free samples were subsequently used to determine the structural carbohydrates and lignin with a two-step acid hydrolysis method. Biological samples were fixed by adding ethanol to a final concentration of 50% (v/v) pending DNA and RNA extractions. The fixed samples were sent for sequence analysis using the BioProphyler approach. High-throughput sequencing was performed on an Illumina MiSeq. The reads, maximal 301 bp in size, were processed using in-house developed BioProphyler software. The sequence reads were first run through a quality filter named Trimmomatic, followed by a comparison to sequences stored in GenBank using the BLASTn algorithm. Reads were also compared to the nr database by using the RAPSEARCH2 algorithm. Identifications were ranked by tag abundance.

3 Results and discussion

The CMYs of co-digestion of CM and SM at mixing ratios of 3:1, 1:1, and 1:3 were 175, 200, and 210 mL/gVS$_{added}$, respectively (Fig.1(a)-(e)), which showed a higher methane yield of 11.6% -30.5% than mono-digestion of CM.

The removal of cellulose and hemicellulose in SM alone (56% and 54%, respectively) was significantly higher than that in CM (38% and 31% respectively). Moreover, the removal of cellulose and hemicelluloses in mixtures of CM and SM was significantly higher than CM alone, ranging from 43% to 56% and 38% to 55%, respectively.

Enzymes such as cellulase, glycogen phosphorylase and alpha-amylase are known for hydrolysing polysaccharides. On day 0, compared with CM, SM possessed more kinds of bacteria which could excrete those enzymes (Table 1(a)). Besides, it was observed uniquely in SM the activity of cellulase excreted by *Bacteroides sp*. and an uncultured bacteria species which is responsible for cellulose and/or hemi-cellulose degradation. In addition, glutamate decarboxylase found in SM was also supposed to be involved in cellulase pathway. Coenzyme-B sulfoethylthiotransferase excreted by *Methanothrix soehngenii* (*Methanosaeta*) accounted for 50% or even more in all CM, SM as well as their blends. In addition, Coenzyme-B sulfoethylthiotransferase excreted by *Methanoculleus sp*.was also active in high SM addition (CM:SM=1:1 and 1:3), reaching 31% and 29%. Additionly, phosphoglycerate dehydrogenase and phosphoserine transaminase excreted by bacteria *Candidatus Cloacimonas acidaminovorans* were observed in all CM and SM scenarios, indicating its functional role in methane metabolism. Overall, the addition of SM introduced active enzymes on lignocellulosic compounds degradation and enriched the methane metabolism pathway, especially at high SM addition.

The daily methane yield at steady stage (day50-day100) was 146 mL/g/d with the average methane yield 56%. When CM was half replaced by SM from day 101 on, significantly higher daily methane yield was observed (179mL/g/d), which was in line with batch results (p<0.05). Besides, methane content (61%) was also significantly higher than CM alone (56%), indicating the addition of SM could enhance both methane production and methane quality (p<0.05). From day 151 onwards the feeding was changed back to CM alone, the daily methane yield obtained was 159mL/g/d, increased by 10% compared with initial period.

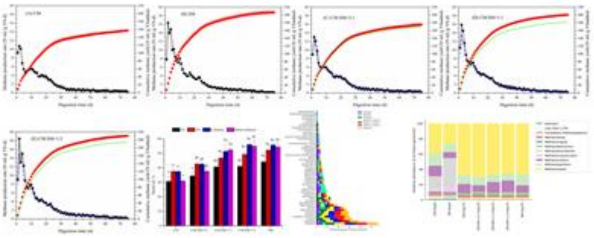

Key-enzymes	Function	Species	Treatment
Cellulase	Cellulose hemi-cellulose metabolism	Bacteroides sp.	10
		Uncultured Bacteria sp.	10
glutamate decarboxylase	Butanoate metabolism	Barnesiella intestinihominis	10
glycogen phosphorylase	Starch and sucrose metabolism	Clostridium sp. CAG 448	10
alpha-amylase	Starch and sucrose metabolism	bacterium P201	10
		Bacteroides sp. 43_108	10
		Alistipes	9;10
		Entamoeba dispar SAW760	9;10
		Entamoeba invadens IP	10
coenzyme-B sulfoethylthiotransferase	Methane metabolism	Methanoculleus sp.	134
		Methanoculleus marisnigri	1345
		Methanoculleus sp. MH98A	1234
		Methanoculleus thermophilus	12345
		Methanoculleus chikugoensis	23
		Methanoculleus sediminis	4
		Methanolinea tarda	125
		Methanobacterium petrolearium	13
		Methanobacterium formicicum	135
		Methanobacterium sp.	15
		Methanomassiliicoccus luminyensis	3
		Methanothrix soehngenii	12345
		Methanospirillum hungatei	1245
		Methanospirillum hungatei JF-1	5
tetrahydromethanopterin S-methyltransferase	Methane metabolism	Methanoculleus marisnigri	3
		Methanoculleus sp. MH98A	4
		Methanobacterium sp. SMA-27	5
		Methanothrix soehngenii	12
methylenetetrahydromethanopterin	Methane metabolism	Methanoculleus marisnigri	3

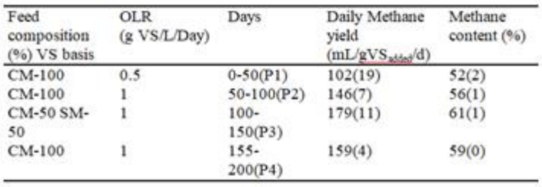

Feed composition (%) VS basis	OLR (g VS/L/Day)	Days	Daily Methane yield (mL/gVS$_{added}$/d)	Methane content (%)
CM-100	0.5	0-50(P1)	102(19)	52(2)
CM-100	1	50-100(P2)	146(7)	56(1)
CM-50 SM-50	1	100-150(P3)	179(11)	61(1)
CM-100	1	155-200(P4)	159(4)	59(0)

Fig.1. (a)-(e) CMYs of CM and SM as well as their blends; (f) TS VS cellulose and hemi-cellulose removals; (g) predominant bacteria genus; (h) predominant archaea genus; Table.1(a). Functional enzymes; Table.1(b). Performance of continuous reactor

4 Conclusions

(1) Synergistic effect of co-digesting of CM and SM was obtained.

(2) enzymes excreted by *Bacteroides*, *Candidatus Cloacimonas acidaminovorans* and *Methanoculleus* contributed to a higher lignocellulostic compounds degration and higher cumulative methane yield observed in co-digestion of CM and SM than CM alone.

(3) The prolonged positive influence of co-digesting SM with CM was also observed in long-term continuous AD, reflected by higher methane production (159 mL/g/d) when fed back to CM compared with feeding CM at the beginning (146mL/g/d)

Reference

[1] Yu et al Co-digestion of cow and sheep manure: Performance evaluation and relative microbial activity RENEW ENERG (accepted)

Anaerobic co-digestion of paper waste and sewage sludge: The effects of paper waste ratio

○Aijun ZHU[1]*, Yu Qin[1], Jing WU[1] & Yu-You Li[1,2]

[1] Department of Civil and Environmental Engineering, Graduate School of Engineering, Tohoku University, 6-6-06 Aoba, Aramaki-Aza, Aoba-Ku, Sendai, Miyagi 980-8579, Japan;

[2] Department of Frontier Science for Advanced Environment, Graduate School of Environmental Sciences, Tohoku University, 6-6-20 Aoba, Aramaki-Aza, Aoba-Ku, Sendai, Miyagi 980-8579

*E-mail: zhu.aijun.t4@dc.tohoku.ac.jp

Abstract

The aim of this study was to investigate the effects of different paper waste content in substrate on anaerobic digestion. The single-stage mesophilic anaerobic digestion in lab scale continuously stirred tank reactor (CSTR) systems fed semi-continuously with sewage sludge containing paper waste were studied to evaluated their performance, energy balance and reaction processes. The CSTR were operated under mesophilic(35±1oC) in order to enhance methanogenesis. The reactor was fed with substrate containing different mixture of paper waste to improve the methane production and organic removal efficiency. The mixing ratios of sewage sludge and paper waste was ranged from 4:0, 4:2,4:4,4:6 based on TS. The TS, VS, carbohydrate and COD removal efficiency was almost the same at different conditions and protein showed negative removal efficiency.

The experimental results showed the different substrate containing various mixture ratio of paper waste substrate has good performance at a hydraulic retention time (HRT) of 30 d.

Keywords: co-digestion; paper waste; sewage sludge; mesophilic anaerobic digestion

1. Introduction

Sewage sludge(SS), the byproduct of biological wastewater treatment processes, is expected to increase continuously in the next decade, due to increasing population connected to sewage networks, building new waste water treatment plants (WWTPs) and upgrading existing plants to meet the more stringent local effluent regulations. Treatment of sewage sludge via anaerobic digestion has been carried out widely, and the technology has recently received increased interest in many countries due to the renewable energy it can produce. However, despite its high carbohydrate content, the anaerobic treatment of sewage sludge is quite problematic due to its low bicarbonate alkalinity high COD concentration and tendency to rapid acidification. biodegradation, the low C/N ratio of sewage sludge also a serious problem to the anaerobic digestion. Although, an optimum C/N range in feedstock for the anaerobic digestion is still debatable in the literature, 20/1–30/1 is a most acceptable range.

One method to avoid excessive ammonia accumulation is to adjust low feedstock C/N ratios by adding high carbon content materials, thereby improving the digestion performance. Paper waste(PW) has a C/N ratio ranging from 173/1 to greater than 1000/1. Both wastes are produced in large quantities and in many places, and much research has focused on this particular issue. Co-digestion using paper waste and sewage sludge as substrate may enhance the performance of the anaerobic digestion (AD) due to better carbon and nutrients balance. That is, the use of a co-substrate that in most cases improves the biogas yields due to positive synergisms established in the digestion medium and the supply of missing nutrients by the co-digestion. For high-solids digestion of DS, the addition of FW not only improved system stability but also greatly enhanced volumetric biogas production.

System performances of co-digestion systems were mainly determined by the mixing ratios of DS and FW. Biogas production and volatile solids (VSs) reduction in digestion of the co-mixture of DS and FW increased linearly with higher ratios of FW. A kinetic model, which aimed to forecast the performance of co-digestion and to assist reactor design, was developed from long term semi continuous experiments.

2. Materials and Methods

2.1 Materials

The sewage sludge was consisted primary sludge of waste activity sludge 1:1(based on wet mass) from the Senen waste water treatment plant as substrate. The collected sewage sludge was ground and homogenized in a blender and stored at 4°C before feeding.

The paper waste was consisted of office paper, toilet paper and newspaper which are the largest amount of recycling paper in Japan. The ratio of three paper waste was 1 : 1 : 1 based on wet mass, cut by shredder before mixing with sewage sludge for feeding.

Seed sludge was from a mesophilic sewage sludge digester at the Sendai municipal sewage treatment plant located along Sendai, Japan.

2.2 Analytical methods

Daily biogas production is measured by wet gas meter, the composition of biogas (CH_4, CO_2 and N_2) were measured by a ShimadzuGC-8A gas chromatograph. and pH, COD, TS, ammonium nitrogen, alkalinity, VS and VSS were measured according to Standard Methods. Sludge samples were sampled twice a week from the digesters and the substrate tank to determine the total and soluble parameters. Samples

Table 1 the operating conditions in this study

		Run 1	Run 2	Run 3	Run 4
work volume		3 L			
Substrate	SS	4%	4%	4%	4%
	PW	0	2%	4%	6%
HRT（d）		30	30	30	30
Operation time（d）		1-120	121-182	183-253	254-315
OLR gVS/L/d		1.01	1.63	2.27	2.96

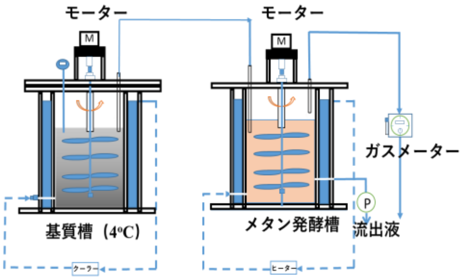

Fig. 1. Schematic diagram of the single-stage system used in this study for methane production

Table 2 the stability of the reactor

		Run 1	Run 2	Run 3	Run 4
biogas	(L/L/d)	0.51±0.24	0.75±0.11	1.38±0.13	1.68±0.24
	L/g-TS	0.38±0.05	0.37±0.02	0.53±0.02	0.53±0.05
	L/g-VS	0.46±0.06	0.42±0.02	0.60±0.02	0.61±0.06
N_2 content (%)		0.01±0.00	0.01±0.01	0.01±0.01	0.01±0.01
CO_2 content (%)		0.38±0.02	0.43±0.02	0.43±0.06	0.45±0.02
CH_4 content (%)		0.61±0.02	0.56±0.02	0.54±0.03	0.54±0.02
pH		7.16±0.05	7.14±0.08	7.11±0.09	7.10±0.06
alkalinity (g-$CaCO_3$ /L)		3.85±0.24	3.62±0.15	3.55±0.16	3.54±0.16
ammonia(g /L)		1.21±0.11	1.10±0.0	0.93±0.11	0.70±0.07
H_2S(ppm)		543.33±40.41	726.67±25.17	540±14.14	68±5.66

for the analysis of soluble items, such as soluble COD (SCOD), total ammonia nitrogen (TAN), VFAs and alkalinity, were centrifuged at 8,000 rpm for 15 min and then filtered with 0.45 μm filters before they were analyzed. A GC, equipped with a flame ionization detector ((GC-FID, Shimadzu GC-14B) and a DB-WAXetr column, was utilized to detect VFAs and ethanol. A 0.5 mL filtrate was collected in a 1.5 mL GC vial, and 0.5 mL 0.1 mol/L HCl solution was also added to achieve an acidic pH.

2.3 Reactors start-up and operation

Experiments were carried out in a single-stage continuous anaerobic process. On the first day of the experiments, 3.0 L seed sludge was added to the reactor, which was operated semi-continuously (twice-a day draw-off and feeding). The OLR was increased stepwise before normal performances could be achieved at designed paper waste mixture ratio. The mixing ratios based on TS substrate for each reactor were shown in Table 1. As the mixing ratios based on TS were accurately controlled, reactor was operated for four different paper mixture ratio.

The continuous operation of the reactor started at HRT of 30d. Sludge samples were sampled twice a week from reactors under continuous stirring conditions and analysed, for monitoring each reactors performance. Experiments were conducted successively to determine the optimum and maximum paper waste ratio for methane production. Organic loading rate (OLR) was increased by increasing the paper waste ratio. The reactor was operated at different feeding substrate of paper waste and food waste. The tested stability and gas production in the system are summarized in Table 2.

3.Results and Discussion

In mono high-solids anaerobic digestion of sewage sludge, ammonia concentration was the highest in all the condition, reaching 1.2 g/L. Cause of the low OLR(1.01 gVS/L/d), the reactor was running stable. With the paper waste addition, despite of OLR had increased，the reactor was running stable until the PW content reaching 8%TS.

The pH，alkalinity, ammonia concentration were decreased with the paper waste increasing, maintained stably under the steady stage. The experimental results about organic removal efficiency obtained at steady-state with the various PW content ranged 0% to 6%. The TS, VS, carbohydrate and COD removal efficiency was almost the same in different conditions. The maximum organic removal rate was achieved for TS(61.3±1.8%), VS(71.5±1.3%), carbohydrate (82.78±8.7%) and COD (85.9±5.3%). Meanwhile, the protein showed negative removal efficieny during the all periods. The biogas production also increased with the OLR increased. However, the methane content was decreased with the paper waste addition, cause of the carbonhydrate content increasing.

In the mesophilic fermentation, stable methane fermentation in high organic loading rate utilizing mixture of sewage sludge and paper waste was possible at OLR 2.96 gVS/L/d. And the mixing ratio of paper was found to have an important role in the whole process. The processing was operating stably if the paper ratio was less than 8% TS.

Manifold Analysis of Pacific Islands Climate Data

○ Ming-Che HU[1*], Yi-Hsuan Shih[1], Tai-Yi Liu[1]
[1]Department of Bioenvironmental Systems Engineering, National Taiwan University, Taipei, Taiwan.
*E-mail: mchu@ntu.edu.tw

Abstract

Dimensional reduction is an important issue while dealing with complex datasets. Traditional methods, such as principal component analysis (PCA) or multidimensional scaling (MDS), are usually based on Euclidian distance. However, this may underestimate the true distance between data points while there exists a curved structure of data. In order to solve the problem above, nonlinear dimensional reduction methods based on manifold learning, such as isometric feature mapping (Isomap) or locally linear embedding (LLE), are proposed. In this study, Isomap is applied to help us understand the structure of climate data in the Pacific Islands. In Isomap, the neighborhood graph is constructed based on the original distance. Next, geodesic distances is approximated by the shortest path calculated by using Dijkstra's algorithm. Finally, the geodesic distance matrix is imported into multidimensional scaling (MDS) to create a two-dimension map representing their dissimilarities in a higher dimension. Results have shown that the first Isomap dimension has a relationship with latitude. The sensitive analysis of variables has shown that though some countries are spatially close, their temperature or rainfall distance are much farther. Also, we can observe the change of data structure along time through this research.

Keywords: Multidimensional scaling (MDS); Nonlinear dimensionality reduction; Manifold learning; Isometric feature mapping (Isomap), Pacific islands climate data

1 Introduction

The analysis of the temporal and spatial pattern of hydrological data has always been a concerned topic, especially under the deteriorating situation of climate change, where extreme weather events have caused changes in distribution of rainfall and temperature. If we can understand these trends, it will be quite helpful for us to make strategy or plan policies of adjustment or adaptation to climate change.

In this study, Section 2 introduces the methodology used in this, including theory of the linear dimension reduction method MDS, details of Isomap, and the method, Procrustes analysis, applied to compare configurations. Section 3 describes the the results of this research, and finally this work will be concluded in Section 4 and some future directions will be point out.

2 Methods

In this study, we use Isomap to help us understand the structure of climate data in Pacific islands. Isomap is a nonlinear method consisting two parts, one is to calculate the geodesic distance on manifold, and second is to map the geodesic distance into a low dimension space remaining the global structure. Hence, we will first introduce the linear dimension reduction method, MDS. Next, how the geodesic distances are calculated will be presented. Finally, we will apply a method of comparing configurations.

Multidimensional scaling (MDS) is a linear dimension reduction method widely used in sociology, marketing and psychology. The purpose of MDS is to build a lower dimension space maintaining the dissimilarities between data. In some cases, we can get similar results using either MDS or Principal component analysis (PCA), however, the difference between two methods is that the input of PCA is linear combinations of the dataset, MDS only needs the distance matrix. When the properties of data are quantitative, metric MDS can be used. Classical MDS, one of the metric MDS is introduced in this study.

3 Results and Discussion

In this part of research, we will observe how the climate data structure varies under different ratios. Different kinds of distance matrices, including spatial, rainfall and temperature distance are displayed. In each figure, the darker the grid the larger the distance between countries. In order to compare different kinds of distance, every matrix is scaled from zero to one.

Figures show the results in which only rainfall or temperature data is considered. The figure illustrates how the stress value changes with the embedding dimension p in both cases . From the figure, we can observe that it is not inappropriate to set the embedding dimension as two. The embedding coordinates are plotted, and the first and second dimension values are listed. Since it is not straight forward to observe the relationship between countries, the dendrogram of the 24 countries are thus listed. In the dendrogram, the hierarchical relationship between objects is shown in the diagram. Dendrogram can be considered as a summary of the distance matrix, the height of the dendrogram indicates the order in which the clusters were joined.

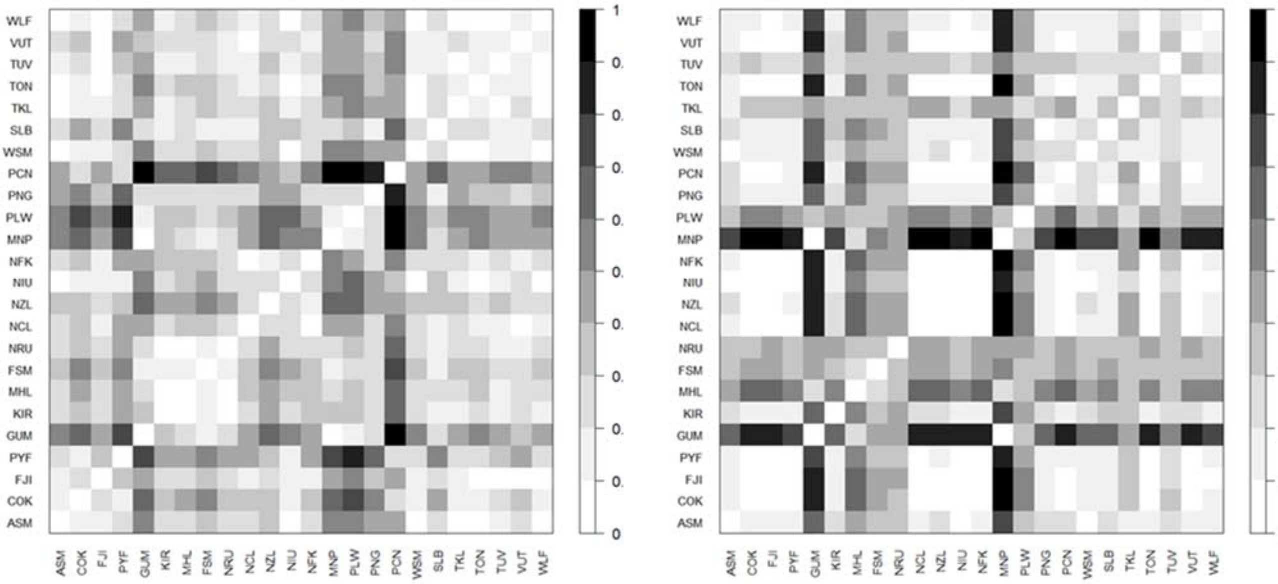

(a)

(c)

Fig. 1. Scaled correlation of islands (a) Geographic distance (b) Rainfall distance (c) Temperature

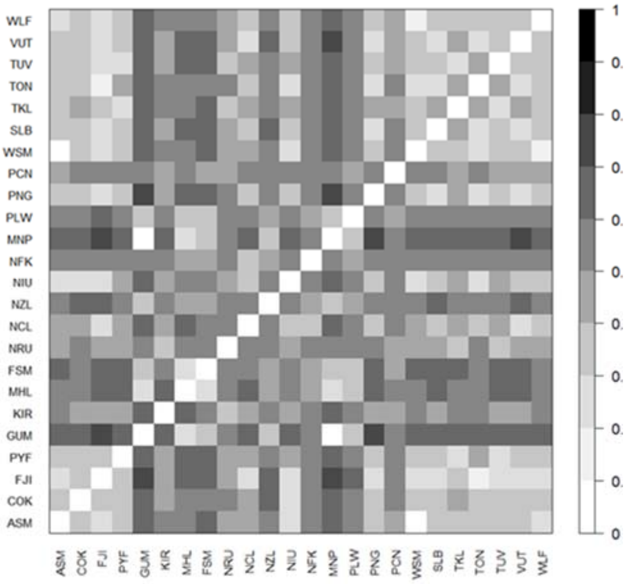

(b)

4 Conclusions

In this research, the embedding dimension p is set to be 2. From the result, we can find out that at least 70% of variation can be explained by the first two Isomap dimension.

By projecting the first Isomap dimension on the map, we can observe that the structure of both rainfall and temperature have relationship to latitude. The values will first decrease then increase from north to south Pacific in rainfall cases, however, the values just decrease in temperature cases.

By applying Procrustes analysis, we can compare different configurations. In the sensitive analysis of variables, we can conclude that for some countries, they may be short in the spatial distance, however the temperature or rainfall distance may be much farther. In the other part, we can observe how the climate data structure varies under climate change.

The distance of temperature and rainfall in this research is defined as one half of the Pearson distance, however, this is just one of the method to calculate dissimilarity. In the future, it is possible to see how the structure of the climate data structure will perform under different definition of distance.

In this research, we only considered temperature and rainfall. Besides the two data, more variables can be analyzed, such as wind speed, frequency of typhoons. In addition, we may focus on some species, specified on the characteristic of their favorable habitat, or concentrate on other issues.

This research applies a nonlinear dimensional reduction method based on manifold learning, here we present the low dimension embedding of climate data. In the future, we may combine the concept of network theory, topology or group theory, and build a temporal spatial prediction model based on manifold learning. The prediction of the hydrological changes in the Pacific Islands can be a reference for the decision-making on disaster adaptation or water resource distribution.

A preliminary study on development flood early warning system in Southeast Sulawesi Province

○ N. Fajar JANURIYADI[1*]
[1]Department of Civil Engineering, Pertamina University, Jakarta 12220, Indonesia.
[*]E-mail: nurul.fj@universitaspertamina.ac.id.

Abstract

Flood early warning system (FEWS) is one of the alternatives for reducing flood risk, which can allow people to prepare for flooding and to protect assets and property. Lacking information is one of the obstacles to develop a flood early warning system. The study aims to obtain the information of 2019 flood inundation extents and to find the appropriate rainfall stations number. The multi-temporal Sentinel-1A images were employed to identify the flood inundation extents while kriging with external drift (KED) used to find the appropriate rainfall station numbers. The study found that the inundation areas of the 2019 flood event estimated 49.9 km^2, while the required additional rainfall stations in the watershed are 8 stations. The results of this study are expected being used as the basic information to develop FEWS.

Keywords: FEWS; Sentinel-1A; KED.

1 Introduction

Flooding is one of the major natural disasters that make suffer the human being life. In 2018, there were 127 flood events of 315 climate-related and geophysical disaster events recorded in the EM-DAT, over 34 million people were affected by flooding [1]. In Indonesia, flooding contributed 26 % of natural disaster events that occurred in 2018, with the affected people over 470 thousand or 78 % of total affected people due to natural disasters. [2]. The latest flood event occurred at the beginning of June 2019 in Southeast Sulawesi Province (SSP). The flood event is one of the biggest floods in SSP, which inundated three regencies. The flood event has shown the destructive impact that flooding can have on people and property. More than 1500 houses inundated and 8000 people become refugees. Furthermore, many people isolated for a few days due to no sufficient time that allowing people to be evacuated from areas at risk, and to move vehicles and personal assets to safety.

Flood early warning system (FEWS) could be one of the alternatives to reduce the flood risk. FWES could provide the lead time to reduce the fatalities risk and to allow people to prepare for flooding and to protect assets and property. Flood prevention actions may also be taken to reduce flooding; for example, by operating river control structures and installing temporary barriers. FEWS is expected to provide the information location, time and magnitude of the flood, the information of predicted exposures both people and properties, and the information on how to respond effectively [3]. This project focuses on providing the information on location, time and magnitude of the flood and the information of predicted exposures, by developing a flood forecasting model. Lasolo river selected as the study site, because it is one of the rivers that contributed to the flood in SSP. The first step of this project is obtaining the information related to the latest flood event. One of the obstacles to the project is lacking data. Therefore, we used some approach to obtain the data, for example, flood inundation areas of flood derived from Sentinel-1A dataset. This paper shows the flood inundation areas obtained from the Sentinel-1A dataset and the information of rain gauge network that design using kriging external drift method.

2 Data and Methodology

2.1 Data

The Sentinel-1A dataset provided from the European Space Agency (ESA), which performing C-band synthetic aperture radar imaging to acquire imagery regardless of the weather. Four images of Sentinel-1A IW GRDH (Ground Range Detected in High resolution) are employed to identify the flood inundation in SSP. One dataset was acquired three months before the flood event (March 3rd,2019), while the other datasets were acquired during the flood event (May 28th, June 9th, and June 21st, 2019).

The information rainfall stations were collected to identify whether the numbers and location of the stations sufficient or not. Seven rainfall stations are located in the Lasolo watershed as shown in Fig. 2 (red dots).

2.2 Inundation Area Identification

This study used the Sentinel-1A dataset to identify the flood inundation extents. The sentinel-1A images include pre- and during the flood event. The pre-processing of the images is the removal of speckle noises. The speckle noises removal was done using a median filter of window size 3*3. The second step is image processing, the water areas, and non-water areas are separated from the Sentinel-1A images. Subsequently, the separated images are compared before and during flood events [4].

2.3 Kriging with External Drift

An approach to add external information in the interpolation technique is kriging with external drift (KED). Some studies also used this method to interpolate the rainfall data [5]–[7]. This study uses the digital elevation model as additional information. In the case of KED, predictions at new locations are estimated using Eq. 1 and 2:

$$\hat{z}_{KED} = \sum_{i=1}^{n} w_i^{KED}(s_0) \cdot z(s_i) \qquad (1)$$

$$\sum_{i=1}^{n} w_i^{KED}(s_0).\, q_k(s_i) = q_k(s_0); \qquad k = 1, \dots, p \qquad (2)$$

Where z is the target variable, q_k are the predictor variables i.e. values at a new location (s_0), p is the number of predictors. The variance of predictor error is estimated using Eq. 3.

$$\sigma_{KED}^2(s_0) = (C_0 + C_1) - \boldsymbol{c}_{\mathbf{0}}^{KED\mathbf{T}} \cdot \lambda_{\mathbf{0}}^{KED} \qquad (3)$$

Where σ_{KED}^2 is KED variance, $\lambda_{\mathbf{0}}^{KED}$ is the vector of solved weights and $\boldsymbol{c}_{\mathbf{0}}^{KED}$ is the extended vector of covariances at the new location. The square root of the kriging variance, also named as kriging standard error (KSE), is used as a gauge network evaluation factor that can reflect the performance of optimal gauge combination [8].

3 Results and Discussion

The comparison of Sentinel-1A images before and during the flood event shown in Fig.1. The figure shows the water body increase during the flood event. The water body areas slightly increase on May 28th, which indicates the flood began to inundate several areas around the Lasolo river. Furthermore, the image on June 9th shows a significant increase in the water body areas in Lasolo River, which indicates the peak of flood occurred. On June 21st, the image shows water body areas decrease, which identifies the flood began to recede. Based on the June 9th image, the total areas of flood inundation was approximately 49.9 km^2. Even though this study succeeds to identify the flood inundation extents, the distribution of flood depths is not identified yet. Also, adding the image data from the other dataset (e.g. Sentinel-1B) required to improve the information of flood inundation extents.

Fig. 2 shows the KED result of average annual rainfall in Lasolo watershed and the kriging standard error. Fig. 2a and Fig.2b show the KED result and KSE values for the existing stations. The figure shows that the high KSE values in the north part or upstream region of watershed, which indicates those areas require additional rainfall stations. This study recommends adding eight additional stations on the upstream region. The additional stations determined based on the highest KSE values location. Fig. 2c and Fig. 2d show the KED result and KSE values after adding the stations. The new KSE values are lower compared to before adding the stations, which indicates adding new stations could reduce the prediction error on rainfall interpolation.

As explained above, this paper is the introduction step of the project of the development flood early warning system in SSP. Additional data analysis is required to obtain more accurate results before developing the flood forecasting model. The next steps of this project are adding the image data from the other sources and analyzing the distribution of flood inundation depth. Also, the project will generate the land cover map from historical satellite images data, which can be used as the input parameters in the flood forecasting model.

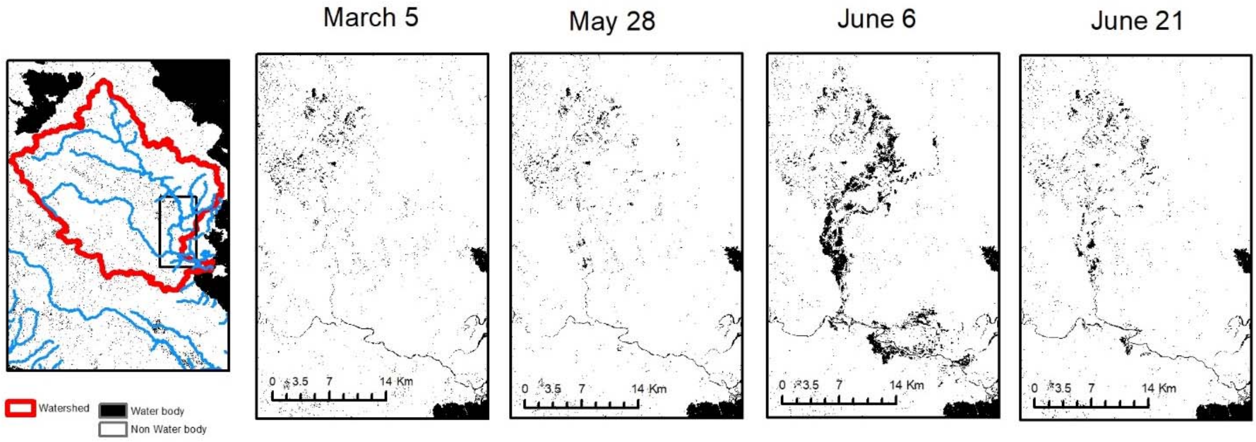

Fig. 1 Comparison of sentinel-1A images before and during flood event

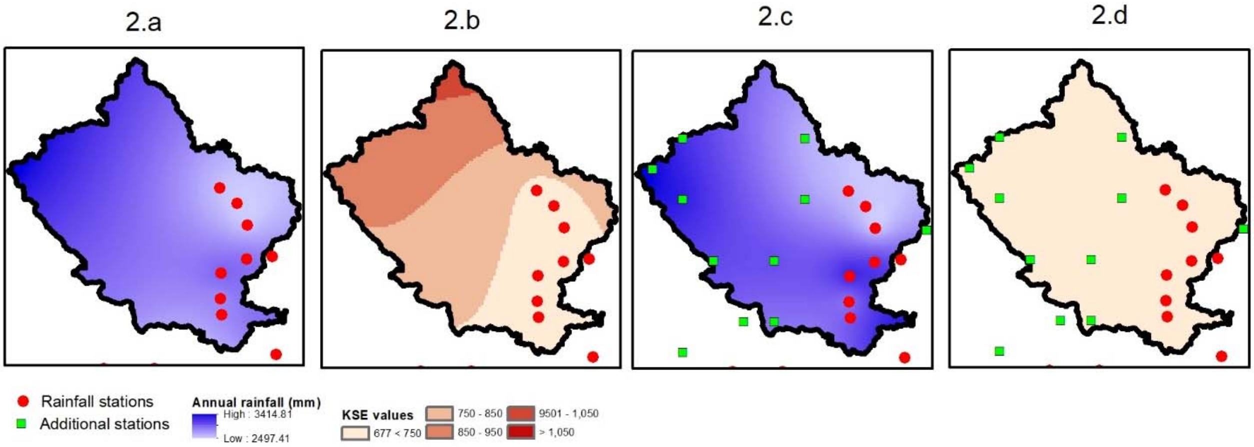

Fig. 2 Annual average rainfall and kriging standard error before and after adding the rainfall stations

4 Conclusions

This paper presented a preliminary study on the development of a flood early warning system, which consists of the detection of flood inundation extents and estimation of the appropriate numbers of rainfall stations. The results show the flood inundation areas of the 2019 flood event estimated 49.9 km^2, which is detected by the Sentinel-1A image on June 9th. The study also found that the inappropriate existing rainfall stations number in the watershed, particularly in the upstream region. Eight new rainfall stations should be added in the watershed for obtaining more reliable rainfall interpolation. The results of this study are expected being used as the basic information to develop the flood forecasting model.

Reference

[1] CRED, "Natural Disasters 2018: An opportunity to prepare," CRED, Brussels, 2019.
[2] BNPB, "Natural disaster in 2018," 2019. [Online]. Available: https://bnpb.cloud/dibi/laporan5. [Accessed: 10-Oct-2019].
[3] K. Sene, *Flood warning, forecasting and emergency response*. New York: Springer, 2008.
[4] N. Anusha and B. Bharathi, "Flood detection and flood mapping using multi-temporal synthetic aperture radar and optical data," *Egypt. J. Remote Sens. Space Sci.*, p. S1110982318303041, Feb. 2019.
[5] E. Rabiei and U. Haberlandt, "Applying bias correction for merging rain gauge and radar data," *J. Hydrol.*, vol. 522, pp. 544–557, Mar. 2015.
[6] A. M. J.-C. Wadoux, D. J. Brus, M. A. Rico-Ramirez, and G. B. M. Heuvelink, "Sampling design optimisation for rainfall prediction using a non-stationary geostatistical model," *Adv. Water Resour.*, vol. 107, pp. 126–138, Sep. 2017.
[7] A. Verworn and U. Haberlandt, "Spatial interpolation of hourly rainfall – effect of additional information, variogram inference and storm properties," *Hydrol. Earth Syst. Sci.*, vol. 15, no. 2, pp. 569–584, Feb. 2011.
[8] P. Xu *et al.*, "A kriging and entropy-based approach to raingauge network design," *Environ. Res.*, vol. 161, pp. 61–75, Feb. 2018.

Spatial Representativity of AMeDAS Gauge Rainfall over Radar/Rain Gauge-Analysed Precipitation

○ Masafumi Yamada
[1]Disaster Prevention Research Institute, Kyoto University, Uji 611-0011, Japan.
*E-mail: yamada.m.hydra@gmail.com.

Abstract

In the studies of climate change impact, ensemble climate datasets, e.g. d4PDF [1], are commonly used to know the probabilistic aspects of these impacts [2]. These ensemble datasets inevitably include the model-output biases, and in order to overcome these weak points, various bias correction methods have been developed. For Japan area, Watanabe et al. [3] proposed the bias correction method of d4PDF precipitation, using long-term rain gauge observation data, and confirmed its performance.

Keywords: d4PDF; AMeDAS; climate change.

1 Introduction

In order to use the point-based rain gauge data, whether it is from actual observation or from bias corrected data, for the analyses taking the 2-D precipitation data as input (e.g. runoff analysis), it is needed to spatially interpolate the multi-point rain gauge data. The simplest way is the Thiessen polygon: dividing the plain into some regions for that within each region all cells have the same nearest rain gauge, and this method is still common in runoff analysis [2]. Therefore, the spatial representativity of each rain gauge data over the region covered by that rain gauge is crucial for the reliability of the analyses with the rain gauge data as an input. So far, many researches have discussed the effect of input data on the outcome of runoff analysis [4]. However, as far as the authors know, the simple comparative study between the point-based rain gauge data and spatial precipitation data, focusing on the spatial representativity of the rain gauge, has not been undertaken. This study aims to examine how the AMeDAS gauge rainfall data, the most common rain gauge dataset in Japan, is spatially representative over the 2D precipitation dataset, Radar/Rain gauge-Analysed Precipitation (hereafter R/A), and also to quantify the associated biases.

AMeDAS, acronym of "Automated Meteorological Data Acquisition System", is a dense network of climate data observation points, managed by Japan Meteorological Agency (JMA). In September 2019, there are around 1300 AMeDAS point all over Japan, and each point covers approximately 17km grid area. We collected the nationwide AMeDAS data from 1988 to 2018 as one of the inputs of our research.

On the other hand, R/A is a reanalysis dataset issued by Japan Meteorology Agency (JMA) from April 1988, based on the AMeDAS rain gauge measurement, and MLIT (Ministry of Land, Infrastructure, Transport and Tourism) and JMA radar observation. The R/A is developed for the forecast and prevention of disasters triggered by heavy rainfalls like landslides and flashfloods, and it is now used as the basic input data for various sort of disaster prevention calculations, including the flood risk prediction and heavy rainfall warning. Despite some reports pointing out the over-estimation trend of R/A dataset compared to the rain gauge data [5], R/A is widely accepted as the basic dataset of rainfall in Japan. We use R/A as the other input of our research. The spatial resolution of R/A is not consistent over time: ca. 5km from April 1988 to March 2001, ca. 2.5km from April 2001 to December 2005, and ca. 1km from January 2006 to December 2018. In order to assure the data recording period enough long to do the statistical analysis, we upscaled the R/A after April 2001 so that all data have ca. 5km spatial resolution [6]. The coverage period of 5km R/A data is from 1998 April to 2018 December, around 31 years. In addition to that, we set the period from January 2006 to December 2018, 14 years, also as the research target with the finest resolution of 1km.

As the coverage area of each AMeDAS rain gauge point, we set the 20km*20km grid around each AMeDAS point. Each covering area contains 16 grids of 5km resolution R/A, or 400 grids of 1km resolution R/A. In order to quantify the spatial representativity of rain gauge data to R/A, we carried out two analyses below:

1) quantify the distribution of the ratio of AMeDAS rain gauge data and the R/A precipitation of each cell in the area, for each section of AMeDAS rain gauge data, and

2) for each rainfall event, defined by at least 24 hours non-precipitation period, quantify the difference of area average total precipitation amount between AMeDAS and R/A with two different resolution.

Reference

[1] Mizuta, R. and co-authors. Over 5000 years of ensemble future climate simulations by 60 km global and 20 km regional atmospheric models. Bull. Amer. Meteor. Soc., pp.1383-1398, 2017.

[2] Abe, S., Watanabe, S., Yamada, M., Kotsuki, S., Watanuki, A. Impact of observed rainfall and pattern of sea surface temperature on flood analysis using massive climate prediction data. J. of Japan Soc. of Civil Eng, Series B1, in press. (in Jpn with Eng abstract)

[3] Watanabe, S., Nakamura, M., and Utsumi, N. The development of bias corrected hourly precipitation dataset for AMeDAS stations based on the projections from d4PDF. J. of Japan Soc. of Civil Engineers, Series B1, Vol.75, pp.I_1399-I_1404, 2018. (in Jpn with Eng abstract)

[4] Fekete, B. M. and Vörösmarty, C. J. Uncertainties in Precipitation and Their Impacts on Runoff Estimates. J. of Climate, Vol. 17, pp.294-304, 2003.

[5] Ishizaki, H. and Matsuyama, H. Distribution of the Annual Precipitation Ratio of Radar/Rain gauge-Analyzed

Precipitation to AMeDAS across Japan. SOLA, Vol.14, pp.192-196, 2018.

[6] Urita S., Saito, H., and Matsuyama, H. Temporal and spatial discontinuity of Radar/Rain gauge-Analysed Precipitation that appeared in relation to the modification of its spatial resolution, Hydrological Research Letters, Vol.5, pp. 37-41, 2011.

Estimating Irrigated Area through a Combined Use of MODIS and Land Surface Model in the Amu Darya Delta

○ Jacqueline Muthoni MBUGUA[1*], Yoshiya TOUGE[1] & So Kazama[1]
[1]Department of Civil and Environmental Engineering, Tohoku University, Miyagi 980-8579, Japan.
[*]E-mail: mbugua.jacqueline.muthoni.s8@dc.tohoku.ac.jp.

Abstract

Secondary salinization coupled with the frequent droughts causes the irrigation area to constantly change for farmers to adapt to cropping environmental problems and the changing annual climate in this region. However, obtaining an accurate report of the actual distribution of the irrigated area has proven to be difficult even to the local government and agricultural institutes. This study aims to assess the potential of using Land Surface Temperature (LST) from MODIS and a Land Surface Model (LSM) to detect annual changes in irrigated area. 3 indices were developed using LST by MODIS and LSM based on the concept of heat capacity difference between water and soil. The LSM provides LST for ideal conditions while MODIS provides the actual LST. A combination of the two enables the elimination of external influence on LST such as rainfall and geological variations which may impact on the LST. A distributed map of all the 3 indices shows the potential of LST in detecting drought. The irrigation fraction during a drought year was observed to be lower as compared to that of a normal year. This was true especially further away from the water source due to water scarcity.

Keywords: Irrigation; MODIS; LSM; Drought; Amu Darya delta.

1 Introduction

Irrigation water is an important part of the hydrology cycle and has thus been included in recently developed hydrological models both at the basin and global scales. These hydrological models are however based on the concept of fixed land use. The variability of irrigated area is an important component to be considered as it impacts the heat and water balance in the basin. Central Asia is a region where the land use changes dynamically. It is difficult to obtain an accurate estimation of the irrigated area because collecting data in a wide region is difficult especially in developing countries.

Since global land cover products such as the Global Land Cover Characterization (GLCC) map are static, the land cover classification provided does not reflect land cover variability which may be caused by a reduction of the irrigated area especially during drought or dry years. In this case, the non-irrigated area may incorrectly be classified as irrigated.

In addition, some of the native plants in this study area have long roots of between 10 to 30m enabling the plants to flourish. This makes it difficult to identify the area of land under irrigation using NDVI. Irrigated area in statistical databases such as FAO AQUASTAT is mentioned as 'area equipped for irrigation'. This is the definition of irrigable land and not the actual irrigated area

In this research, a combination of satellite analysis and Land Surface Modelling approach was performed to detect the irrigated area. A global dataset developed by Doll (2002) showing the percentage of area equipped for irrigation was used to identify the irrigable area in the basin. The LST obtained from both MODIS and a LSM considering conditions with and without irrigation was used to detect the irrigation effect on heat balance in the basin. The objective of this study is to assess the annual changes in the irrigated area so as to facilitate an understanding of changing water demand through climatic variables.

2 Methodology

Since water has a higher heat capacity than soil, soil with high soil moisture does not immediately respond to temperature changes. Moreover, increased evapotranspiration as a result of the presence of irrigation water further reduces the LST in the day time. LST by the satellite represents the actual conditions on the ground while the LSM was used to provide the estimated ideal LST for both conditions with and without the influence of irrigation. The mesh was assumed to be fully irrigated when simulating irrigation conditions and fully non-irrigated while simulating conditions without irrigation. Since MODIS provides the surface temperature for the actual conditions on the ground, when attempting to detect irrigation, it is sometimes impacted upon by precipitation. Additionally, effects on LST due to geological variability cannot be isolated. The purpose of the simulation of LST using the LSM is to remove the influence of this climatology and geological variability which results in temperature difference.

2.1 Satellite data

MOD11A1 product with a temporal resolution of 12 hours and a spatial resolution of 1km was used for LST data. MODIS collects daily observations from the study area at approximately 4 pm and 3 am local time. This study used MODIS data from 2001 when it was first available.

2.2 SiBUC Land Surface Model

Simple Biosphere including Urban Canopy (SiBUC) by Tanaka (2005) is developed based on the Simple Biosphere (SiB). It considers artificial water operation in irrigated land and water and heat balance on an urban area. The basic concept of the irrigation scheme is to maintain soil moisture of the green area above minimum soil moisture defined for each growing stage of the crop. Irrigation scheme in this model was improved based on field investigation to consider local furrow irrigation rules in the basin (Touge et al. 2015).

For meteorological input, Japanese 55-year Reanalysis (JRA-55) was used to provide forcing data to the model. Since all the data is provided at a temporal resolution of between 3 and 6 hours, hourly data was linearly interpolated and spatial interpolation was done using Inverse distance weighting (IDW). Global Satellite Mapping of Precipitation (GSMaP) version 6 data was used for precipitation data. This is a real-time radar derived dataset and it was used in order to isolate irrigation effect on soil moisture from that caused by rainfall.

2.3 Irrigation indices

The following Eq.(1-(3) 下の were used to develop LST based indices in an attempt to detect the irrigated area.

$$R_1 = \Delta ST_{SAT} - \Delta ST_{LSM\_NI} \quad (1)$$

$$R_2 = \frac{ST_{SAT}^{day} - ST_{LSM\_NI}^{day}}{ST_{LSM\_IR}^{day} - ST_{LSM\_NI}^{day}} \quad (2)$$

$$R_3 = \frac{ST_{SAT}^{day} - ST_{LSM\_NI}^{day}}{AveST_{SAT}^{day} - AveST_{LSM\_NI}^{day}} \quad (3)$$

where, R is irrigation index, ST is surface temperature, ΔST is surface temperature difference between day and night, $AveST$ is long term average of surface temperature. And suffix of SAT means observed by satellite, LSM_IR and LSM_NI means simulated with full irrigation and without irrigation, respectively, and day means daytime.

Eq.(1) 上の was used to remove the climatic influences and the geological difference that may affect ΔLST in order to identify the irrigation effect in a mesh. Eq. (2) compares the irrigation effect observed by MODIS with the ideal simulated irrigation effect. Since this is the rate of the actual irrigation effect from the ideal irrigation effect, it would reflect the irrigation fraction in the mesh. Eq.(3) compares the irrigation effect observed by MODIS with the average simulated irrigation effect. This is used to detect a drought event by comparing the irrigation effect in a given year to an average year.

3 Results and Discussion

Fig.1 below shows the potential of the 3 indices to detect drought effect on irrigated area during the irrigation season. During a dry year, the irrigation fraction away from the water source is reduced due to water scarcity resulting in a higher LST. The indices were computed from a 10-day average of LST data.

Fig.1 (a-c) shows a higher value for all the indices in the month of August 2001 especially in the northern part of the delta. In 2001, some areas in the north were severely affected by drought and could not be irrigated. This can be clearly viewed by the proposed LST indices. R_1 shows changes to the irrigated area due to anthropogenic effect which in this case, relates to the reduction of the irrigated area due to drought. R_2 seems to be directly related to the irrigation fraction and therefore has a much clear result on the impact of drought than R_1 and R_3. It compares an ideal natural simulated effect of irrigation and the actual irrigation condition. R_3 seems least suitable of the 3 since it compares the actual condition to average changes which may include drought conditions in the past. Fig.1 (d-f) shows an average year where the irrigation fraction is much larger as compared to 2001.

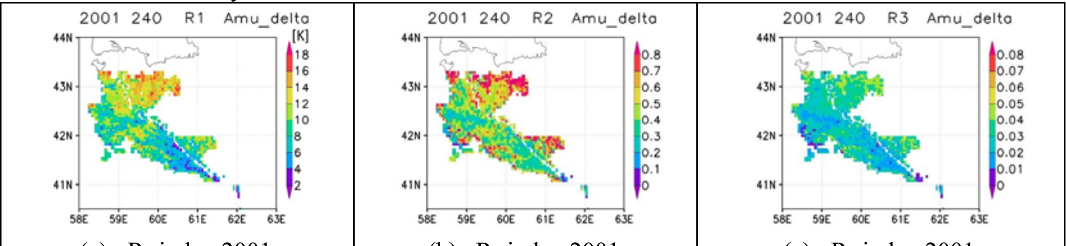

(a) R_1 index 2001 (b) R_2 index 2001 (c) R_3 index 2001

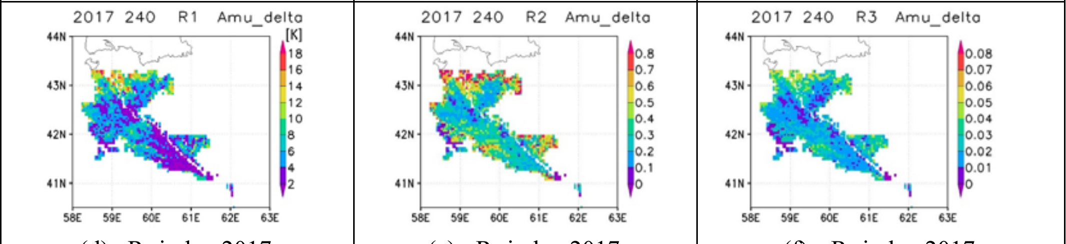

(d) R_1 index 2017 (e) R_2 index 2017 (f) R_3 index 2017

Fig.1 Effect of drought on LST in the irrigated area

4 Conclusions

(1) Due to the difference in heat capacity between water and soil, it was expected that soil with high moisture content will not respond immediately to temperature changes. Therefore, 3 indices were developed to detect the irrigated area.

(2) Irrigation fraction during a drought year was observed to be lower as compared to that of a normal year especially further away from the water source due to water scarcity.

Reference

[1] Tanaka, K., Development of the New Land Surface Scheme SiBUC Commonly Applicable to Basin Water Management and Numerical Weather Prediction Model, PhD Thesis, Kyoto University., (2005).

[2] Touge, Y. et al, Developing a Water Circulation Model in the Aral Sea Basin Based on in Situ Measurements on Irrigated Farms, Journal of Arid Land Studies 25 (3) (2015) 133–36.

Estimating fire severity map based on representative plots in the Kamaishi 2017 forest fire

○ Grace Puyang Emang[1*], Yoshiya TOUGE[1] & So KAZAMA[1]
[1]Department of Civil and Environmental Engineering, Tohoku University, Miyagi 980-8579, Japan.
[*]E-mail: grace.puyang.emang.r2@dc.tohoku.ac.jp.

Abstract

Fire severity in a forest fire varies within the burned area and this variation will cause different impacts towards the forest such changes to hydrological processes and carbon dioxide emission. Thus it is important to map the fire severity to assess the magnitude of such impacts. These fire severity can be observed using satellite, field investigation or both. Thus in this study, the estimation of fire severity map was studied using 15 representative plots of four different fire severity levels that were based on the probability of tree mortality. The threshold of each fire severity level was based on the maximum NDVI difference between pre and post-fire images of each representative plots. The resulting fire severity map showed a coarse delineation of fire severity indicating the thresholds used were insufficient due to the small number of representative plots used.

Keywords: forest fire; fire severity; NDVI; Landsat 8.

1 Introduction

Fire severity is a term to describe how fire intensity affects ecosystems where the effects are often varied within and between different ecosystems. Some studies have reported increased in sedimentation concentration observed in burned watersheds and higher sediment production rates were found in high severity forest than a moderate and low severity forest fire. The increase in sedimentation rate and heavy precipitation events post-fire will lead to deterioration of water quality.

Variation in fire severity existed in a burned area for the same fire event because it is influenced by various factors such as fire intensity, heating and duration, soil and plant dryness, topography and climate. Hence it is vital to estimate and map the various fire severity in order to quantify and mitigate the effects of a forest fire.

Fire severity can be measured through the loss or change of above and below ground organic matter by field observation or satellite images. The fire severity and indices used in most studies were defined and measured according to the studies purpose and localised to the study areas which are insufficient in other study areas because of different ecosystem and climates. The common satellite index used to study fire severity is Normalise Burn Ratio (NBR) but another index which could be viable in detecting fire severity and related directly to forest growth is Normalise Difference Vegetation Index (NDVI). The assumption in this study was that various fire severity will result in a different probability of tree mortality due to various damages on trees so these trees are expected to grow differently after the fire was suppressed and its growth rate should be different from trees growing in an unburned area. These changes in trees growth due to various fire severity can potentially be detected using NDVI.

In this study, fire severity were visually identified during field investigation by the percentage of scorch crown height and were then categorised into three levels of fire severity (low, moderate and high severity) to match the probability of tree mortality (low, moderate and high tree mortality) which were based on the percentage of scorch crown height. This study aims to estimate the fire severity map based on representative plots in the Kamaishi 2017 forest fire.

2 Study Area and Methodology

2.1 Study Area

The study area is located around Takanosu Mountain in Kamaishi city, Iwate Prefecture and forested mainly with needleleaf trees (pine and cedar) and sparsely with broadleaf trees. A fire which broke out on 8 May 2017 and suppressed on 22 May 2017, lasted for 14 days and the estimated total burned area, as indicated in Fig.1, was 413ha which is greater than the total of burned area for the whole of Japan in 2016. The burned area was extensive due to the strong presence of wind and low accessibility of vehicle into the burned area which was surrounded with steep cliffs, Komatsu Bay on the east and Ozaki Peninsula on the northeast.

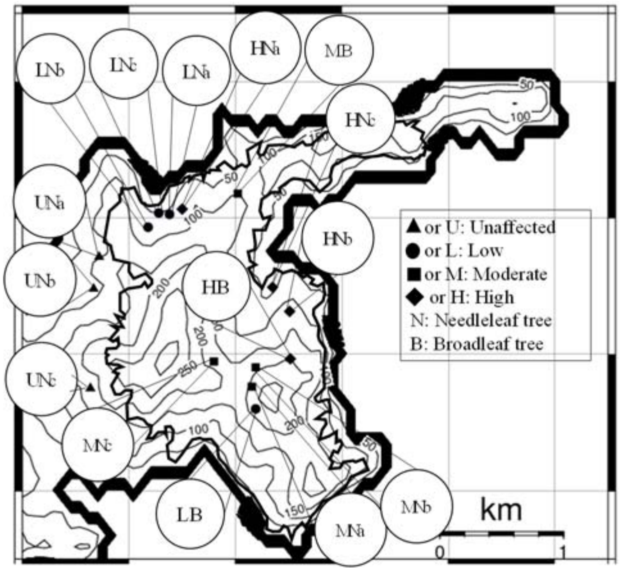

Fig.1 Study area drawn in solid line based on burned and unburned areas as indicated by information from Kamaishi Forestry Association and the distribution of 15 trees used in this study

2.2 Ground Truth and Fire Severity Classification

The study area is forested mostly with needleleaf trees so three needleleaf trees and a broadleaf tree were used in each fire severity levels. In total, 15 trees were used in this study as shown in Fig.1 with 12 trees in the burned area and the remaining trees were from unaffected areas.

Fire severity was observed by visually estimating the percentage of scorch crown height relative to its total crown height. These percentages were categorised into three levels (low, moderate and high severity) so to match the probability of tree mortality: low (scorch crown height less than 30 % of crown height), moderate (scorch crown height more than 30 % but less than 80 % of crown height), and high tree mortality (scorch crown height more than 80 % of scorch crown height) as shown in Table 1.

Table 1 Classification of fire severity levels used based on the probability of tree mortality[17].

Fire severity	Percentage of scorch crown height
Low	Less than 30 %
Moderate	More than 30 % but less than 80 %
High	More than 80 %

2.3 Satellite Images

NDVI images free of cloud and snow on 30 April 2017 (pre-fire) and 24 June 2017 (post-fire) from Landsat 8 were used in this study and calculated as Eq. (1).

$$NDVI = \frac{(NIR - R)}{(NIR \ + R)} \quad \ldots\ldots..(1)$$

where NIR is spectral reflectance of the near infra-red band (0.85-0.88 micrometres) and R is spectral reflectance of the red band (0.64-0.67 micrometres).

The NDVI difference between these two images was determined for all 15 trees in the representative plots. The maximum NDVI difference from each fire severity level was used as thresholds of severity levels as indicated in Table 2.

Table 2 NDVI thresholds in each fire severity level based on the maximum NDVI difference of the 15 trees used.

Fire severity	NDVI threshold used in delineating fire severity area
Unaffected	less than 0
Low	More than 0 but less than 0.03
Moderate	More than 0.03 but less than 0.33
High	More than 0.33

3 Results and Discussion

The resulting fire severity delineated areas in the spatial distribution map in Fig.2 was coarse, suggesting the thresholds used based on the 15 trees were inappropriate and determining the thresholds with limited observation points are inadequate. Some areas which were forested with broadleaf trees showed no changes in NDVI suggesting observing broadleaf trees by NDVI are difficult due to its canopy being less dense than needleleaf trees.

However, it is possible the prior fire conditions in broadleaf trees areas could have led to a minimal decrease in NDVI for broadleaf trees. NDVI of pre-fire image showed the areas of the broadleaf trees had lower NDVI than other areas but a higher NDVI in the post-fire image indicating these broadleaf trees might have not been affected by the fire and continued to grow or the higher NDVI is due to the growth of grass in the sparsely forested broadleaf areas captured by Landsat 8.

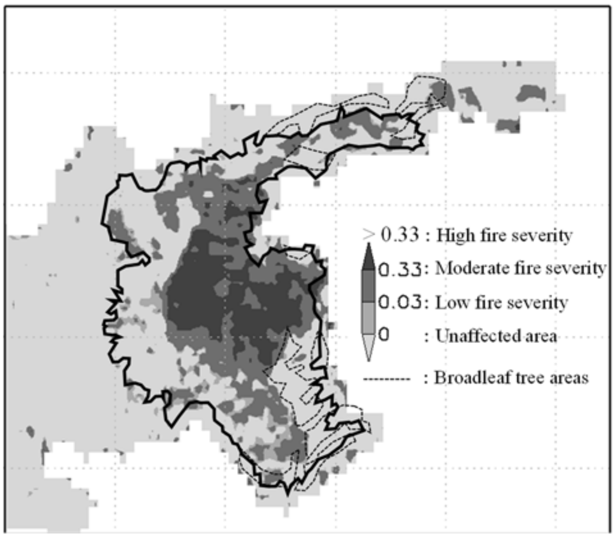

Fig. 2. Delineation of fire severity areas based on NDVI threshold

4 Conclusions

(1) The small number of representative plots were not sufficient in determining the NDVI threshold used to estimate the fire severity map.

(2) Estimation of fire severity map using both field observation and satellite is needed by increasing number of representative plots to enhance understanding of forest fire effects towards forest ecosystem and provide insights to the relations of different fire severity with dryness conditions prior to and after a forest fire.

Reference

[1] Keeley, J. E. Fire intensity, fire severity and burn severity: A brief review and suggested usage, Int. J. Wildl. Fire, 18, (2009) 116–126.

[2] Silins, U., Stone, M., Emelko, M. B. & Bladon, K. D. Sediment production following severe wildfire and post-fire salvage logging in the Rocky Mountain headwaters of the Oldman River Basin, Alberta Catena, 79 (2009) 189–197.

[3] Benavides-Solorio, J. D. D. & MacDonald, L. H. Measurement and prediction of post-fire erosion at the hillslope scale, Colorado Front Range, Int. J. Wildl. Fire, 14, (2005) 457–474.

[4] Chatto, K. & Tolhurst, K. A review of the relationship between fireline intensity and the ecological and economic effects of fire, and methods currently used to collect fire data, Research Report No. 67, Department of Sustainability and Environment, pp. 1-20, 2004.

[5] Ryan, K. C. Techniques for assessing fire damage to trees, Proceedings of the Symposium on Fire -- Its Field Effects, pp. 1–11, 1982.

[6] Touge, Y., Emang, G. P., Kazama, S., Takahashi, Y. & Sasaki, K. Introduction of the Tohoku Forest Fires on May 2017; case in Kamaishi city of Iwate Prefecture and Kurihara city of Miyagi Prefecture. *自然災害科学 J. JSNDS*, Vol. 36, pp. 361–370, 2018.

Understanding flood hazard and crop yield loss relationship using hydrodynamic and remote sensing model

○ Vempi Satriya Adi HENDRAWAN[1*], Daisuke KOMORI[2]
[1]Graduate School of Environmental Studies, Tohoku University, Miyagi 980-8572, Japan.
[2]Department of Civil and Environmental Engineering, Tohoku University, Miyagi 980-8579, Japan.
[*]E-mail: vempi@dc.tohoku.ac.jp.

Abstract

The existing evaluation methods to understand flood impact on agricultural crop are mostly to utilize a damage function. However, constructing a damage function is time-consuming as it requires ex-post survey data and experimental analysis based on historical event. Therefore, developing an alternative approach is needed, particularly for an area where a stage damage function has not been developed yet and agricultural flood impact data are limited. This study is aimed to develop an alternative approach to understand the relationship between flood characteristics and associated crop yield loss.

1 Introduction

In most Asian countries, low land rice crop cultivation has suffered huge losses during wet monsoon season due to extreme river flooding [1]. The existing evaluation methods to understand flood impact on agricultural crop are mostly to utilize a damage function. However, constructing a damage function is time-consuming as it requires ex-post survey data and experimental analysis based on historical event [2]. Therefore, developing an alternative approach is needed, particularly for an area where a stage damage function has not been developed yet and agricultural flood impact data are limited.

This study is aimed to develop an alternative approach to understand the relationship between flood characteristics and associated crop yield loss. The approach proposed by [3] was adopted to achieve abovementioned purpose. The previous studies used capability of near real time remote sensing technology to record vegetation greenness condition to build empirical crop yield model. Whereas the inundation and flood parameters was simulated by a hydrodynamic model. A relationship between crop loss and flood parameter then was obtained. Moreover, the applicability of those approach for different climate, geographical condition and different crop behavior is still unknown. Therefore, another case study was employed in this study to test the applicability of the approach and to develop an alternative flood-loss relationship curve. Timeseries smoothing were also taken into consideration to overcome image noise disturbances that was not considered in the previous study.

To achieve the purpose of this study, some objectives were defined as follows: 1) To estimate crop yield loss using smoothed satellite images, 2) To simulate flood propagation in the crop field, and 3) To understand relationship between flood characteristic and its associated damage.

2 Materials and Methods

2.1 Case study and flood event

Solo river basin was selected as a case study (Figure 1). Solo river basin is the largest river basin in java island Indonesia with approximately 16,100 km2 of the total area. It has rice crop cultivated in the basin 31% of the total basin area. There are mainly two paddy-crop pattern system in the river basin [4]: (1) October-January and February-June and (2) December-April and April-June. It is varying spatially and temporary based on local farmer's practice and climate condition.

The flood event occurred in the basin from the 25th December 2007 to 10th January 2008 was chosen as an event for flood simulation. The flood occurred during newly-planted paddy-crop growth stage in the eastern part of basin and maturity stage in western part of basin variously. It damaged about 60,630 ha paddy field [4].

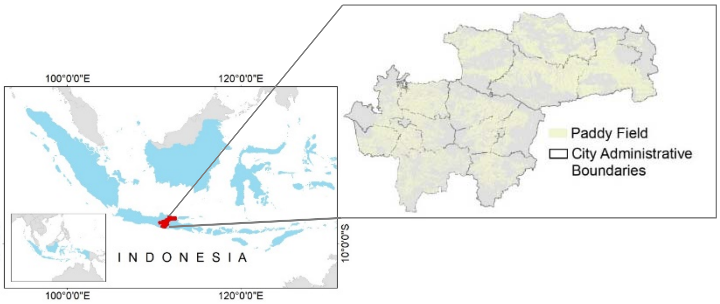

Figure 1 Solo river basin and rice field

2.2 Methodology

This study consists of three main analyses, crop yield loss estimation, flood characteristics simulation, and obtaining relationship of flood characteristics and its associated loss estimation.

1) *Crop Yield Loss Estimation*

MODIS Vegetation indices (MOD13Q1) product was used to develop statistical crop yield model to estimate the potential crop yield. The multiple linear regression model based on the city level yield as a dependent variable and several NDVI and EVI value within the period of the flood event was performed. The yield loss was obtained by making a ratio between assumed normal year and flood affected year

2) *Flood characteristics simulation*

A flood model, Rainfall-Runoff-Inundation (RRI) model developed by [5] was used to simulate the inundation and output flood parameters.

3) *Flood-loss relationship*

Then the relationship between flood parameters and crop yield loss then was obtained to understand flood characteristic affecting crop yield.

3 Results and Discussion

3.1 Crop Yield Loss Estimation

Crop yield model was established by using smoothed time series images that was performed by TIMESAT [6]. Multiple linear regression model was used to estimate yield using city scale NDVI and EVI in both 2007 and 2015 year. Relatively satisfactory reliability of the model could be achieved with the coefficient of determinant by 0.65 and 0.63 for 2007 and 2015 model respectively (Table 1).

Table 1 Yield Regression Model

Year	Regression Equation	R^2_{adj}
2007	Y = 4.18 - 8.53*EVI14sep07 + 12.82*EVI16oct07	0.65
2015	Y = 4.81 - 11.08*NDVI30sep15 + 15.7*NDVI1nov15	0.63

In order to estimate the potential loss, we use the ratio value between normal and affected year:

$$Ratio = \frac{Yield_{2007}}{Yield_{2015}}$$

From above ratio formula, then the range value from 0 to 1 was considered as a loss ratio, meaning that the yield in 2007 as affected year is lower than 2005 as normal year.

3.2 Flood Characteristic Simulation

From the result, flood characteristics in the basin then were obtained in both river and slope plain in spatial distribution. A huge inundation area is shown in the downstream area where rice crop field is cultivated. The maximum depth within all inundated pixels is 3.55 m and the maximum velocity is 0.26 m/s. While maximum duration for > 1-meter depth inundation is 13.5 days. The spatial distribution of those parameters was also obtained in the same resolution with crop yield model. Then those was used to obtain flood-loss relationship.

3.3 Flood-Loss Relationship

In order to obtain the relationship, we used interval 1% of ratio to obstruct average each flood parameter value within those pixels, rather than using every single pixel. We used maximum velocity, duration and depth to represent flood hazard. While, loss ratio was obtained by following formula. Higher loss ratio means higher potential loss.

$$Loss\ Ratio = 1\ - Ratio\ (<1)$$

Loss ratio was obtained by rating 2007 yield and 2015 yield. Ratio value was used is less than 1 meaning that there was loss in 2007 yield as mentioned above.

Taking one into discussion, depth-loss relationship shows that there are two side of loss ratio resulted from the same flood parameter (i.e. 20 – 40 cm in) (Figure 2). However, it shows a clear relationship from 40 cm water depth meaning that more than 40 cm water depth would result a damage on the rice crop. The results are inline the previous study showing that rice plants may suffer considerable yield losses when water depths are at 20 to 50 cm water depth [1].

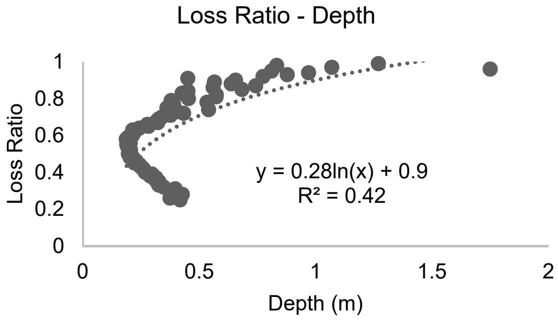

Figure 2 Flood-loss relationship

4 Conclusion

This study is aimed to develop an alternative approach to understand the relationship between flood characteristics and associated crop yield loss. This study consists of three main analyses, crop yield loss estimation, flood characteristics simulation, and obtaining relationship of flood characteristics and its associated loss estimation.

From the case study we find that remote sensing-based model could be potentially used to assess the crop yield loss. Integrating spatial crop yield loss model and flood simulation could result a new relationship. The results show clear relationship between flood parameter and the potential loss. In depth-loss relationship solely, it shows that more than 40 cm water depth would result a damage on the rice crop. The results are inline the previous study.

For further research, it is needed to build more reliable crop yield loss model and to validate the loss resulted from the hazard. Field observation seems able to fill the gap between predicted and observed yield loss. Proposed by a number of studies taking sample of Vegetation Indices of crop field is also promising to get better crop yield model.

References

[1] Singh A.et al., 2017. Genetics, Physiological Mechanisms and Breeding of Flood-Tolerant Rice (Oryza sativa L.), Plant and Cell Physiology, Volume 58, Issue 2, February 2017, Pages 185–197.

[2] Brémond, P., Grelot, F. and Agenais, A.L., 2013. Economic evaluation of flood damage to agriculture–review and analysis of existing methods. Natural Hazards and Earth System Sciences, 13(10), pp.2493-2512.

[3] Chen, H. et al., 2017. Integrated remote sensing imagery and two-dimensional hydraulic modeling approach for impact evaluation of flood on crop yields. Journal of Hydrology, 553, pp.262-275.

[4] Shrestha B. B et al., 2016. Assessment of Disaster Damage due to Flood Hazard in the Solo River Basin of Indonesia. 7th ICWRER.FAO. 2015. The impact of disasters on agriculture and food security. Rome.

[5] Sayama T et al., 2012, Rainfall-Runoff-Inundation analysis of Pakistan flood 2010 at the Kabul river basin, Hydrological Sciences Journal, 57(2), 298-3.

[6] Eklundh, L. and Per, J., 2017. TIMESAT 3.3 With Seasonal Trend Decomposition and Parallel Processing Software Manual.

Assessing the impact of human-induced land-use change on natural water cycle at watershed scale based on land surface model

----a case study in the Loess Plateau Region, North Central China

○ Linghao Meng[1*], Daisuke Komori[1, 2]
[1]Department of Frontier Science for Advanced Environment, Tohoku University, Miyagi 980-8579, Japan.
[2]Department of Civil and Environmental Engineering, Tohoku University, Miyagi 980-8579, Japan.
[*]E-mail: meng.linghao.t8@dc.tohoku.ac.jp.

Abstract

Human activities have become one of the most crucial factors of the natural water cycle. This research is to assess the impact of human activities, especially land use and vegetation changes on the natural hydrological factors in the Loess Plateau Region (LPR), a region suffered the most severe soil erosion over the world. From 1999 the water conservation project, forest and grass land increased significantly to replace most of the field land to more than 25%. three stations at the watershed are used to analyze water cycle parameter changes. Climate and land use data are divided into three parts and thus nine cases for simulation. The model calibration shows good accuracy of H08 used in the region.

Keywords: Loess Plateau Region, land surface model, land use change, water cycle

1 Introduction

Rapidly expanding human activities have profoundly affected various biophysical and biogeochemical processes of the Earth system over a broad range of scales, and freshwater systems are now amongst the most extensively altered ecosystems (Carpenter et al. 2011). Apart from urbanization, human activities also apparently altered the natural water cycle, with more or less both positive and negative impacts simultaneously. So, it is significant to assess the effects of human activities as a way of nature environment protection project.

So far, various researches about the relationship between water and the environment as well as human activities have been carried out. For example, Gorman (2015) found climate change increased the runoff in Mississippi River Basin and Hanasaki (2017) pointed out that the role that forest plays depends on specific catchment and so on. Researchers usually first investigates the consequences caused by the impact, makes qualitative analysis, and then quantitatively calculates according to the actual data. However, most are focus on climate change; for land use changes the dominant point lies on urbanization and deforestation, human-induced afforestation is rarely being researched. Therefore, this research aims using land surface model to physically simulate the water cycle changes under human afforestation at large watershed scale.

2 Materials and Methods

2.1 Data Preparation

Climate Data

We used the downscale daily climate data in 5-arc minute resolution from three observation datasets provided by H08: 1) the Water and Global Change (WATCH) forcing data for 1980 –1989 (hereafter H for history), 2) the Second Global Soil Wetness Project for 1996 – 2005 (hereafter P for past), 3) the WATCH Forcing Data methodology applied to ERA-Interim data for 2005 – 2014 (hereafter C for current). DEM data and River discharge data from three observation stations (Figure 1) in the Loess Plateau Region were obtained from China Geo-data Sharing Service Platform (CGSSP) and used to calibrate and validate the models.

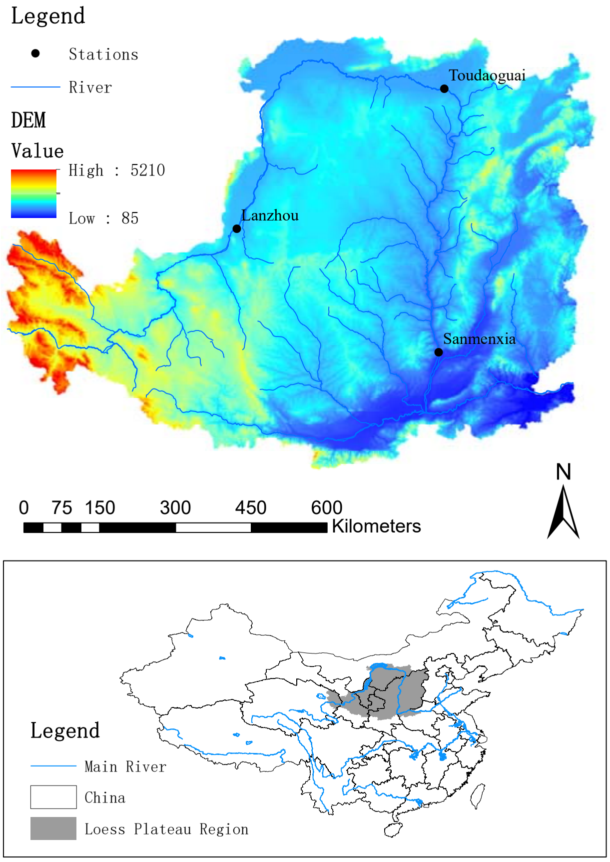

Figure 1. DEM, location and three stations of LPR

Land use data

The LPR is one of the most severe soil erosion area. Chinese government started its water and soil conservation project by reducing the area of field crops into forest. Land use data of

1985 (history), 2000 (past), 2012 (current) were obtained from CGSSP (Figure 2).

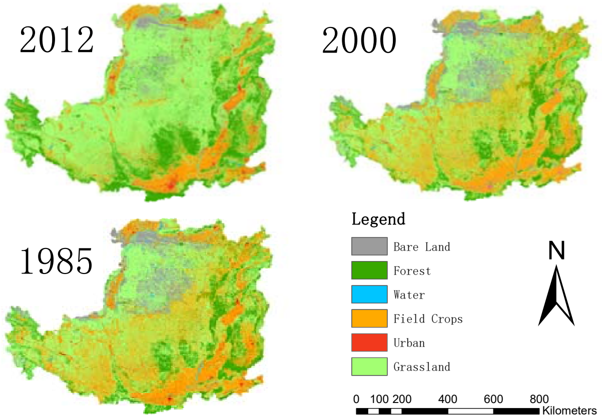

. **Figure 2. Land use in LPR of 1985, 2000, and 2012**

2.2 Analysis Methods

A land surface model called H08 (Hanasaki, 2008) is used to analyze water cycle under different land use scenarios in the LPR. This module is based on a bucket model (Manabe, 1969; Robock et al., 1995) with improvements. The soil water balance and runoff were expressed as follows:

$$\frac{dW}{dt} = Rainfall+Q_{sm}\text{-}E\text{-}Q_{s}\text{-}Q_{sb}$$

Where Q_{sm} is the snow melt rate; Q_s is the surface runoff, Q_{sb} is the subsurface runoff, τ is a time constant as 100 days × 86400 (s) and the γ is set at 2 which are global constant (Hanasaki, 2008)

Nine simulation will be conducted in this research as shown in table 1.

Table 1. Details of nine simulations

Case	Data		Case	Data		Case	Data	
	Climate	Land Use		Climate	Land Use		Climate	Land Use
H-H	1980-1989	1985	P-H	1996-2005	1985	C-H	2005-2014	1985
H-P	1980-1989	2000	P-P	1996-2005	2000	C-P	2005-2014	2000
H-C	1980-1989	2012	P-C	1996-2005	2012	C-C	2005-2014	2012

2.3 Model Calibration

Observed daily discharge of three stations in the LPR named Landzhou, Toudaoguai, and Sanmenxia (hereafter station 1, 2, and 3) was used for model calibration. Parameters of the H08 model that are susceptible to river discharge and related to land use (Mateo et al., 2012) are soil depth (SD), bulk transfer coefficient (CD), time constant for daily maximum subsurface runoff (τ), and a shape parameter (γ) that is related to subsurface flow (Hanasaki et al., 2014). The model can be calibrated by changing the values of the parameters based on land use type and evaluated using the Nash-Sutcliffe Efficiency Coefficient (NSE).

The C-C case of each station is used to calibrate the model. By changing the 4 parameters to find the optimal match of the parameter sets. Later on, the H-H and P-P case of each station will be used for model validation.

3 Results and Discussion

As shown in figure 2, forest and grassland increased significantly while crop field dramatically decreased because of the Water and Soil Conservation Project. By calculation, the total ratio of forest and grassland increased from 53% to 80% while field crops deceased from 33% to 12%.

Figure 3 showed the result of model calibration. The NSE of each station is 0.84, 0.78, 0.88, which means the H08 has high accuracy when applying to LPR.

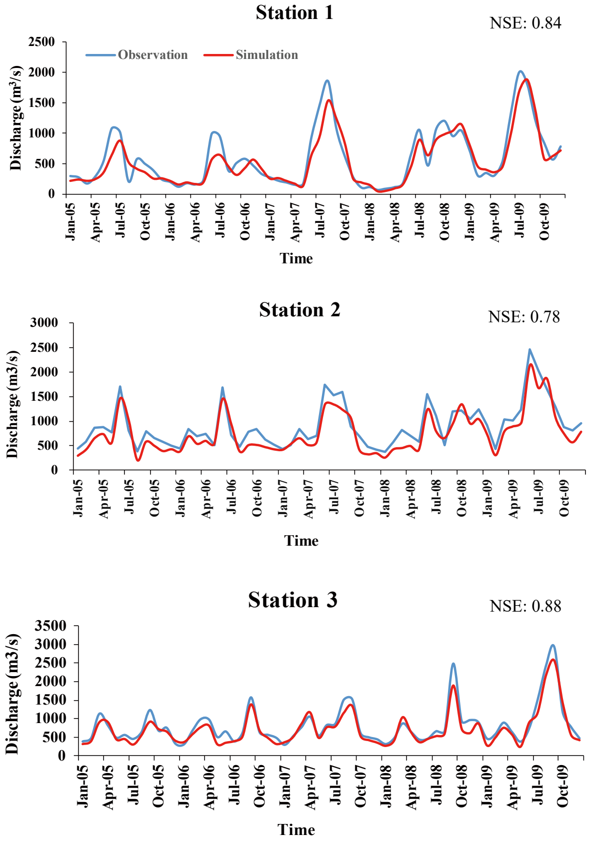

. **Figure 3. Model calibration of three stations**

4 Conclusions

(1) Human-induced afforestation have exerted great changes in the land use pattern of the LPR. Forest and grassland have greatly replaced the crop fields which used to be the dominant land use type.

(2) The simulation of 3 selected stations shows satisfactory accuracy in calibrating the models, which means it can be applied to simulate the water cycle in the studied area. Later another two senarios will be used for model validation.

Reference

AghaKouchak A, Norouzi H, Madani K, Mirchi A, Azarderakhsh M, Nazemi A, Nasrollahi N, Farahmand A, Mehran A, Hasanzadeh E (2015) Aral Sea syndrome desiccates Lake Urmia: call for action. J Great Lakes Res 41(1):307–311.

Carpenter SR, Stanley EH, Vander Zanden MJ (2011) State of the world's freshwater ecosystems: physical, chemical, and biological changes. Annu Rev Environ Resour 36(1):75–99.

Ghimire, C. P., van Meerveld, H. I., Zwartendijk, B. W., Ravelona, M., Lahitiana, J., Razakamanarivo, H., ... & Jones, J. (2015). Effects of reforestation on the partitioning of precipitation into evapotranspiration, overland flow and recharge in eastern Madagascar.

Hanasaki N., (2008). An integrated model for the assessment of global water resources–Part 1: Model description and input meteorological forcing. Hydrology and Earth System Sciences, 12(4), 1007-1025.

Hanasaki N., (2014). A quasi-real-time hydrological simulation of the Chao Phraya River using meteorological data from the Thai Meteorological Department Automatic Weather Stations. *Hydrological Research Letters*, *8*(1), 9-14.

Estimation of the flood damage caused by Climate change and effect of the adaptation

○ Tao Yamamoto[1*], So Kazama[1] ,Yoshiya Touge[1], Tsuyoshi Tada[2], & Takeshi Yamashita[3]
[1]Department of Civil and Environmental Engineering, Tohoku University, Miyagi 980-8579, Japan.
[2]Department of Civil and Environmental Engineering,National Defense Academy,Kanagawa 239-8686,Japan
[3] Information Infrastructure Division, Information Department, Tohoku University,Miyagi, 980-8578, Japan
*E-mail: tao.yamamoto.r4@dc.tohoku.ac.jp.

Abstract

This study shows and compares the effect of the mitigation and the adaptation for the flood caused by climate change. It was estimated that the flood depth and the damage using 2D non-uniform flow model and the flood control economy investigation manual. Furthermore, it was estimated that the future flood damage using GCM (Global Climate Model)s and two RCP(Representative Concentration Pathways) scenarios. And we considered the land use control as the adaptation. We consider the reduction if we withdraw the land based on the 100 year return period flood depth as the effect of the land use control.

Keywords: *global warming, land use control, GCM, future climate.*

1 Introduction

Due to the impact of climate change associated with global warming, there are concerns about the increase in various water disaster risks in Japan. According to Wada et al., daily precipitation at the end of the 21st century with a recurrence period of 100 years is predicted to increase by 20% nationwide compared to the present 1). This suggests an increasing trend in the number of flood disasters such as heavy rain in July 2018. Based on these trends, it is necessary to consider the impact and adaptation measures. As a previous study about flood disasters, Tezuka et al. quantitatively evaluated future flood damages in Japan2). Tanaka et al. estimated the amount of damage caused by flood and storm surge combined disasters throughout Japan3). However, in these studies, the resolution of the analysis was about 1km square, and small rivers such as mountainous areas could not be represented. As for the evaluation method of adaptation measures, the difference between the two damages when the flood control level was raised and when it was raised was evaluated as the effect of adaptation measures. This method cannot individually evaluate the effects of various adaptation measures. Although land use control can be cited as an adaptation measure against floods, the effects of the entire country have not been verified.

Therefore, the purpose of this study is to quantitatively evaluate the amount of flood damage with higher resolution data, and to individually evaluate the effects of adaptation measures using the future climate. We also compare the effects of adaptation and mitigation measures against floods.

2 Datasets

In order to estimate the amount of damage in the future climate, the rate of increase of future precipitation relative to the current precipitation is calculated. For this, we used the daily precipitation that was downscaled by the 1km regional climate scenario / multi-meteorological element version in Japan4). There are six GCMs: GFDL-CM23, HadGEM2-ES, MIROC5, MRI-CGCM3, CISRO-Mk3-6-0, and IPSL-CM5A-LR. There are two scenarios: RCP8.5 and RCP2.6. The target period was 1981 to 2005(current) and 2031 to 2055(near future).

The input data for flood calculation is shown below. The national land numerical information was used for elevation and land use data. In addition, for daily precipitation data, we used the probabilistic flood-contributing rainfall distribution, which is a rainfall distribution that generates floods at any point of time, calculated from the relationship between the catchment area and runoff coefficient created by Tezuka et al.

3 Method

In this study, we used a two-dimensional unsteady flow model that has been used in previous studies as an inundation model. The resolution was increased to about 250m square. Based on the inundation depth obtained from these, referring to the flood control economic survey manual, the damage rate corresponding to the inundation depth and the unit price of damage according to land use are set, and the damage amount is calculated based on them.

The future climate estimation method is shown. For the GCM data shown in the data set, we extracted the maximum daily precipitation for each year at 50 locations nationwide. The parameter of the generalized extreme value distribution GEV (Generalized Extreme Value) distribution was estimated by using the Probability Weight Moment (PWM) method, and precipitation with a recurrence period of 100 years was calculated. The ratio of precipitation obtained during the two periods was taken as the rate of future precipitation increase. Figure 1 shows the distribution of precipitation increase rates created based on MRI-CGCM3. By multiplying this with the above-mentioned stochastic flood-contributing rainfall distribution in the current climate, the future probabilistic flood-contributing rainfall distribution was created.

Next, the calculation method of the annual expected damage(AED) is shown. According to the method of Tezuka et al., it was assumed that the flood control equipment withstands floods with a recurrence period of 50 years, and floods with a recurrence period of 100 years or more with a low probability of occurrence do not have a significant impact on the annual expected damage. Based on this assumption, the AED is calculated by multiplying the section average damage amount and section probability between the recurrence periods of 100 and 50 years.

Finally, the land use control method is shown. In this study, land use was changed according to the inundation depth during floods with a recurrence period of 100 years in the current climate. For example, the land use of house and building land that was flooded for more than 3m was uniformly changed to the land use of forests that did not account for damage. The amount of damage was calculated using the land use distribution after the control as an input value.

4 Result and Discussion

The expected annual damage due to flooding in the whole country was estimated to be 1.39 trillion JPY. If the inundation depth is over 3m and the mesh that is residential and commercial land is withdrawn , and the damage amount of the mesh is not counted (hereinafter referred to as 3m control), the national expected damage amount is 947 billion JPY. It decreased by 31.8% from the current expected damage. Therefore, the effect of land use control is estimated to be 42.2 billion JPY in annual expected amount. The annual expected damage was estimated to be 1.33 trillion JPY when the control inundation depth standard was set to over10m (hereinafter referred to as 10m control, which was 55.7 billion yen less than the current AED.

The amount of damage in the future climate is shown below. The AED due to flooding in the future in the future climate was estimated to be 1.43 trillion JPY for the RCP2.6 scenario and 1.45 trillion JPY for the RCP8.5 scenario. They increased by 2.7% and 4.1%, respectively, from the current expected damage. However, the damages of four combinations of CISRO-Mk3-6-0 and MIROC5 RCP2.6 and GFDL-CM23 and MIROC5 RCP8.5 were reduced.

In addition, when 3m control is performed in the future climate, AED is calculated as the average value of 6GCMs, which is 988 billion JPY in the RCP2.6 scenario and 1.01 trillion JPY in the RCP8.5 scenario. They decreased by 30.7% and 30.3%, respectively, from the expected future damage without land use control. AED for the 10m control was estimated to be 1.37 trillion JPY for the RCP2.6 scenario and 1.39 trillion JPY for the RCP8.5 scenario. Both were reduced by 4.0% from the expected future damage in the absence of land use control. Therefore, AED reduction effect in the future climate with land use control is estimated to be about 438 billion JPY in both RCP scenarios in the 3m control. In the 10m control, both RCP scenarios are estimated to be 57.6 billion JPY. The above results are shown in Table 1. From Table 1, the effect of adaptation measures based on land use control is estimated to be about 438 billion JPY for the 3m control and about 57.6 billion JPY for the 10m control. The effect of mitigation measures can be regarded as the difference in the amount of damage when mitigating the RCP scenario from 8.5 to 2.6. Therefore, the effect of mitigation measures is considered to be about 19.2 billion JPY. This shows the effectiveness of adaptation measures.

5. Conclusion

1) AED of flood disaster nationwide in current climate is 1.39 trillion JPY.
2) AED of flood disasters in the future climate is 1.43 trillion yen based on the RCP2.6 and 1.45 trillion yen based on the RCP8.5.
3) If land use is restricted to land with a flood depth of more than 3m during a flood with 100 years return period, there is an effect of reducing AED amount of about 438 billion JPY in both the present and future. In addition, if land use is restricted to land with a flood depth of more than 10m during a flood with a 100 years return period in the current climate, there is an AED reduction effect of approximately 57.6 billion JPY in both the present and future.
4) AED reduction of floods when mitigating global warming from RCP8.5 to RCP2.6 is about 19.2 billion JPY, while AED reduction due to land use regulations is 57.6 billion JPY to 438 billion JPY.

Reference

1) 和田一範，村瀬勝彦，冨澤洋介：地球温暖化に伴う降雨特性の変化と洪水・渇水リスクの評価に関する研究，土木学会論文集，No.796/II-72，pp.23-37，2005.
2) S. Tezuka, H. Takiguchi, S. Kazama, A. Sato, S. Kawagoe, R. Sarukkaliged, Estimation of the effects of climate change on flood-triggered economic losses in Japan, International Journal of Disaster Risk Reduction, Vol.9, pp.58-67, 2014.
3) 田中裕夏子，風間聡，小森大輔： 洪水・高潮複合災害リスク評価， 土木学会論文集 G(環境), Vol.74, No.5, pp. I_257-I_264, 2018.
4) 西森基貴・石郷岡康史・桑形恒男・遠藤伸彦・飯泉仁之直・雨貝裕介（2017）：日本における影響評価・適応研究のためのメッシュ気候シナリオデータセット群について，日本農業気象学会 2018 年全国大会.

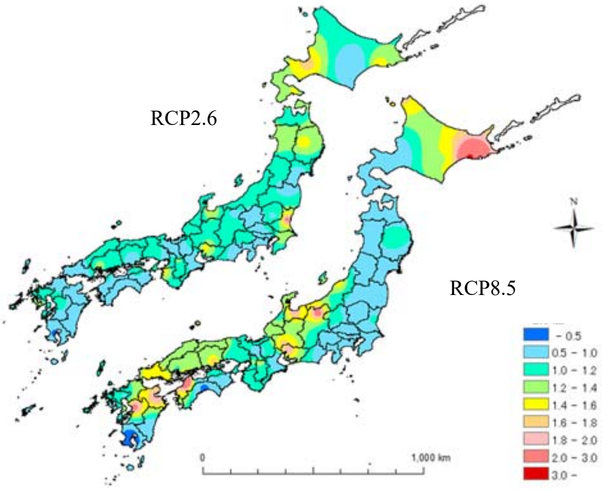

Fig.1 The distribution of precipitation increase rates created based on MRI-CGCM3

Table.1 AEDs of each senarios

Expected Annual Damage(trillionJPY)	current climate	RCP2.6 2050	RCP8.5 2050
no control	1.39	1.43	1.45
3m control	0.947	0.988	1.01
10m control	1.33	1.37	1.39

Analysis of Flood Inundation Area in Naruse River Basin by RRI Model toward Consideration of Paddy Field Dams

○Yikai CHAI*, Yoshiya TOUGE & So KAZAMA
Department of Civil and Environmental Engineering, Tohoku University, Miyagi 980-8579, Japan.
*E-mail: chai.yikai.r1@dc.tohoku.ac.jp.

Abstract

In recent year, to mitigate flood damage due to increasing of the intensity and frequency of torrential rain events, the Miyagi prefecture, Japan, has adapted measures using paddy field by installing runoff control devices named paddy field dam, and utilizing rainwater storage capacity potentially of irrigation ponds. The purpose of this study is to analysis the flood inundation area caused by typhoon in 1986 in Naruse River Basin toward consideration of paddy field dams and small irrigation ponds by Rainfall-Runoff-Inundation (RRI), which is a two-dimensional model capable of simulating rainfall-runoff and flood inundation simultaneously. As an input data, 3 arc-second HydroSHEDS Digital Elevation Model (DEM) and daily observation rainfall data are used. According to reduction of inundation damage, drop in channel water level and decrease in discharge volume using combined flood routing and hydrologic analyses. The result showed that the paddy field dam has a temporarily effect on the inundation area and the peak discharge.

Key word: Paddy field dam; RRI Model; Naruse River Basin.

1 Introduction

Flood caused by Typhoon or torrential rains is one of the most devastating natural disasters in the world. In recent year, flood risks are expected to increase in the year to come. Although Japan is very small, it is very prone to flooding. Hence, flood-risk assessments in those regions are crucial.

In order to estimate the flood damage in the area affected by flooding, the inundation area within a short time after the disaster must be calculated by hydrological model simulation. In recent years, a variety of flood inundation models have been developed and have been applied in river basins all over the world. One of the models is the Rainfall-Runoff-Inundation (RRI) model, which can simulate maximum water depth, river discharge and inundation area, even subsurface flow. One of the advantages of RRI Model is the prediction of flood events development by considering the effects of river discharge and floods inundation. Therefore, the model is designed to address the problems of simulated flooded areas in paddy fields and irrigation ponds.

The paddy field dam which is low material installation cost and high immediate effect with extensive address, is one of the flood mitigation measures during torrential rains. By artificially enhancing the flood control function of the paddy fields, the rainwater is temporarily stored in the paddy field during torrential rains, and the flood peak discharge of the paddy field is controlled to reduce the disaster of the farmland downstream of the paddy field.

The purpose of this study is to analysis the flood inundation area caused by typhoon in 1986 in Naruse River Basin toward consideration of paddy field dams and small irrigation ponds by Rainfall-Runoff-Inundation (RRI). The Naruse River Basin is choosed as the study area because of its small footprint and the river bed slope. Except for a few towns along the Yangtze River, most of the mid-to-downstream region consists of paddy fields and irrigation ponds. As an input data, 3 arc-second HydroSHEDS Digital Elevation Model (DEM) and daily observation rainfall data are used. According to the maximum water depth and inundation area obtained by RRI model, it is showed that the paddy field dam has a temporarily effect on the inundation area and the peak discharge.

2 Methodology

2.1 Study Area

For the case study, the Naruse River with a length of about 89 km, which is located in Miyagi Prefecture, Japan, is one of the most important river for agriculture, infrastructure and transportation of Miyagi Prefecture. The Naruse River originates from the Funagata Mountain at the junction of Miyagi and Yamagata Prefecture, and merges with Tagawa River, Hanagawa river, Tadakawa River and an artificial river named Shineaigawa. In addition, the Yoshida River originates from Kurokawa District Yamato town. Finally, the Naruse River and the Yoshida River which is the right tributary, also belong to first-class river, converges into the Pacific Ocean, and the mouth is located in 38°22′34″N 141°10′29″E. The Naruse River Basin area is approximately 1130km2. Geographically, the Naruse River Basin is surrounded by forest and hills in the north and south, and Ouu mountain range in the west. The slope of the water arising from the mountains is significant large, ranging from 1/100 to 1/500, and the slope of the plain is only 1/2500 to 1/5000, therefore, if the river bursts its banks, serious disasters will occur. The basin consists of 8 cities and 3 villages including Osaki City. The population of the basin is about 180,000 people, and the land use in the basin is about 72% such as mountain, about 22% such as paddy fields and upland areas, and about 6% of urban areas such as residential areas.

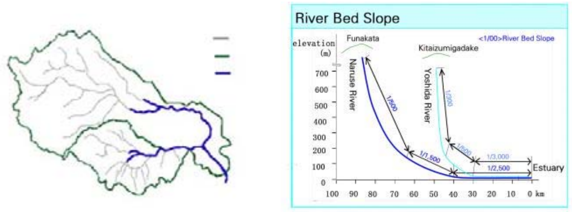

Figure 1. Naruse River Basin and River Bed Slope

2.2RRI Model

Rainfall-Runoff-Inundation (RRI) Model is a two-dimensional model capable of simulating rainfall-runoff and flood inundation simultaneously (Sayama et al., 2012). The model deals with slopes and river channel respectively, and assumes that both slope and river channel are positioned in the same grid cell. The channel is discretized as a single line along the center line of the overlying slope grid cell. The flow on a grid cell is calculated by the Two-Dimensional diffusion wave model, and the channel flow is calculated by One-Dimensional diffusion wave model. The advantage of the RRI Model is the simulation also including lateral subsurface flow, vertical infiltration flow and surface flow in order to better representations of the rainfall-runoff and flood inundation process. Considering saturated subsurface flow and surface flow, a discharge-hydraulic gradient relationship is used to treat the more important lateral subsurface flow in mountainous regions. On the other hand, the vertical infiltration flow rate was estimated using the Green-Ampt model. Based on the different overflow formulas, the flow interaction between the river channel and slope is estimated based on the water-level and the levee-height condition.

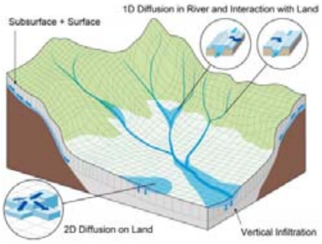

Figure 2. Schematic diagram of RRI Model.

The Rainfall-Runoff-Inundation model equations are derived based on the following (1) mass balance Equation and (2) momentum Equations and (3) for gradually varied unsteady flow:

$$\frac{\partial h}{\partial t}+\frac{\partial q_x}{\partial x}+\frac{\partial q_y}{\partial y}=r-f \qquad (1)$$

$$\frac{\partial q_x}{\partial t}+\frac{\partial u q_x}{\partial x}+\frac{\partial v q_x}{\partial y}=-gh\frac{\partial H}{\partial x}-\frac{\tau_x}{\rho_w} \qquad (2)$$

$$\frac{\partial q_y}{\partial t}+\frac{\partial u q_y}{\partial x}+\frac{\partial v q_y}{\partial y}=-gh\frac{\partial H}{\partial y}-\frac{\tau_y}{\rho_w} \qquad (3)$$

The second terms of the right side of Equations (2) and (3) are calculated with Manning's Equations (4) and (5).

$$\frac{\tau_x}{\rho_w}=\frac{gn^2u\sqrt{u^2+v^2}}{h^{1/3}} \qquad (4)$$

$$\frac{\tau_y}{\rho_w}=\frac{gn^2v\sqrt{u^2+v^2}}{h^{1/3}} \qquad (5)$$

h = Height of the water from the local surface
qx, qy = Unit width discharges in x and y directions
r = Rainfall intensity
f = Infiltration rate
u, v = Flow velocity in x and y directions
g = Gravitational acceleration
H = Height of the water from the datum
τx, τy = Shear stress in x and y directions
ρw = Density of water
n = Manning's roughness parameter

2.3 Paddy Field Dam Model

Sayama et al. (2012) applied the RRI model to the Niigata Prefecture Niigata City Yokoe drought drainage basin in Japan. The runoff analysis construction consists of a mountain city module, a paddy field module and a river channel module, meanwhile, the runoff control measures play an effective role. In the flood model, the unsteady flow is calculated from the momentum equation and the continuity equation. In the river model, based on characteristic of topographically adjustable cell's and topographically adjustable cell's production, the geometric properties of the organizational unit are used to calculate the flood flow. In the land-use flow model, a new definition was introduced, namely the introduction of the terminal drains and the calculation of the flow of rice fields, farmfield area and urban area.

2.4 Analysis method

The Naruse River Basin is covered by the GSMaP radar-rainfall product, which is available from 2000 onward at an approximately 1-km spatial and an hourly temporal resolution. Due to the flooding event that this study used is in 1986, this means that the method to obtain rainfall data only base on the observation station data. Beacuse only 4 observation stations in Naruse River Basin, it is not enough to simulate accurately, for decrease the uncertainty, according to the three days rainfall data obtained from observation station in Miyagi Prefecture, simulate the precipitation in entire Miyagi Prefecture by ArcGIS and try to generate a hourly rainfall time series for longer. As an input data, 3 arc-second HydroSHEDS Digital Elevation Model (DEM), flow direction data, and flow accumulation data modified by ArcGIS, through RRI Model combined with paddy field model, reduction of inundation damage, drop in channel water level and decrease in discharge volume where is regulated and unregulated by paddy field dam.

Stepwise regulation of endogenous free ammonia to improve short-chain fatty acids production from waste activated sludge alkaline fermentation

○ Min YE[1*], Yu-You Li,[1,2]

[1] Department of Civil and Environmental Engineering, Tohoku University, Miyagi 980-8579, Japan.
[2] Department of Frontier Science for Advanced Environment, Tohoku University, Miyagi 980-8579, Japan.
[*]E-mail: 402093078@qq.com

Abstract

Short-chain fatty acids (SCFAs) derived from waste activated sludge (WAS) is a promising alternative as carbon source for denitrifying processes, while the free ammonia present in the fermentation supernatant requires more attention. Stepwise regulation of endogenous FA under 24 h accumulation at phase I and removing FA from supernatant at phase II were conducted to improve SCFAs production and carbon source availability simultaneously from WAS alkaline fermentation. The results show that a maximal SCFAs production in the pH=9 + Ammonia stripping reached 431.4 mg chemical oxygen demand (COD)/g volatile suspended solid (VSS), i.e., 9.0% and 119.8% higher than that of the pH=9 and the control, respectively. The WAS-derived SCFAs availability as carbon source also increased by 58.7% than the pH=9.

Keywords: Short-chain fatty acid; free ammonia; waste activated sludge; alkaline fermentation.

1 Introduction

Waste activated sludge (WAS), a by-product from BNR processes, has drawn more and more attraction. WAS contains abundant organic matters like proteins (25-62%) and carbohydrates (7-19%) which could be degraded to added-value of short-chain fatty acids (SCFAs) via anaerobic fermentation. It is well known that SCFAs could be used as the carbon sources to biological nutrient removal (BNR) in wastewater treatment. However, the SCFAs production is always limited because of a low hydrolysis efficiency.

Additional pretreatments are always needed to promote WAS fermentation, such as thermal, ultrasonic and microwave-assisted processes. Among them, alkaline fermentation has been demonstrated to be a promising strategy to improve SCFAs production by enhancing WAS solubilization and/or hydrolysis as well as inhibiting subsequent SCFAs consumption by methanogens. However, the conventional alkaline fermentation at pH=10 needs numerous alkaline reagents with high costs. In addition, it is noted that even though alkaline conditions produced substantial dissolved organic matters (DOMs) via strongly abiotic effect, they may concomitantly inhibit the biotic effect, and thereby hinder SCFAs production maximization.

In fact, WAS alkaline fermentation not only produces SCFAs but also releases ammonium as a byproduct. Alkaline fermentation with a very high pH favors mainly free ammonia (FA) rather than ammonium ion in the supernatant. FA can easily diffuse from cell membrane into the cytoplasm and lead to intracellular proton imbalance or potassium deficiency. On one hand, FA was indicated as an inhibitory factor for hydrolysis and acidogenesis process. On the other hand, adding FA was also demonstrated as an effective pretreatment to WAS disintegration. However, the actual functions of endogenous FA in previous WAS alkaline fermentation studies was not be confirmed. Therefore, stepwise regulation of endogenous FA for its positive function maximization during WAS fermentation at weak-alkaline condition could be a potential approach to enhance the SCFAs production.

In this study, batch trials of WAS alkaline fermentation process were conducted to investigated the contributions of endogenous FA accumulation to WAS disintegration at early fermentation stage and its removal at later fermentation stage to SCFAs production promotion.

2 Materials and methods

2.1 Characterization of WAS

The WAS was collected from the second sedimentation tank of a municipal WWTP. The WAS was concentrated by natural settling for around 24 h at 4 ºC refrigerator prior to using. The characteristics of WAS are as follows: pH 7.1-7.4, total suspended solid (TSS) 17.9 g/L, volatile suspended solid (VSS) 12.9 g/L, TCOD 22.3 g/L, SCOD 89.2 mg/L, total carbohydrate 2552.8 mg COD/L, total protein 11477.3 mg COD/L, SCFAs 60.8 mg COD/L, ammonium 17.1 mg N/L, total nitrogen (TN) 5.7% in sludge dry weight.

2.2 Batch trials

The release of endogenous FA and its effect bring about to WAS solubilization on alkaline condition was carried out in six identical reactors with working volume of 0.2 L. The reactors were divided into the control (neutral pH), the pH=9 + Ammonia stripping, the pH=9, the FA 100, the FA 300, and the FA 500. Specially, the pH=9 + Ammonia stripping was conducted with intermittent nitrogen gas stripping to regulate FA at a low level, which on behalf of the sole pH=9 effect to WAS. In addition, the different initial FA reactors (i.e. FA: 100, 300, 500 mg/L) were conducted by adding a series NH_4HCO_3 (NH_4^+concentration of 188.9, 566.9, and 944.8 mg/L). The initial FA concentration was calculated with conditions of pH, temperature and total ammonia nitrogen concentration (TAN). Each reactor was lasted for 24 h in an air-bath shaker (160 rpm, 35 ºC), during which the pH was maintained at pH=9 via using 2M HCl and 2M NaOH.

Batch WAS fermentation tests were conducted to assess the removal of endogenous FA to SCFAs production, and carried out in the working volume of 500 mL reactors. The reactors were divided into the control (without pH adjustment), the pH=9 fermentation, and the pH=9 + ammonia stripping. The pH in alkaline fermentation was controlled via adding 2M HCl and 2M NaOH. The pH=9 + ammonia stripping fermentation included two phases: (1) endogenous FA accumulation during first 24 h; (2) the FA was reduced by in-situ ammonia stripping until fermentation ending. The intermittent stripping intensity was controlled at 12 L_{gas}/L_{WAS}/min by high purity nitrogen gas. Each reactor was firstly flushed with nitrogen gas for 5 min to remove oxygen, and then placed in air-bath shaker (160 rpm, 35 ^{o}C) for 8 days anaerobic fermentation.

2.3 Analytical methods

Determination of TSS, VSS, TN, ammonium, were carried out following standard methods. COD was measured via a spectrophotometer (HACH DR890, USA) coupled with a HACH DRB200 reactor. The pH was detected using a pH-meter. The proteins and carbohydrates were determined by Lowry-Folin method and phenol-sulfuric method. SCFAs concentration and composition were measured using gas chromatography (Shimadzu, Japan) equipped with a Stabilwax-DA chromatographic column and a flame ionization detector (FID).

The FA concentration was determined by total ammonium nitrogen (TAN) according to the following equation.

$$\frac{[NH_3]}{[TAN]} = 1/(1+\frac{10^{-pH}}{10^{-(0.09018+\frac{2729.92}{T})}})$$

where $[NH_3]$ and [TAN] are FA and TAN concentrations, respectively, and T the medium temperature, K.

3 Results and discussion

Fig. 1a-1c shows the effect of endogenous FA production to WAS solubilization during first 24 h. The FA was fast released from 49.3 mg/L (6 h) to 210.6 mg/L (24 h). Compared to without FA accumulation via in-situ stripping ammonia from supernatant, the SCOD concentration (6303.8 mg/L) in the pH=9 was increased by 26.0%. In addition, adding initial FA (100, 300, 500 N mg/L) into WAS achieved a fast SCOD release rate, but the maximal SCOD value at 24 h was similar to the pH=9. Therefore, keeping endogenous FA accumulation at first 24 h could be a useful way to perform FA-induced abiotic effect and promote WAS solubilization.

The process of WAS alkaline fermentation at pH=9 was divide into two phases by stepwise regulation of FA: phase I, endogenous FA pretreatment for 24 h; phase II, removing endogenous FA from supernatant in later fermentation. Fig. 1d-1e indicated that the maximal SCFAs production in the pH=9 + ammonia stripping reached up to 431.4 mg COD/L at day 7, which was higher than the pH=9 (395.7 mg COD/L) and the control (193.8 mg COD/L). With respect to SCFAs composition in fermentation supernatants, acetic acid (accounting for 50-60% of total SCFAs) all constituted the most abundant component, followed by propionic acids and butyric acids. While in the pH=9 + Ammonia stripping, the final FA concentration fell into a range of 5-20 mg N/L after a peak accumulation at 24 h. Furthermore, removing FA was contributed to SCOD, SP, SC increment, in which FA-induced inhibition to hydrolysis and acidogenesis was mitigated (as seen in Fig. 1f-1i).

Fig. 1m-1o demonstrated that the WAS-derived SCFAs availability as carbon source was effectively enhanced by improving SCFAs production and reducing ammonium. The available COD in the pH=9 + Ammonia stripping was 5437.9 mg COD/L, which was higher than that of the pH=9 (3426.4 mg COD/L) and the control (879.7 mg COD/L). stepwise regulation endogenous FA could be a potential application of SCFAs-containing WAS fermentation supernatant for effective denitrification processes in wastewater treatment plants.

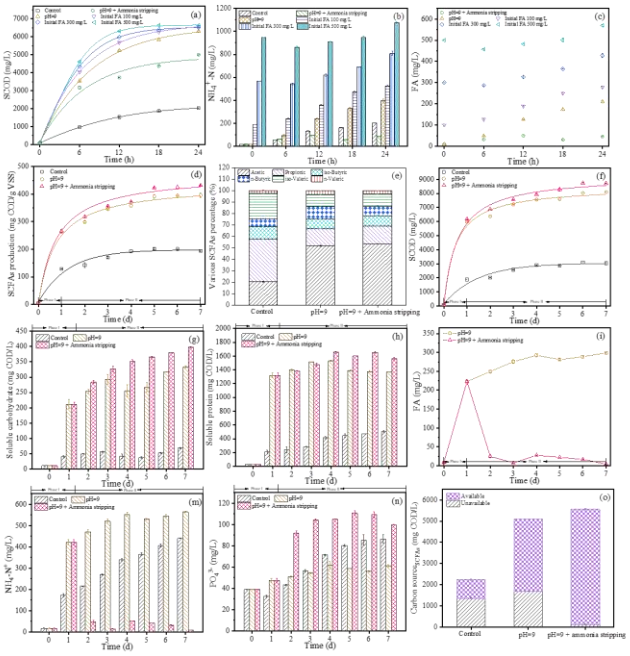

Fig. 1. The SCOD (a), NH_4^+-N (b), FA (c) release from WAS with different initial FA during 24 h; the SCFAs production (d) and components (e), SCOD (f), soluble carbohydrate (g), soluble protein (h), FA (i), NH_4^+-N (m), PO_4^{3-} (n), carbon source availability (o) from WAS fermentation at pH=9 by regulating endogenous FA.

4 Conclusions

(1) The endogenous FA accumulated in supernatant during first 24 h, could be an effective strategy to WAS solubilization, compared with adding initial FA.

(2) Stepwise regulation endogenous FA (phase I: FA accumulation for WAS pretreatment, phase II: removing FA from WAS to mitigate FA-induced biotic inhibition) realized a higher SCFAs production and an enhancement of carbon source availability.

Reference

[1] Wang, X., Li, Y., Zhang, Y., Pan, Y.R., Li, L., Liu, J., Butler, D. Stepwise pH control to promote synergy of chemical and biological processes for augmenting short-chain fatty acid production from anaerobic sludge fermentation. Water Res., 155(2019), 193-203.

[2] Liu, Y., Ngo, H.H., Guo, W., Peng, L., Wang, D., Ni, B. The roles of free ammonia (FA) in biological wastewater treatment processes: A review. Environ. Int., 123(2019), 10-19.

Gradual deterioration in methanogenic degradation of N, N-dimethylformamide under the anaerobic condition

○ Tianjie WANG[1*], Zhe KONG[1] & Yu-You LI[1]

[1]Laboratory of Environmental Protection Engineering, Department of Civil and Environmental Engineering, Graduate School of Engineering, Tohoku University, 6-6-06 Aza-Aoba, Aramaki, Aoba Ward, Sendai, Miyagi 980-8579, Japan

[*]E-mail: wang.tianjie.s3@dc.tohoku.ac.jp.

Abstract

The stability of the methanogenic degradation of *N*, *N*-dimethylformamide (DMF) was evaluated under a constant DMF concentration of approximately 2000 mg L-1 using a lab-scale up-flow anaerobic sludge blanket (UASB) inoculated with activated sludge. While the UASB realized a nearly 100% degradation of DMF and a high methane production for the first two months, both the removal efficiency and methane production continued to decrease until the end. The characterization of the prokaryotic community reveals that those DMF-hydrolyzing bacteria (DHB) originating from the activated sludge were responsible for the effective degradation of DMF. However, even when fed with a constant concentration of DMF, the DHB kept decreasing all the time while methane-producing archaea were rapidly cultivated. The variation of prokaryotic community suggests that the DHB could not proliferate anaerobically without assimilating the intermediate products from the hydrolysis of DMF, resulting in an unstable DMF-degrading consortium. The cultivation of DHB under the anaerobic condition of the UASB was therefore difficult.

Keywords: *N*, *N*-dimethylformamide; UASB; methanogenic degradation; anaerobic digestion; DMF-hydrolyzing

1 Introduction

N, *N*-dimethylformamide (DMF) [$(CH_3)_2NCHO$] is widely implemented in a wide variety of chemical industries as a versatile organic solvent due to its excellent miscibility in water and many other organic liquids (Nisha et al., 2015; Sanjeev Kumar et al., 2013; Yang et al., 2014). However, this nitrogenous compound is also toxic and because it remains refractory and recalcitrant in aquatic environment, the excessive discharge of DMF-containing wastewater results in serious environmental problems, like eutrophication (Rahmaninezhad et al., 2016; Vidhya and Thatheyus, 2013; Xiao et al., 2016).

DMF-hydrolyzing bacteria (DHB) provide a hydrolytic enzyme (known as DMFase) to hydrolyze DMF into dimethylamine (DMA) and formic acid (HFc): these intermediates are then fermented into methane by methylotrophic and hydrogenotrophic methanogens (Kong et al., 2019c). The stoichiometric equation of DMF methanogenic degradation is described below:

$$(CH_3)_2NCHO + 2.5H_2O \xrightarrow{\qquad\qquad} 1.75CH_4 + 0.25CO_2 + NH_4^+ + HCO_3^-;\ \Delta G^0 = 28.01\ kJ\ mol^{-1} \qquad (1)$$

In this study, a lab-scale UASB reactor was used to investigate the long-term behavior and stability of the DMF methanogenic degradation under a constant concentration of approximately 2000 mg L^{-1}. The UASB reactor was inoculated with the activated sludge as the sole seed inoculum because it is widely acknowledged that activated sludge lacks archaea (methanogens) (Kobayashi et al., 2009).

2 Materials and methods

2.1 Analytical reagents and method

Biogas production and gas temperature were recorded by a wet tip gas meter (Shinagawa, Japan). The components (%) of the biogas including N_2, CH_4 and CO_2 were measured using a gas chromatograph (GC-8A, Shimadzu, Japan), and pH was measured by a HM-30R pH meter (DKK-TOA, Japan). The DMF concentrations were determined using the Waters ACQUITY UPLC H-class system (Milford, USA). All ions including ammonium (NH_4^+), DMA ($(CH_3)_2NH_2^+$), MMA ($CH_3NH_3^+$) and HFc (OOH-) were determined by capillary electrophoresis (7100CE, Agilent Technologies, USA).

2.2 Experimental apparatus and procedure

The lab-scale UASB used in this study obtains a maximum volume of 5 L and was kept at the mesophilic condition at around 35 °C by a thermostatic water circulation system. An inoculum of 5 L DMF-degrading activated sludge was inoculated to the UASB as the seed sludge.

DMF-containing wastewater with a concentration of approximately 2000 mg L^{-1} was prepared in a 120 L substrate tank and was dosed with sufficient trace elements. The hydraulic retention time (HRT) was kept at a constant of 24 h in order to maintain a relative constant organic loading rate (OLR) around 3 g COD L^{-1} d^{-1}. The extraction of genome DNA, the sequencing procedure of PCR and Illumina, and the processing of sequencing data were all consistent with those reported in previous studies (Kong et al., 2018c, 2019c). The operational taxonomic units (OTUs) were generated on the basis of 97% similarity. Singleton OTUs were removed and sequences were randomly selected to unify the sequence number of each sample to 50,000 as the standard number.

3 Results and discussion

3.1 Rapid start-up and stable methanogenic degradation of DMF

As shown in Fig. 2 (b), it took about a week for the UASB to realize a rapid start-up: the reactor obtained a high DMF removal efficiency of 81.97% on the first day, and reached 98.17% on Day 7. As can be clearly seen in Fig. 2 (a) and (c): The effluent pH reached a high of 8.45 because of the high concentration of the alkaline compound DMA, at 786.23 mg L^{-1}, detected on the first day (Ferguson et al., 2000). Besides, the growing trend of the biogas production rate from merely zero on the first day to a high of 1.02 L L^{-1} d^{-1} on Day 7 can be obviously seen in Fig. 2 (d). The methane content of the biogas also significantly increased from a low of 14.62% at the very beginning to a high of 84.71% on Day 7, which can be seen in Fig. 2 (e).

For a two months period from Day 7 until Day 56, the relatively stable and remarkably high DMF removal efficiency of over 95% (even reached 99.99% on some days). During this period, the effluent DMF concentration was basically lower than 10 mg L^{-1}, and the pH remained stable at around 7.50. The thorough mineralization of DMF also resulted in a stable effluent ammonium concentration of around 500 mg L^{-1}, which was in good accordance with the stoichiometric calculation using Eq. (1). As can be seen in Fig. 2 (d) and (e), the majority of DMF was successfully recovered as biogas with an average production rate of 1.15 L L^{-1} d^{-1}, in which the bio-methane accounted for nearly 90% (the highest methane content recorded was 91.58%) of the components with an average production rate of 1.03 L L^{-1} d^{-1}. This was also in good accordance with stoichiometric Eq. (1).

3.2 Deterioration of DMF methanogenic degradation

The operation of the UASB began to deteriorate after Day 70. As shown in Fig. 1 (b), the removal efficiency of DMF continued to drop: By the end of the experiment, the DMF removal efficiency had dramatically dropped to a low of 32.79%. Due to the insufficient degradation of DMF, the ammonium concentration in Fig. 1 (c) also kept decreasing from around 500 mg L^{-1} to 156.66 mg L^{-1}. As shown in Fig. 1 (d), the biogas production rate dramatically dropped from 1.10 L L^{-1} d^{-1} to a low of 0.26 L L^{-1} d^{-1}. However, the methane content in the biogas still remained high, at over 86%, as can be seen in Fig. 1 (e). In order to reveal the reason for this deterioration, the entire prokaryotic community structure was investigated in detail.

The variation of the total abundance of these DMF-degrading candidates (or DHB) illustrated in Fig. 2 (a) shows an obvious decreasing trend from 34.27% on the first day to just 5.37% on the last day. The continuous decrease in the total abundance of these DMF-degrading candidates suggests that most of these DHB were unable to proliferate under the anaerobic condition even though some of them were actually facultative anaerobes (Nisha et al., 2015; Vidhya and Thatheyus, 2013). While these bacteria seemed to successfully survive under the anaerobic condition of the UASB and they "temporarily" retained their DMF-hydrolyzing ability or ability to produce hydrolytic enzyme, the fact is that these bacteria kept decaying all the time and the hydrolytic enzymes produced from these bacteria were left in the reactor, maintaining the DMF-hydrolyzing activity for about two months. Meanwhile, the total abundance of the DMF-degrading candidates in the entire prokaryotic community was calculated as 9.98% on Day 56 in Fig. 2 (a). This suggests that only when the abundance of DHB accounted for more than 10% of the total prokaryotic community could the system realize the thorough methanogenic degradation of DMF under a constant OLR of around 3 g COD L^{-1} d^{-1}.

4 Conclusions

The performance of DMF methanogenic degradation and the corresponding variation in microbial community were investigated in detail, leading to a better awareness of the mechanisms and requirements in the anaerobic treatment of DMF-containing wastewater. These can be summarized as follows:

1) While the DMF-degrading methanogenic consortium realized a quick start-up within a week, the performance of DMF methanogenic degradation gradually weakened even though the system was operated at a constant DMF loading rate.

2) DMF-hydrolyzing bacteria are difficult to cultivate under the methanogenic condition because they are incapable of assimilating DMA and HFc even though they are facultative anaerobes.

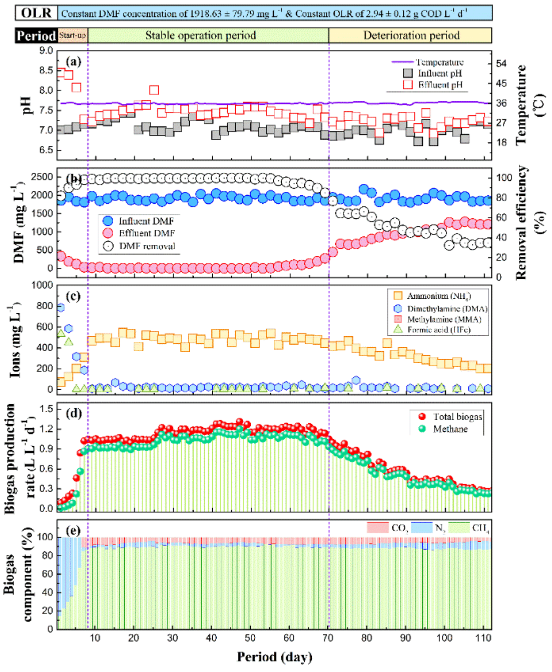

Fig. 1. Operational results of the continuous experiment conducted using a lab-scale UASB.

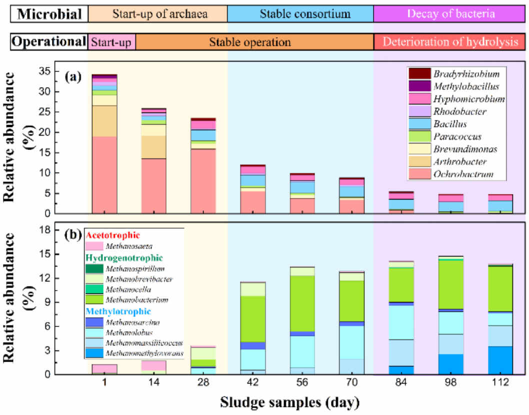

Fig. 2. Variation of the total relative abundance of the DMF-hydrolyzing bacteria and methanogens

Antibacterial effect of food waste hydrolysate on Escherichia Coli

○ Yuanyuan REN[1,3*], Qunhui WANG[3] & Yu-You LI[1,2]

[1] Department of Civil and Environmental Engineering, Graduate School of Engineering, Tohoku University,
6-6-06 Aoba, Aramaki-Aza, Aoba-Ku, Sendai, Miyagi 980-8579, Japan;
[2]School of Energy and Environmental Engineer, University of Science and Technology Beijing, 30 Xueyuan
Road, Haidian District, Beijing 100083, China

[3] Department of Frontier Science for Advanced Environment, Graduate School of Environmental Sciences,
Tohoku University, 6-6-20 Aoba, Aramaki-Aza, Aoba-Ku, Sendai, Miyagi 980-8579
*E-mail: ren.yuan.yuan.t7@dc.tohoku.ac.jp.

Abstract

With the development of the economy and social progress, people's pursuit of quality of life is getting higher and higher. According to the survey, the amount of food waste generated is increasing every year. The treatment of food waste mainly includes landfill, incineration and anaerobic digestion. But it takes time from the generation of food waste to the transport to disposal location. During this period, due to the high organic content of food waste, a large number of harmful bacteria breed. Moreover, because of the corruption of food waste, it will affect the urban environment and people's health. Previous studies have shown that the amount of harmful bacteria in food waste can be greatly reduced under anaerobic preservation conditions. This study focused on the inhibition of Escherichia coli by various hydrolysates generated from hydrolysis of food waste during the anaerobic preservation. The results showed lactic acid and acetic acid have bacteriostatic effect when they exist in a molecular state rather than in an ionic state. And lactic acid, acetic acid and ethanol have a synergistic antibacterial effect between every two materials.

Keywords: Food waste; hydrolysate; bacteriostatic preservation; Escherichia Coli.

1 Introduction

Food waste (FW) is one of the most important components of municipal solid waste, including household food waste, food-processing waste, canteen and restaurant waste. The stacking of FW has gradually become a global problem. It is estimated that the amount of FW sharply increased from 2.78 billion tons to 4.16 billion tons in Asian countries by 2025. Especially in China, the growth rate of FW has increased more than 10% with the acceleration of industrial development and urbanization processes. At present, FW regarded as municipal waste is sent to landfills and incineration plants as final disposal points. In some ways, these processes release some stress from garbage siege; at the same time, a series of problems are emerging including the rising cost of waste disposal, the lack of land space, groundwater pollution by leachate, and the emission of toxic and greenhouse gases. Moreover, FW with high concentrations of organic matter (volatile solids/total solids [VS/TS]: 0.8–0.9), high moisture content, and good biodegradability have been regarded as the most promising anaerobic substrates (Ren et al., 2018). Large-scale FW recycling is a current major issue because the collection of FW is dispersed. Consequently, the collection and transport of FW before being transported to the anaerobic treatment plant takes time. During this period, FW easily promotes bacterial growth because it is rich in water and organic substrates to affect urban environment. if the FW is not sterilized, the pathogenic bacteria represented by Escherichia coli will multiply to affect the health of people. The bacteriostatic preservation of FW is a key problem in FW recycling. Therefore, how to effectively inhibit the growth of spoilage bacteria during transportation is the primary problem to be solved in this study. The traditional solutions mainly include cryopreservation, high temperature sterilization, dry dehydration, and addition of preservatives to alleviate the problem of rapid decay of FW, but these methods require relatively high costs. Therefore, finding a cost-effective way to prevent and cure FW is an urgent problem to be solved. Previous studies have shown that the anaerobic preservation of FW can effectively inhibit the proliferation of pathogenic bacteria (Zhao et al., 2016). This study conducted further bacteriostatic effects analysis on various acidic substances in anaerobic preservation samples.

2 Materials and methods

2.1 Substrate Preparation

FW was obtained from a student canteen in the University of Science and Technology in Beijing. Large bones and pericarps of FW were first removed. The remaining waste was shredded and then stored at −20 °C. The substrates were thawed and kept at 4 °C before use.

The Escherichia Coli stored at -70 °C were taken out of the refrigerator and immediately placed in a 38-40 °C water bath until the icing was completely dissolved. The appropriate amount of Escherichia Coli was firstly added to the sterilized LB liquid medium, and the culture was completed by incubating at 150 r/min and 37 °C for 24 h. The activated Escherichia Coli was then added to a new LB liquid medium with a certain inoculum for subsequent bacteriostatic experiments.

2.2 Experiment methods

The checkerboard assay was used to assess the bacteriostatic preservation effect. The antibacterial materials and Escherichia Coli were added 100 ul into every hole in the 96-well sterile microplate, and then the 96-well plate was placed in a multi-function microplate reader, and incubated at 37 ° C for 24 h with shaking. The OD600 was measured every 1 h, and taken out after 24 h. The minimum inhibitory concentration of the absorbance decreased by more than 80% compared with the non-medicated blank group was the minimum inhibitory concentration MIC80 of the drug. The interaction was judged by calculating a fractional inhibitory concentration (FIC).

To evaluate the interaction of hydrolysate against Escherichia Coli, the fractional inhibitory concentration index (FICI) was calculated for each combination. The FICIs were calculated using the following equation: $FICI=FICA+FICB=C_A^{comb}/MIC_A^{alone}+C_B^{comb}/MIC_B^{alone}$ where MIC_A^{alone}, MIC_B^{alone} are the MICs values of compound A and B when acting alone, and C_A^{comb}, C_B^{comb} are the concentrations of compound A and B at the isoeffective combinations. The FICI was interpreted as follows: a FICI $\leqslant 0.5$ demonstrated synergy; a FICI between 0.5 and 4 indicated no interaction; and a FICI >4 showed antagonism.

3 Results and discussion

3.1 Materials in the hydrolysate

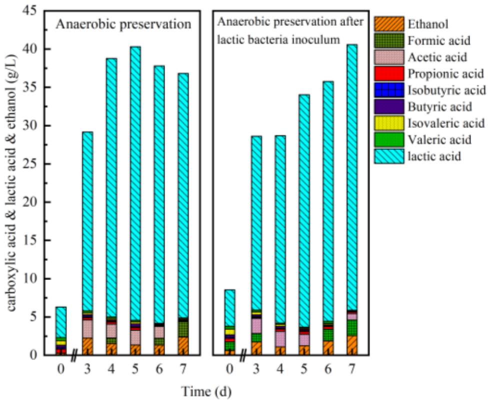

Fig. 1. The concentration of carboxylic acid, lactic acid and ethanol in hydrolysate.

Fig. 1 showed the concentration of carboxylic acid, lactic acid and ethanol in hydrolysate. The majority of material was lactic acid, meanwhile the concentration of acetic acid and ethanol can also reach about 5 g/L. After anaerobic preservation for 4 days, the concentrations of organic acids and lactic acid in the two groups were 38.77 g/L and 28.88 g/L, respectively. However, the lactic acid concentration in the anaerobic preservation group can reach the maximum value on the fifth day. A large amount of lactic acid can be generated quickly, so that the antibacterial effect can be better.

3.2 Antibacterial effect of different materials

The Time–kill assay of lactic acid, acetic acid and ethanol is shown in Fig. 2. With the increasing concentration of bacteriostatic substances, the measured OD600 value is getting smaller and smaller, and the bacteriostatic effect is more and more obvious. It is considered to have antibacterial effect when the OD600 is more than 80% lower than the growth curve after 24h culture. After calculation, the minimum inhibitory concentrations of lactic acid, acetic acid and ethanol are 2.5g/L, 1.25g/L and 35g/ L, respectively. While sodium lactate and sodium acetate did not inhibit the growth of E. coli even at 40 g/L and 20 g/L.

It is indicated that lactic acid and acetic acid have bacteriostatic effect when they exist in a molecular state, while they have no bacteriostatic effect when they exist in an ionic state. From the synergistic inhibition experiments, it can be concluded that the three substances have a synergistic effect between every two materials.

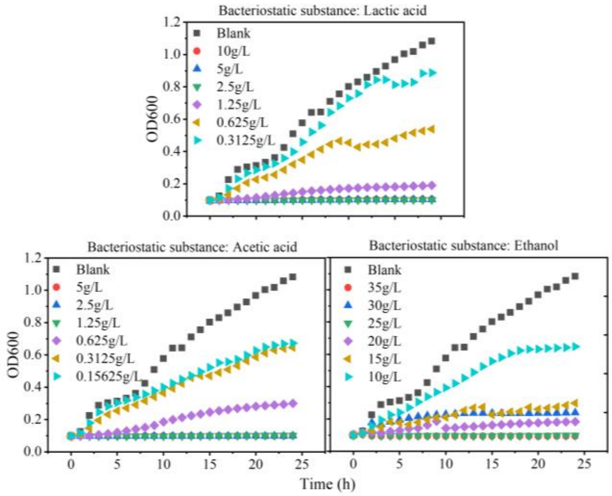

Fig. 2. Time–kill assay of lactic acid, acetic acid and ethanol.

Table 1 the MIC80 and interpretation relationship of different hydrolysate.

Hydrolysate	MIC80（g/L）	FIC	Interpretation
Lactic acid	2.5	-	-
Acetic acid	1.25	-	-
Ethanol	35	-	-
Sodium lactate	-	-	-
Sodium acetate	-	-	-
Lactic acid + Acetic acid	0.625/0.625	0.17	synergistic
Lactic acid + Ethanol	1.25/1.25	0.03	synergistic
Acetic acid + Ethanol	0.625/7.5	0.22	synergistic

4 Conclusions

(1) After anaerobic preservation for 4 days, the concentrations of organic acids and lactic acid in the two groups achieved 38.77 g/L and 28.88 g/L, respectively.

(2) Lactic acid and acetic acid have obvious bacteriostatic effect when they exist in a molecular state rather than in an ionic state.

(3) Lactic acid, acetic acid and ethanol have a synergistic antibacterial effect between every two materials.

Reference

[1] Ren, Y., Yu, M., Wu, C., Wang, Q., Gao, M., Huang, Q., Liu, Y., 2018. A comprehensive review on food waste anaerobic digestion: Research updates and tendencies. Bioresource Technology, 247, 1069-1076.

[2] Zhao, N., Yu, M., Wang, Q., Song, N., Che, S., Wu, C., Sun, X., 2016. Effect of Ethanol and Lactic Acid Pre-fermentation on Putrefactive Bacteria Suppression, Hydrolysis, and Methanogenesis of Food Waste. Energy & Fuels, 30, 2982-2989.

Anammox-dependent nitrogen removal process using up-flow fixed-bed bioreactor

○ Ying SONG[1*], Yu-You LI[2]
[1]Department of Environmental Engineering, Environmental University, Miyagi 980-8579, Japan.
[2]Department of Frontier Science for Advanced Environment, Tohoku University, Miyagi 980-8579, Japan.
*E-mail: song.ying.q2@dc.tohoku.ac.jp

Abstract

The treatment of wastewater containing high-strength nitrogen, represented as the wastewater of fermentation, has been obtaining ever-increasing attention due to far-ranging applications of biogas process. Anammox-based technologies as a cost-effective and high-capacity process have been considered a promising alternative to treat high ammonium concentration wastewater. In this thesis, the fixed-bed biofilm reactor was applied and successfully started up after inoculation and stably operated with growing nitrogen loading rate (0.74g-N/L/d~2.56±0.03g-N/L/d) and nitrogen removal rate(0.39±0.34g-N/L/d~1.99±0.04g-N/L/d) by increasing the substrate concentration at a constant hydraulic retention time(HRT) of 8h. The total nitrogen(TN) removal efficiency was in the range of 76.12±4.82%~87.98±3.72%. Along with the increasing nitrogen loading rate, the biomass attached to biofilms as well as the suspended biomass was largely improved because of the interception impact provided by the biofilms. Spatial distribution of fixed-bed UASB Anammox reactor for nitrogen removal capacity was also investigated .Nitrogen removal efficiency of bottom was around 90% of total nitrogen removal efficiency, which indicated that the bottom bacteria possesses outstanding activity.

Keywords: Anammox, Nitrogen removal, fixed-bed biofilm, spatial distribution

1 Introduction

Anaerobic ammonium oxidation (Anammox) has been considered as a high-efficient, cost-effective and environmental-friendly alternative for nitrogen removal to conventional nitrogen removal process as nitrification/denitrification process. The mechanism of anammox process is producing molecular nitrogen gas with ammonium as the electron donor (energy source) and nitrite as the electron acceptor according to the following reaction:

$$NH_4^+ + 1.146NO_2^- + 0.07HCO_3^- + 0.057H^+ \rightarrow$$
$$0.986N_2 + 0.161NO_3 + 0.071CH_{1.74}O_{0.31}N_{0.20} + 2.002H_2O$$

Remaining issues of this process are long start-up period due to generation time of ca.15 days, mainstream application and sensitivity to operational conditions. Also, the production of the nitrogen gas poses a side effect on sludge floating. What's more, the accumulation of extracellular polymeric substance (EPS) tends to give rise to sludge floatation when the Anammox bacteria is inhibited. Fixation and entrapment of anammox biomass are key to efficient start-up. Hence, in order to retain and enrich the functional bacterial in anammox reactors, fixed-bed biofilm is designed to culture Anammox bacteria with the purpose of obtaining and maintaining high nitrogen removal rates.

2 Materials and methods

A cylindrical UASB reactor are set up for Anammox cultivation. The volume filling rate and working volume of the reactor are 5.29% and 3.06L. Inoculum was originated from granule Anammox bacteria which is gently smashed to particles for the biofilm culturing. Temperatures was set around 35 ˚C which is optimal for Anammox bacteria.

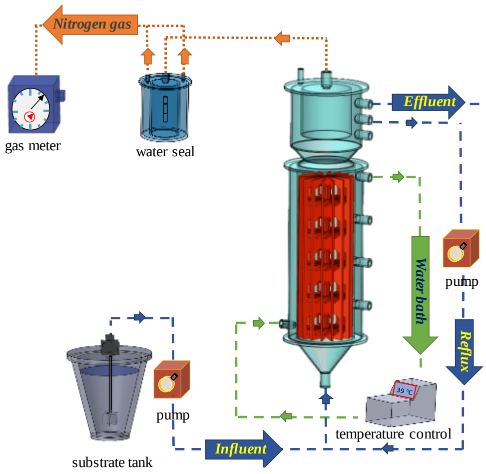

Fig.1 Diagram of experimental set-up

Influent and effluent samples were filtered by 0.45μm membrane filter and stored in a refrigerator at 4 °C before analysis. Nitrogen components of NH_4^+-N, NO_2^--N and NO_3^--N were analyzed by a capillary electrophoresis (CE) system (Agilent 7100).

3 Results and discussion

3.1 Nitrogen removal performance

As shown in Fig.2, Anammox reactor was started up at nitrogen concentration of 250mg-N/L with NLR of 0.7g-N/L/d and nitrogen removal efficiency was around 76% since beginning. Then nitrogen concentration of influent was gradiently increased to 660mg-N/L with nitrogen concentration of effluent lowering than 100mg-N/L/d stable nitrogen removal efficiency of 76-85%. However, the Δ NO_2^--N/Δ NH_4^+-N of effluent was increased from 1.25 to

1.82 and then decreased to 1.2 while the Δ NO_3^--N/Δ NH_4^+-N was stayed relatively stable during this capacity enhancement period. This phenomenon might be caused by the loss of Anammox bacteria because the granule Anammox bacteria was smashed to little ones before inoculation, releasing extra ammonium. From 52nd, the nitrogen concentration of 1000mg-N/L resulted in the slight deterioration of the performance. Therefore, the nitrogen concentration of influent was reduced to 750mg-N/L in case of further inhibition of reactor. After stable operation of 22 days, the NLR was increased to 2.5g-N/L/d by increasing nitrogen concentration of influent to 830mg-N/L and the nitrogen concentration of effluent was at 200mg-N/L/d owing to FA concentration of 20-45mg-N/L or inadequate growth of Anammox bacteria.

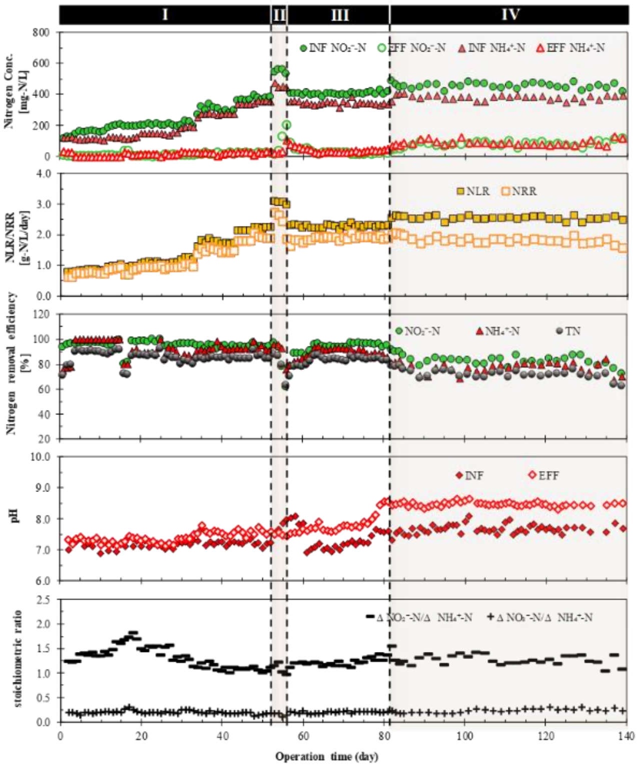

Fig.2 Performance of Anammox process

3.2 Spatial distribution

reactor for nitrogen removal capacity was also investigated (shown in Fig.3). The reactor was divided into upper, middle and lower parts, and the effective volume from bottom to top are 0.865L,1,73L and 0.865L, respectively. The nitrogen removal efficiency of bottom was around 90% of total nitrogen removal efficiency, which indicated that the bottom of the reactor was the most functional area. As Fig.3 a shows, the NRR of the bottom reached up to 6.5g-N/L/d compared to the average value of 1.9g-N/L/d while NRR of the middle and the top was only 0.17 g-N/L/d and 0.28 g-N/L/d. The specific activity (from aspect of Heme C color) and quality of the Anammox bacteria down the reactor were much higher than that of the middle and the top from visual inspection.

As reported, hydrodynamic problems like clogging and turbulence occur in fixed-bed biofilm reactors, mainly due to the production of EPS and their accumulation in the channel of the bed, leading to a gradual decline in performance, which ultimately would lead to system collapse. Therefore, the fixed-bed was arranged in the longitudinal direction in the reactor, and each fixed biofilm was vertically cut 5 circular hole, which could facilitate N_2 elimination and relieves channeling. In the phase IV, clogging and stuck EPS were witnessed along with the increased NLR, resulting higher nitrite and ammonium concentration of effluent.

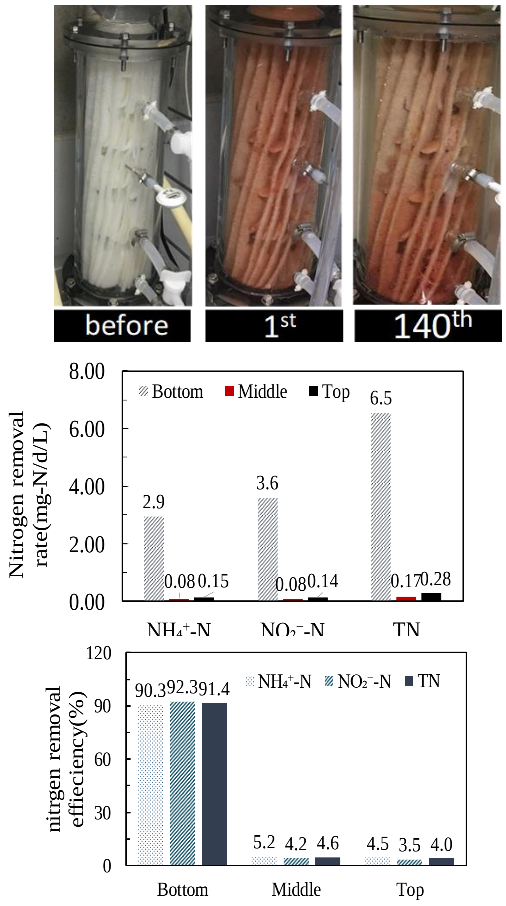

Fig.3 Spatial distribution of fixed-bed UASB Anammox reactor

4 Conclusions

Anammox process using two-stage fixed-bed biofilm configuration has exhibited a commendable performance during the start-up period. The Anammox reactor was able to stably operated with around 70% total nitrogen removal efficiency under the slight pressure of FA and FNA. The acclimated tolerance of FNA and FA of Anammox reactor assure the resistance of trifling performance of partial nitritation. Nitrogen removal capacity was most attributed to the bottom of the reactor where biofilm culturing and suspended granule were much more enriched.

Reference

[1]Cláudio Antonio Andrade LimaI; Rogers RibeiroII; Eugenio ForestiII; Marcelo ZaiatII,2005. Morphological study of biomass during the start-up period of a fixed-bed anaerobic reactor treating domestic sewage. ENGINEERING AND TECHNOLOGY.48, no5.

Anaerobic digestion of milk waste and sewage sludge by using hollow fiber anaerobic membrane reactor

○ Ziang HE[1*], Xueqin Lu[2] ,Chenglei XIE[3]&Yu-You Li[3]
[1]Department of Frontier Science for Advanced Environment, Graduate School of Environmental Sciences,
Tohoku University, 6-6-20 Aoba, Aramaki-Aza, Aoba-Ku,Sendai, Miyagi 980-8579,
[2]School of Ecological and Environmental Science, East China Normal University, PR China
[3]Department of Civil and Environmental Engineering, Tohoku University, 6-6-06 Aramaki Aza Aoba, Aoba-ku, Sendai, Miyagi, 9808579, Japan
*E-mail: he.zi.ang.p8@dc.tohoku.ac.jp

Abstract

In this study, the performance of a mesophilic (37℃) HF-AnMBR (hollow fiber type anaerobic membrane bioreactor) in treating sewage sludge with milk waste for 132 days is studied and its effectiveness is evaluated. The milk waste used in this study was made of crusher liquid, yogurt and concentrated permeate. The organic loading rates (OLR) of HF-AnMBR was gradually increased from 0.97g-COD/L/d to 8.82 g-COD/L/d by shortening the hydraulic retention time (HRT) from 30d to 3.5d. Respectively, the COD conversion efficiency was as high as 96.04%, 97.35%, 98.98% and 96.79% at OLRs of 0.97, 2.94, 6.35 and 8.82 g-COD/L/d. Meanwhile, membrane fouling is the serious problem for MBR, which affects the performance of reactor, so the relationship between the reversible fouling resistance and irreversible fouling resistance was evaluated by this kind of substrate under flux of 11 L/m^2/h. The long-term stable performance of AnMBR indicates that sewage sludge with milk waste were suitable to decompose under condition of mesophilic.

Abstract: Milk waste, sewage sludge, co-digestion, AnMBR

1 Introduction

Nowadays, wastewater treatment plants have to face critical issue with strict regulation of water discharge quality. The food industry generates a plenty of milk product waste in stock breeding. According to the key facts on food loss and food waste by the Food and Agriculture Organization of the United Nations (FAO), 1/3 of food is lost or wasted during production process and human consumption globally [1]. The increasing production of food waste like milk product waste worldwide and new international regulations call for the development of new technologies to treat this biowaste. Due to high-organic content (81.9%) of milk waste, many researchers have investigated the use of the anaerobic digestion in treatment of milk waste, which are able to treat efficiently organic wastes, producing at the same time different value-added compounds, such as methane.

However, in anaerobic digestion system, HRT and sludge retention time (SRT) is the same parameter compare to conventional activated sludge process (CAS). Meanwhile, due to the low growing rate of archeae. The anaerobic digestion system needs a large reactor volume to maintain capability of treatment [2]. In recent years, anaerobic membrane bioreactor (AnMBR) was invented, which can separate HRT and SRT by retaining solids within reactor and discharging permeate through membrane filtration. This combination of MBR with anaerobic digestion brings a high biomass of archeae, which contribute to high organic loading rate (OLR). Meanwhile, applying co-digestion could be one of methods to improve the biogas yield and stability of the anaerobic digester by providing some ways i.e. adjustment of moisture content; supplying trace metal elements; maintaining an optimal pH, enhance capacity of buffer.

The objectives of this study were to assess the performance of an AnMBR treating milk waste with sewage sludge in the co-digestion process as well as the effect of different HRT on membrane fouling.

2 Materials and methods

2.1 Materials

The co-substrate used in this experiment which was made of concentrated triple sewage sludge, crusher liquid, yogurt and concentrated permeate. All the substrates and inoculum sludge were provided by Tokyo Gas Co Ltd.

Table 1 Characteristics of inoculum sludge

Parameters（mg/L）	Inoculum sludge
pH	7.28-7.50
Total COD（g/L）	24.6±0.27
Total Carbohydrates	1862±99
Total Protein	13617±34
TS（g/L）	26.75
VS（g/L）	21.92
TSS（g/L）	22.62
VSS（g/L）	19.21
NH_4^+-N	1316.38

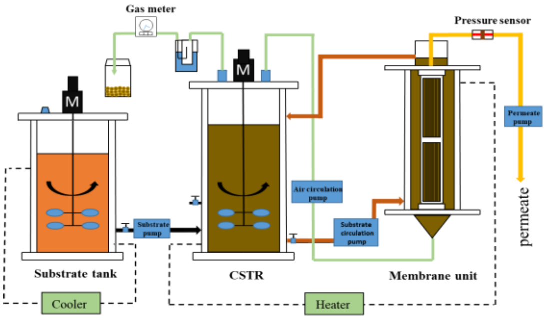

Fig. 1. The schematic diagram of HF-AnMBR.

Table 2 The operation conditions and removal rate in reactor

Temperature	37℃											
Operation time（d）	1-13			13-31			31-52			52-71		
OLR (g COD L/d)	0.97			2.94			6.35			8.82		
HRT (d)	30			10			5			3.5		
ITEM	Substrate	Permeate	Removal rate	Substrate	Permeate	Removal rate	Substrate	Permeate	Removal rate	Substrate	Permeate	Removal rate
T-COD (g/L)	29.15	1.15	96.04%	29.13	0.7	97.35%	31.77	0.31	98.98%	30.86	1.01	96.79%
S-COD (g/L)	15.77	0.96	93.90%	17.85	0.66	97.49%	17.16	0.27	99.12%	16.52	0.98	96.80%
T-Protein (g/L)	3.6	0.07	97.96%	5.38	0.3	93.42%	5.41	0.05	99.14%	5.63	0.08	98.52%
S-Protein (g/L)	0.4	0.04	90.10%	0.88	0.18	95.89%	0.81	0.04	99.19%	0.58	0.07	98.70%
T-Carbohydrates (g/L)	3.6	0.07	97.96%	8.12	0.05	99.30%	6.18	0.05	99.13%	7.01	0.03	99.86%
S-Carbohydrates (g/L)	1.45	0.06	98.17%	6.26	0.04	99.43%	4.51	0.03	99.41%	5.61	0.01	99.73%
T-P (mg/L)	385.84	177.06	54.04%	402.58	191.16	52.60%	467.73	289.37	35.20%	407.84	100.14	75.35%
VS (g/L)	17.54	0.97	94.79%	18.65	0.8	95.93%	19.91	0.68	96.39%	20.33	1.38	93.23%
VSS (g/L)	10.82	0.54	95.09%	8.42	0.28	98.09%	10.35	0.32	96.90%	10.76	0.22	98%
NH4-N (mg/L)	124.98	770.74	-516.69%	251.08	610.16	-143.01%	200.86	222.55	-0.84%	200.86	222.55	-10.79%

2.2 Analysis methods

Daily biogas production is measured by wet gas meter, the composition of (CH_4, CO_2 and N_2) were measured by a ShimadzuGC-8A gas chromatograph, and COD, carbohydrate, protein, ammonium nitrogen, alkalinity, TS, TSS, VS and VSS were measured according to Japan Standard Testing Method. Sludge samples were taken from the digesters and the substrate tank three times a week. The total effective volume was 15L.The membrane unit was made of polytetrafluoroethylene, with a mean pore size of 0.2 μm and an effective filtration area of 0.1m2

3 Results and discussion

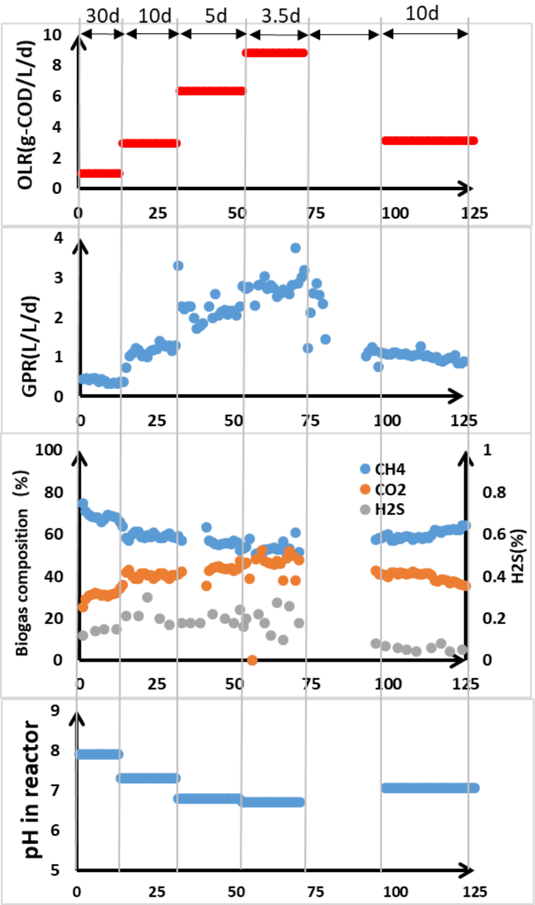

Fig. 2. Reactor performance.

The treatment performance of AnMBR is shown in Fig.2. The start-up period (HRT=30d) began with a gas production rate of around 0.54 L/L/d, after 11 day, the composition of methane rose to 62.3%. However, the substrate pump has a problem about timer setting, so the content of methane shows a little lower. The value of COD removal efficiency was around 96% with the OLR was about 0.97 g COD L/d.

After 15 day, the OLR was increased to 2.94 g COD L/d by shorten HRT from 30 day to 10 day. The biogas production rate achieved a value of 1.15 L/L/d, 112.9% higher than the initial value, due to the high treatment capacity of the anaerobic biomass.

From the 76th day, reactor became possible to operate continuously under HRT of 5 days. From the 45th day to the 90th day, gas production rate was 0.39 ± 0.05 L/L/d as HRT was reduced stepwise and reactor volumetric load increased from 1,3 to 8.82 kg-COD/m3/d 1.15 ± 0.16 L/L/d, increased from 2.20 ± 0.41 L/L/d to 2.7 ± 0.22 L/L/d. The methane content was maintained at 55-58%. When the COD volumetric load was increased to 8.82 kg-COD/m3/d, the methane content 53.23% tended to decrease gradually.

4 Conclusions

In this study, we conducted continuous experiments on membrane-type methane fermentation for milk waste and sewage sludge and examined important parameters for plant design. The main results are summarized as follows.

Based on the generation rate of waste liquid in the factory, the HRT was changed step by step to improve the OLR. As a result, HRT was over 5 days, OLR was 6.35 g COD L/d, the reactor maintains good operation performance. When the OLR was increased to 9 kg-COD / m3 / d, there was storage of organic acids. From these results, it is considered that the limit of the AnMBR for maintaining the absence of organic acid accumulation is about 6.35 g COD L/d.

Reference

[1]H. Cheng, Y. Hiro, T. Hojo, Y.Y. Li, Upgrading methane fermentation of food waste by using a hollow fiber type anaerobic membrane bioreactor, Bioresour Technol, 267 (2018), pp. 386-394.

[2]W. Qiao, K. Takayanagi, M. Shofie, Q. Niu, H.Q. Yu, Y. -Y. Li Thermophilic anaerobic digestion of coffee grounds with and without waste activated sludge as co-substrate using a submerged AnMBR: system amendments and membrane performance.Bioresour Technol, 150 (2013), pp. 249-258

Effect of thermal pretreatment on digestion of sewage sludge in an anaerobic membrane bioreactor

○ Guangze GUO[1*], Yemei LI[2] & Yu-You LI [1,2]
[1]Graduate School of Environmental Studies, Tohoku University, Miyagi 980-8579, Japan.
[2]Department of Civil and Environmental Engineering, Tohoku University, Miyagi 980-8579, Japan.
[*]E-mail: guo.guangze.t1@dc.tohoku.ac.jp

Abstract

The treatment of sewage sludge has become an important environmental issue all over the world. Anaerobic digestion is a simple method that converts chemical energy from sewage sludge into biogas like methane as a substitute for fossil fuels in contemporary society while eliminating pathogens and eliminating odors. According to the previous study, hydrolysis becomes a rate-limiting step in the anaerobic digestion process due to the complex floc structure of the sewage sludge (eg, extracellular polymer) and hard cell walls. In order to accelerate the hydrolysis process and increase the efficiency of anaerobic digestion, a thermal pretreatment method is applied to carry out the solubilization reaction to decompose the organic matter in the sludge. This study explored the effects of thermal treatment on sludge properties, methane production efficiency, and membrane reactor performance. Current results showed that thermal pretreatment had a more obvious influence on the property of excess sludge than on that of primary sludge.

Keywords: Thermal pretreatment; Sewage sludge digestion; AnMBR.

1 Introduction

The generation of renewable energy in the field of sewage treatment has been allocated great attention. In 2016, the effective utilization rate of sewage sludge reached more than 70%, but most of the sewage sludge was recycled and used as building materials. In 2017, only 22% of sewage sludge was used as biogas and solid fuel. 68% of sewage sludge is not used as energy. For biogas power generation, about 20% of the sewage treatment plants in the country that use anaerobic digestion will generate biogas for power generation. A sewage treatment plant that does not use biogas to generate electricity mainly utilizes biogas as an auxiliary fuel for digester heating and sludge incineration. Therefore, the effective use of renewable energy in the field of sewage sludge treatment is not good enough.

In the anaerobic digestion of sewage sludge, the main component of the substrate is solid organic matter. The hydrolysis step is a previous step and is also a critical step for determining the rate in anaerobic digestion. Thermal pretreatment causes the lysis of cells, thus making organics and nutrients readily available for microbial growth and metabolic activities. The hydrolysis efficiency and biogas production by organic dissolution are improved through this process. This system of thermal pretreatment combined with anaerobic digestion is called TP / AD (thermal pretreatment anaerobic digestion) system. Since heat treatment of sewage sludge is a simple method and a high pollution dissolution effect can be obtained, thermal treatment temperature conditions which have been extensively studied in recent years are 50℃ to 90℃. However, since the heat treatment of sewage sludge requires a large amount of energy, the TP / AD system is not widely implied. Waste heat from the power plant is able to be used for sludge thermal treatment.

Thus an efficient TP / AD system can be constructed by using waste heat as a thermal treatment energy source for the sewage sludge.

The anaerobic membrane bioreactor is a novel biological treatment technology coupled with anaerobic fermentation and membrane processes. The process has the traditional advantages of anaerobic biological treatment, and the filtration water retention effect of the membrane significantly improves the effluent water quality, while maintaining a high concentration of microorganisms in the reactor, further improving the decomposition and conversion efficiency of organic matter, and effectively making up for the tradition. Insufficient anaerobic biological treatment process. In addition, the process can control the hydraulic retention time (HRT) and sludge residence time (SRT), and extend the SRT to reduce the volume of the anaerobic fermentation tank.

In this research, the changes of the properties of primary sludge and excess sludge by thermal treatment at four different temperatures were studied. The volatile solids (VSS), total solids (SS) and dissolved chemical oxygen demand (SCOD) in the liquid phase were investigated. The effect of thermal treatment temperature and time on the properties of the sludge is determined by the increase of dissolved organic matter and the change of sludge characteristics.

2 Materials and methods

The sewage sludge used for the experiment was withdrawn from a municipal wastewater treatment plant in Sendai, Japan. The sludges were stored at 4℃ in order to maintain freshness.

The method of primary sludge and excess sludge thermal pretreatment is to transfer sewage sludge to glass bottles and heat them in a water bath. Sludge was put into eight 120 ml glass bottles using a 100 ml syringe, and each of bottle was filled with 80ml sludge. After that, placing glass bottles in a 50°C water bath and continuously vibrated in order to evenly heat. It was necessary to discharge the gas in the bottle frequently during the heating process. Eight sludge samples were heated for 10 minutes, 20 minutes, 30 minutes, 45 minutes, 60 minutes, 90 minutes, 120 minutes and 180 minutes respectively. The treated samples were stored in 4℃ refrigerator. Next, keeping the temperature of water bath at 60°C and 8 bottles of 80 ml of the sludge samples were taken again and placed in 60°C water bath for heating the same time as 50°C. In the end, temperature of water was raised to 70°C and 80°C. Primary sludge and excess sludge were treated under 70°C and 80°C conditions.

In order to examine the change in sludge properties after thermal treatment, the SS, VSS, and pH of the sludge were measured by sewage test standard method. The measurement of the dissolved substance requires centrifugation of the sludge at 15,000 rpm for 15 minutes using a high-speed centrifuge. The obtained supernatant is filtered through a 0.45 μm membrane. The dissolved COD and ammonia nitrogen concentrations of the sludge were determined by the Standard Methods, and the carbohydrate content was determined by the phenol-sulfuric acid method. The protein concentration was determined by the Lowry method.

3 Results and discussion

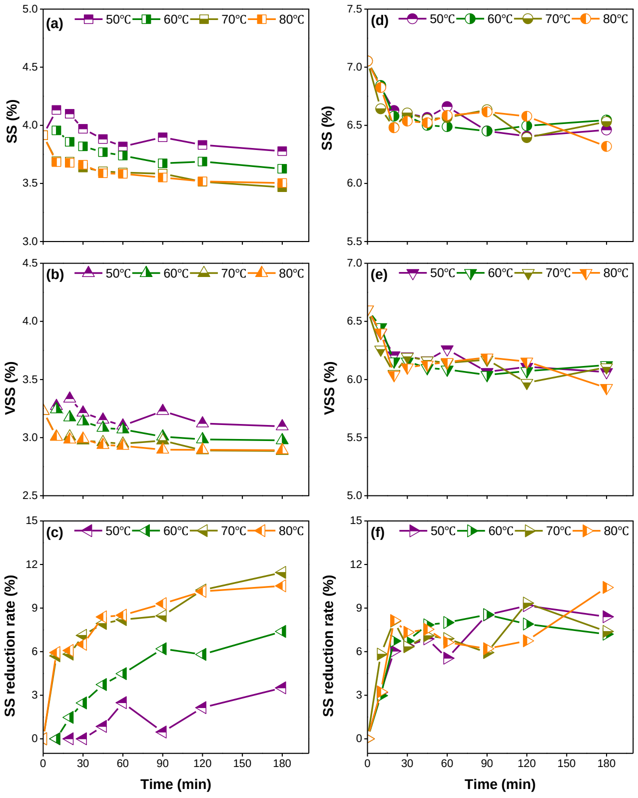

Fig. 1. Changes of (a) SS, (b) VSS and (c) SS reduction rate of excess sludge and (d) SS, (e) VSS and (f) SS reduction rate of primary sludge under different period of pretreatment.

Fig.1 showed the changes of SS, VSS of excess sludge and primary sludge during the three-hour-thermal pretreatment. As the pretreatment time was extended, the concentrations of SS and VSS in the sludge gradually reached equilibrium. Especially for primary sludge, the equilibrium value occurs essentially within thirty minutes of the pretreatment. The temperature showed a slight influence on the SS and VSS levels of primary sludge, while they changed a lot when the temperature changed in excess sludge pretreatment. When the temperature bellow 70℃, the SS and VSS level increased with the increase of temperature. However, when the temperature increased 80℃, the results nearly no changed. That means that 70℃ is a boundary value for excess sludge thermal pretreatment.

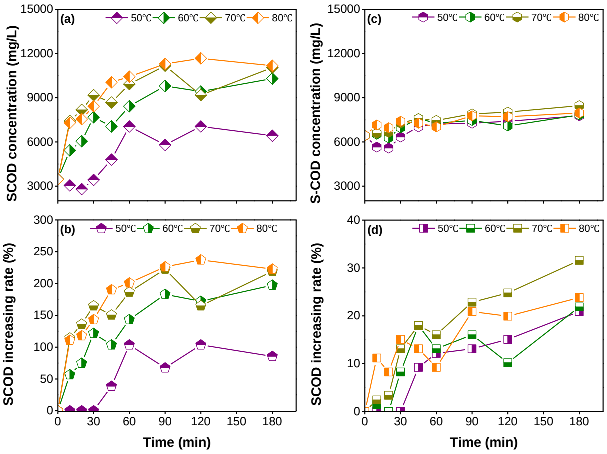

Fig. 2. Changes of (a) SCOD, and (b) SCOD increasing rate of excess sludge and (c) SCOD and (d) SCOD increasing rate of primary sludge under different period of pretreatment.

SCOD is often used to evaluate the effect of pretreatment. Fig. 2 showed the trends of SCOD concentration changed with time and pretreatment temperature during the pretreatment. Similar to that shown in Figure 1, the effect of pretreatment on SCOD in the primary sludge is far less affected by the SCOD in the excess sludge. The change in SCOD levels of primary sludge was not obvious and the SCOD increasing rates were below 35%. In contrast, after the heat treatment of the remaining sludge, the SCOD growth rate can reach nearly 250%.

4 Conclusions

(1) Thermal pretreatment has a little influence on the property of primary sludge while excess sludge change a lot after pretreatment undert 50-80°C.

(2) In general, the 70℃ thermal treatment is more effective than other temperatures.

Reference

[1] Zhen, Guangyin, et al. "Overview of pretreatment strategies for enhancing sewage sludge disintegration and subsequent anaerobic digestion: Current advances, full-scale application and future perspectives." *Renewable and Sustainable Energy Reviews* 69 (2017): 559-577.

Impact of HRT on the performance of AnMBR treating municipal sewage

○ Runda Du[1*], Jiayuan Ji[1], Yujie Chen[1], Yu-You Li[1]
[1]Department of Civil Engineering and Architecture, Tohoku University, 6-6-06 Aoba, Aramaki, Aoba-ku, Miyagi 980-8579, Japan.
*E-mail: du.runda.t3@dc.tohoku.ac.jp.

Abstract

The performance of the municipal sewage treatment process anaerobic membrane bioreactor (AnMBR) was studied through a small reactor with a working capacity of 20 L. In this experiment, the HRT (hydraulic holding time) was changed from 12 hours to 4 hours at 25℃ to explain the effect of HRT. Process performance was evaluated by organic matter removal efficiency, biogas production, sludge production yield, membrane filtration flux and TMP.

Keywords: AnMBR; municipal sewage; HRT.

1 Introduction

The activated sludge process has evolved into a mature method for wastewater treatment for over 100 years. However, there are still some issues such as high energy costs for aeration and mass production of waste sludge to be solved. At the same time, anaerobic membrane bioreactor (AnMBR) has been attached to great attention because its high COD removal rate, low energy demand, low waste sludge generation and even energy recovery (Rong Chen et al., 2017). Although this technology has been successfully applied in the field of industrial wastewater treatment, it has not yet been applied to the treatment of municipal wastewater containing many complex compositions, the contaminants in which have instabilities and low concentrations (Zhen Lei et al., 2018). In this study, a small-scale AnMBR was used for actual municipal sewage to achieve stable operation and investigate the effects of HRT.

2 Materials and methods

A 20L small-scale AnMBR was installed at a Wastewater Treatment Plant (WWTP), so the original sewage could be immediately pumped into the reactor. The membrane was placed in AnMBR filled with anaerobic digested sludge as seed sludge. After the acclimation of microorganisms (about 50 days after beginning), the long-term operation of AnMBR supplied by actual sewage began. The details of operating conditions are shown in Tables 1 and 2.

Table 1 Experiment conditions for AnMBR.

Membrane type	Hollow fiber	**Temperature**	25.2 ± 0.5 ℃
Membrane pore size	0.4μm	**Sewage COD_{Cr}**	400 ± 200 mg/L
Membrane material	PVDF	**Sewage BOD**	150 ± 50 mg/L
Reaction volume	20 L	**Sewage SS**	125 ± 25 mg/L

Table 2 Detail experiment conditions at different HRT.

HRT (h)	24	12	12	6	8	4
Operated period	Day 6-48	Day 49-134	Day 135-145	Day 147-245	Day 246-299	Day 300-
FLUX(m/d)	0.137	0.274	0.274	0.232	0.174	0.348
Membrane area (m^2)	0.146			0.345		
Biogas circulation (m^3/h)	69.76		118.59	116.21		174.31

3 Results and discussion

(1) Removal of organic matters & sludge production yield

Figure 1 shows the average removal efficiency of CODCr, BOD and SS under different HRT conditions. The results of CODCr removal efficiency shows that the values of HRT 8h and 4h were lower, while it is about 90% at 12h and 6h. In terms of BOD removal, the average BOD removal efficiency of HRT 4h is only 87.3%, which is lower than 91% at other HRT conditions. Since the pore diameter of the membrane is 0.4μm, the removal efficiency of SS reaches 100%.

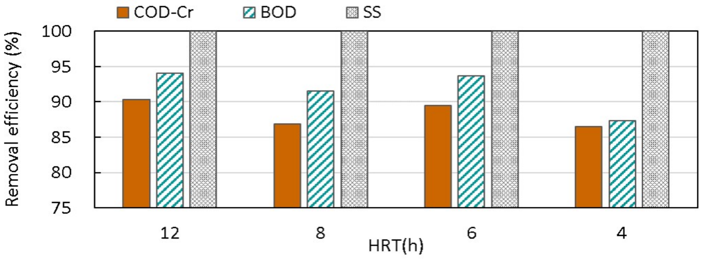

Fig. 1. Average removal efficiency of CODCr, BOD and SS at different HRT

Figure 2 shows the sludge production yield under various HRT conditions. Obviously, as HRT is shortened, sludge production yield has increased. Even the highest sludge yield (0.143 gVSS/gCODCr) shown in HRT 4h is much lower than the theoretical value of the activated sludge process of 0.33 gVSS/gCODCr.

Therefore, it can be seen that the removal of organic matters and SS performs well between HRT 12h and 4h, and sludge production is also low.

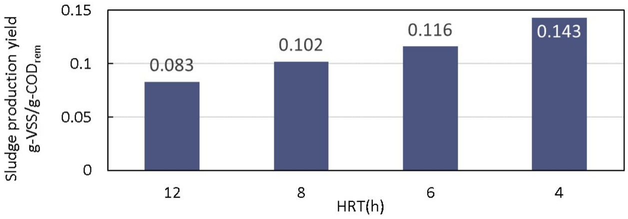

Fig. 2. Average sludge production yield at different HRT

(2) Biogas production

In long-term experiment, the highest biogas production was 0.119 L-gas/L-waterduring at HRT 8h. Average biogas production (Figure 3) also reached 0.103 L-gas/L-water (HRT 12h) and 0.099 L-gas/L-water (HRT 6h). HRT decreased significantly after shortening to 4h. However, in different HRT, the methane gas content was always about 80% of the gas composition. The gas composition was also composed of about 14% and 6% nitrogen and carbon dioxide, respectively.

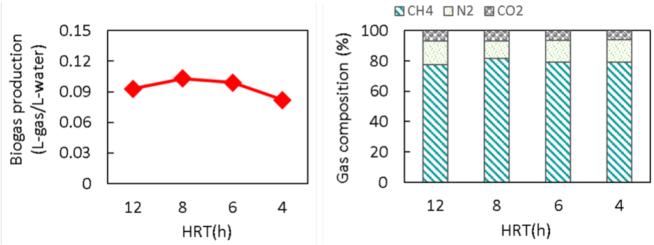

Fig. 3. Average biogas production and gas composition at different HRT

(3) Membrane performance

The TMP and flux datas shown in Figure 4 shows the membrane properties during long-term operation. For flux < 0.27 m/d (HRT6-12h), TMP stabilized at very low values. Since flux > 0.35, TMP rapidly increased due to sludge generation, although there is crossflow by the biogas cycle which is typically used as an effective method to mitigate membrane fouling. This indicates that the concentration of the mixed solution must be tightly controlled to maintain membrane filtration capacity under short HRT conditions (4h).

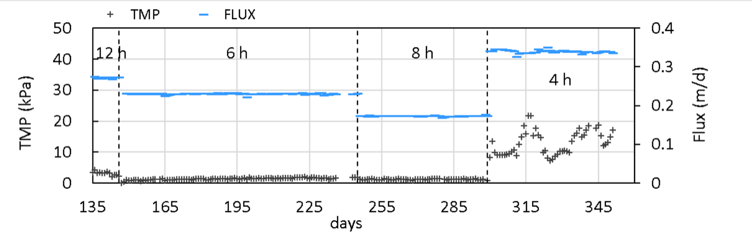

Fig. 4. TMP-FLUX during long-term operation

4 Conclusion

The results so far show that AnMBR can be used for municipal sewage treatment in the HRT range of 6 to 12 hours with good organic removal rates, sludge generation and biogas generation. And the use of HRT for 4 hours or less is not recommended for sewage treatment by AnMBR.

Reference

[1] Rong Chen, Yulun Nie, Jiayuan Ji, Tetsuya Utashiro, Qian Li, Daisuke Komori and Yu-You Li, (2017), Submerged anaerobic membrane bioreactor (SAnMBR) performance on sewage treatment: removal efficiencies, biogas production and membrane fouling, Wat. Sci. and Technol., 76(6): 1308-1317.

[2] Zhen Lei, Shuming Yang, Yu-you Li, Wen Wen, Xiaochang C. Wang and Rong Chen, (2018), Application of anaerobic membrane bioreactors to municipal wastewater treatment at ambient temperature: A review of achievements, challenges, and perspectives. Bioresour. Technol., 267: 756-768.